Aalto-yliopisto
Insinööritieteiden
korkeakoulu

Valtteri Hyvärinen

# Lateral and longitudinal control of electric bus to follow leader vehicle trajectory

Thesis submitted in partial fulfillment of the requirements for the degree of Master of Science in Technology.

Espoo 14.8.2017
Supervisor: Professor Kari Tammi
Instructor: Sami Ruotsalainen

Aalto-yliopisto
Insinööritieteiden korkeakoulu

Aalto-yliopisto, PL 11000, 00076 AALTO
www.aalto.fi

**Diplomityön tiivistelmä**

**Tekijä** Valtteri Hyvärinen

**Työn nimi** Sähköbussin nopeuden ja ohjauskulman säätö edellä ajavan ajoneuvon liikeradan seuraamisessa

**Koulutusohjelma** Konetekniikka

**Pää-/sivuaine** Koneensuunnittelu **Koodi** K3001

**Työn valvoja** Kari Tammi

**Työn ohjaaja(t)** Sami Ruotsalainen

**Päivämäärä** 14.8.2017 **Sivumäärä** 75 **Kieli** Englanti

**Tiivistelmä**

Linja-autojen matkustajakapasiteetti on rajallinen, mikä aiheuttaa ongelmia, sillä sen tulisi olla suurempi. Kapasiteetti on jo nostettu suurimmalle mahdolliselle tasolle, mitä nykyinen infrastruktuuri mahdollistaa. Linja-autolinjan kapasiteettia voisi nostaa ajamalla linja-autoja tiheämmin. Tämä kuitenkin johtaa suurempiin kustannuksiin. Kustannuksia voisi vähentää ajamalla linja-autoja kahden ajoneuvon jonoina, joissa ensimmäistä ajoneuvoa ohjaisi ammattilaiskuljettaja ja toinen olisi autonomisesti ohjattu. Autonominen ajaminen vaatii ajoneuvon nopeuden ja ohjauskulman säätöä. Seuraajalinja-auton pitää pystyä seuraamaan johtajalinja-auton ajamaa ajouraa tarkasti ja välttää törmäämistä johtajaan. Linja-autojen välinen etäisyys on kuitenkin oltava riittävän pieni, jotta se viestisi muulle liikenteelle, että ajoneuvot ajavat jonona.

Kirjallisuus jakaa ohjauskulman säädön yleensä ajouran seuraamiseen ja suoraan seuraamiseen. Ajouran seuraaminen koostuu johtaja-ajoneuvon ajouran saamisesta ja tämän uran seuraamisesta. Ajouran seuraamisen metodit ovat yleensä tarkkoja poikittaisen virheen suhteen, mutta ovat monimutkaisia ja vaativat paljon laskennallista kapasiteettia. Suoran seuraamisen metodit ovat laskennallisesti kevyitä, mutta eivät takaa tarkkaa ajouran seuraamista.

Kahdesta identtisestä linja-autosta koostuva simulaatiomalli kehitettiin. Yksi nopeussäädin ja neljä ohjauskulman säätölakia esitettiin. Nopeussäädin suunniteltiin toimimaan myös tiukoissa käännöksissä, mitä ei ole yleensä tutkittu. Ohjauskulman säätölait perustuivat geometriseen päättelyyn ja ne tarvitsivat vain johtajalinja-auton suhteellisen asentotiedon. Säätölait eivät vaatineet ajoneuvojen välistä kommunikaatiota.

Nopeussäädin toimi järjestelmän alustamisessa ajoneuvojen välisen etäisyyden ollessa 2-10 m. Se toimi hyvin kiihdytys- ja jarrutustesteissä, kun molemmat linja-autot olivat lastattu identtisellä kuormalla, mutta epäonnistui estämään törmäämisen, kun seuraajalinja-auto oli lastattu suuremmalla kuormalla kuin johtaja.

Ohjauskulman säädön testeissä Pure Pursuit ja Modified Pure Pursuit pystyivät seuraamaan johtajaa seuraavilla poikittaissuuntaisilla virheillä: 0,8 m ja 1,1 m (steady-state-testit), 0,8 m ja 0,7 m (u-käännös) ja 0,3 m/0,4 m ja 0,4 m/0,5 m (kaksoiskaistanvaihto, 5 m/s/10 m/s vastaavasti). Spline Pursuit käyttäytyi värähtelevästi eikä seurannut johtajaa hyvin. Circular Pursuit käyttäytyi värähtelevästi eikä seurannut johtajaa hyvin, mutta kuitenkin paremmin kuin Spline Pursuit.

Jää nähtäväksi pystyykö Pure Pursuit tai Modified Pure Pursuit haastamaan monimutkaisempia ajouran seuraamisen metodeja.

**Avainsanat** autonominen ajaminen, suora seuraaminen, ajouran seuraaminen

Aalto University
School of Engineering

Aalto University, P.O. BOX 11000, 00076 AALTO
www.aalto.fi

**Abstract of master's thesis**

**Author** Valtteri Hyvärinen

**Title of thesis** Lateral and longitudinal control of electric bus to follow leader vehicle trajectory

**Degree programme** Mechanical engineering

**Major/minor** Machine design **Code** K3001

**Thesis supervisor** Kari Tammi

**Thesis advisor(s)** Sami Ruotsalainen

**Date** 14.8.2017 **Number of pages** 75 **Language** English

**Abstract**

Buses face problems when the capacity of a bus is limited but it should be larger to be able to carry more passengers. The capacity of a bus is already increased to its maximum that is allowed by the infrastructure. The capacity of a bus line could be increased by driving buses more frequently but it would increase costs, that is unwanted. Costs could be reduced by driving buses as platoons consisting of two buses where only the first bus would be operated by a professional driver and the second would be driven autonomously. Autonomous driving requires longitudinal and lateral control of a vehicle. The follower bus should be able to follow the path driven by the leader bus precisely and avoid inter-vehicular collisions while still driving as close together as possible to indicate other traffic that they move as a platoon.

Lateral control is usually divided into path following and direct following methods in the literature. Path following methods include obtaining the path of the leader vehicle and following of that path. Path following methods are usually accurate in terms of lateral error but are complex and require a lot of computational capacity. Direct following methods are easy to compute but they do not guarantee precise path following.

A simulation model consisting of two identical buses was developed. One longitudinal controller and four lateral control laws were proposed. Longitudinal controller was designed to work also in tight turns which is not usually investigated. Lateral control laws proposed were geometrical in nature and required only input as the relative position of the leader bus. Therefore, they did not require inter-vehicular communication.

Longitudinal controller worked well for initialization of the system with inter-vehicular distances from 2 to 10 m. It worked well in acceleration and deceleration tests when both buses were loaded similarly but failed to prevent collisions when follower bus was loaded more heavily than the leader.

In lateral controller tests, Pure Pursuit and Modified Pure Pursuit methods were able to follow the leader producing following lateral errors: 0,8 m and 1,1 m (steady-state tests), 0,8 m and 0,7 m (u-turn maneuver) and 0,3 m/0,4 m and 0,4 m/0,5 m (double lane change maneuver, 5 m/s/10 m/s respectively). Spline Pursuit method showed oscillatory behavior and did not follow the leader well. Circular Pursuit method showed also oscillatory behavior and did not follow the leader well. However, it showed better performance than the Spline Pursuit.

It remains to be studied whether Pure Pursuit or Modified Pure Pursuit can challenge more sophisticated path following methods.

**Keywords** autonomous driving, direct following, path following

# Preface

*The idea to study the control of a bus platoon originally came from Sami Ruotsalainen from LinkkerBus. My supervisor Kari Tammi proposed the topic which seemed interesting. Klaus Wirtanen had studied the same theme earlier in his own Master's Thesis. The scope of the study was to gather more insight into the control of a bus platoon. I am grateful for Henry Fordin Säätiö for funding my research. Finally, I am very grateful for all the people that have helped me to finish this work, especially my lovely girlfriend for her support.*

Espoo 14.8.2017

Valtteri Hyvärinen

# Table of Contents

# Nomenclature

| | | |
|---|---|---|
| $K$ | | gain parameter |
| $L$ | [m] | length of the bus |
| $L_{fo}$ | [m] | length of the front overhang of the bus |
| $L_{ro}$ | [m] | length of the rear overhang of the bus |
| $L_w$ | [m] | width of the bus |
| $L_{wb}$ | [m] | length of the wheelbase of the bus |
| $M$ | | gain parameter |
| $R$ | [m] | radius of a circle |
| $R_f$ | [m] | turning radius of front |
| $R_{fa}$ | [m] | turning radius of front axle |
| $R_r$ | [m] | turning radius of rear |
| $R_{ra}$ | [m] | turning radius of rear axle |
| $a_c$ | [m/s$^2$] | centripetal acceleration |
| $d$ | [m] | distance |
| $d_0$ | [m] | minimum target distance |
| $d_{lad}$ | [m] | look ahead distance |
| $d_r$ | [m] | distance to right rear corner |
| $d_{target}$ | [m] | target distance |
| $h$ | [s] | time headway |
| $v$ | [m/s] | velocity |
| $v_{leader}$ | [m/s] | velocity of the leader bus |
| $x_{lfa}$ | [m] | relative x-coordinate of leader's front axle |
| $x_{lra}$ | [m] | relative x-coordinate of leader's rear axle |
| $y_{lfa}$ | [m] | relative y-coordinate of leader's front axle |
| $y_{lra}$ | [m] | relative y-coordinate of leader's rear axle |
| $\alpha$ | [°] | angle |
| $\alpha_a$ | [°] | aiming angle |
| $\alpha_r$ | [°] | reflector angle |
| $\alpha_t$ | [°] | angle between the virtual follower's heading and the look ahead distance |
| $\beta$ | [°] | angle |
| $\gamma$ | [°] | relative heading of the leader bus |
| $\delta$ | [°] | steering angle |
| $\delta_{leader}$ | [°] | steering angle of the leader bus |
| $\delta_{target}$ | [°] | target steering angle |
| $\kappa$ | [1/m] | curvature |
| $\tau$ | [s] | sum of all lags |

# Acronyms

| | |
|---|---|
| ACC | Adaptive cruise control |
| CC | Cruise control |
| CTH | Constant time headway |
| DLC | Double lane change |
| FOPID | Fractional order proportional integral derivative |
| HRT | Helsinki Regional Traffic |
| ICE | Internal combustion engine |
| PID | Proportional integral derivative |
| SARTRE | Safe Road Trains for the Environment |
| VTH | Variable time headway |
| V2V | Vehicle to vehicle |

# 1 Introduction

## 1.1 Background

Public transportation is widely used in urban areas. Bus is the most versatile and agile public means of transportation. It is also easy to apply new bus routes into traffic which makes buses as the main means of transportation a very attractive idea.

Electric buses are a new direction in bus driveline systems. Traditional buses use internal combustion engine (ICE) to provide power but the amount of electric buses is rising. They are not very widely used but increasing environmental demands make them a viable option in the future. According to Helsinki Regional Traffic (HRT) the amount of electric buses used in metropolitan area traffic will increase dramatically in near future (HSL, 2014). HRT aims to replace all connection line buses with electrical buses by year 2025. Buses face problems arising during rush hours when more passengers are trying to fit into a bus than it can carry. This leads to the situation when a bus driver is forced to leave excessive passengers to the bus stop which reduces customer satisfaction.

A solution to this situation is to increase the capacity of buses. However, buses cannot grow into any direction, at least for current infrastructure. An increase in the height of the bus would require higher underpasses under bridges. An increase in the width of the bus would require wider roads. And an increase in the length of the bus would require changes into the infrastructure so that it could handle longer vehicles.

A possible solution to the problem is to drive buses more frequently. However, this would eventually lead to buses driving as a platoon because distance between adjacent buses would be so small. Increasing the frequency of buses increases costs which is not wanted. This rises the following question: is it possible to join two buses together so that it would require only one driver to operate the whole vehicle combination?

## 1.2 Scope

This paper concentrates on to the control of electric buses. Even though ICE powered buses are excluded results can probably be applied to those too. Forward motion of the vehicles is only studied, which means that if backward control is needed, other methods should be developed for that purpose.

Bus driving conditions are supposed to be optimal in the study i.e. there is zero sliding between the tires and the road surface. Weather conditions are supposed to be good, which means that all available sensing devices are suitable.

## 1.3 Objectives

The study aims to find an accurate control method to control follower bus laterally and longitudinally. The follower bus must imitate leader's trajectory as precisely as possible. Follower must also maintain appropriate distance to the leader to ensure that there is enough space in case of emergency braking. However, longitudinal distance must also be small enough to indicate that buses move as a platoon and prevent other vehicles and humans to move between the buses.

This means that studied control system must have less than 10 cm maximum lateral displacement error relative to the leader vehicle trajectory. Longitudinal controller must be able to prevent buses from colliding in an emergency braking situation.

Follower bus must be able to operate without information coming from the leader bus. This means that all available information should come from follower bus's own sensors only. If the connection would be lost between the leader and the follower it would result into malfunction of the follower's control. Therefore, it is necessary for a reliable control strategy that the follower bus must be autonomous in that sense.

## 1.4 Methods

Experiments will be done on a simulation model. Simulation modelling offers many advantages over real-world testing. Parameter setting and running through a scenario is faster with a simulation model. Using it is cost and time efficient and it has a smaller environmental impact.

However, building a simulation model can be time-consuming. Simulation model is always an approximation so it does not represent real world perfectly. Therefore, results of a simulation model should always be verified afterwards by real world testing.

# 2 Theory

## 2.1 Platoon

Platoon is a line consisting of multiple vehicles which are joined together. First vehicle, which is called the leader vehicle, is usually driven by a human driver and follower vehicles move autonomously and follow leader vehicle.

Bergenhem et al. (2010) presented the Safe Road Trains for the Environment (SARTRE) concept of platoons and associated challenges with it. The SARTRE definition of platooning implies that the platoon is operated by a lead vehicle driven by a professional driver. Following vehicles are driving autonomously, but a passive driver is located in them to take full control of the vehicle when required. Autonomous driving here means both lateral and longitudinal autonomous control. Platoon should be able to operate without any changes to the infrastructure and when there are non-platoon vehicles operating nearby.

SARTRE project aimed to address cornerstones of transportation issues which are environmental, safety, congestion and driver comfort aspects (Dávila & Nombela, 2010).

The whole point of platooning is that vehicles are able to operate autonomously. Litman (2014) listed numerous advantages and disadvantages of using autonomous vehicles. Benefits include reduced driver stress and costs, mobility for non-drivers, increased safety and road capacity, more efficient parking, increased fuel efficiency and reduced pollution and using autonomous vehicles supports shared vehicles. Problems and costs include increased equipment costs, possible additional risks, security and privacy concerns, social equity concerns, increased travelling using vehicles and reduced employment of professional drivers.

Chan et al. (2012) presented an overview of a control system developed for a five-vehicle platoon consisting of various types of vehicles. Lead vehicle was driven manually and follower vehicles were autonomous. Control system relied on on-board sensor data and vehicle-to-vehicle communication. On-board sensors included radars, lidars and cameras to measure the position of the preceding vehicle. Lateral controller used sensors and vehicle-to-vehicle (V2V) data to determine its target trajectory and controlled steering to follow that trajectory.

Rajamani et al. (2000) implemented an integrated longitudinal and lateral control system for the operation of automated vehicles in platoons. Longitudinal controller used V2V communication to control the distance to the preceding vehicle. Lateral controller used magnets embedded in the center of the lane to calculate vehicle's position on the road to control steering. Lateral control included lane-keeping and lane-change maneuvers. Control system was robust enough to operate 6-8 hours a day for three weeks giving demonstration rides to visitors on a closed highway segment.

Oshima (2016) investigated the impact of Automated Driving Systems on $CO_2$-emissions by changing the traffic flow. When vehicles move as a platoon, follower vehicles achieve lower air resistance if they drive close enough to each other which leads to lower fuel consumption and $CO_2$-emissions. Truck driving with 4 m spacings can lead up to 4,8 % reduction in $CO_2$-emissions.

Chan (2014) measured the fuel consumption of vehicles moving in a platoon with varying inter-vehicle distances. He found out that the lead vehicle makes up to 8 % and following vehicles make up to 16 % fuel savings when vehicles drive close together. The studied platoon consisted of a lead truck, following truck and three following cars and inter-vehicle distances varied from 4 to 25 m.

## 2.2 Connecting the buses and sensing

Shieh et al. (2015) explored the effectiveness of infrared communication for data transfer using various receiver tilt angles to obtain the direction of infrared signals. Authors state that infrared communication is a good choice for vehicle-to-vehicle communication in several intelligent transportation system applications.

Subramanian et al. (2006) developed autonomous vehicle guidance systems for tractor navigating in citrus grove. They found that laser radar based system performed best at low and moderate speeds. Communication speed between the sensor and computer was limiting factor for high speeds. Machine vision based system showed acceptable performance in all speeds. Maximum lateral error was not more than 6 cm in any experiment.

Vehicle state can be sensed for instance through yaw rate sensor, accelerometer, wheel speed sensor and steering angle sensor. Surroundings of the vehicle can be sensed for instance through short/long-range radar sensor, laser scanner (lidar), vision system and ultrasonic sensor. Short-range radar sensors can measure distance, velocity and angle of detection. Lidars have larger field of view than radar sensors but have comparatively slow scanning repetition rate. Vision systems can quite accurately measure angles, but lack distance measurement accuracy when compared to radars and lidars. Ultrasonic sensors can be only used for very short distances to measure distance. (Eskandarian, 2012)

Göhring et al. (2011) presented a real-time algorithm enabling autonomous car to follow other cars. Algorithm combines the advantages of radar and lidar with a sensor fusion approach to provide precise data. Radar sensors provide reliable information on straight lines, but fail in curves due to restricted field of view. Lidar sensors cover large regions but do not provide precise speed information.

## 2.3 Control strategies

When designing steering controller, it is important to understand the dynamics of the system being controlled and to account for the forces acting on front wheels (Yih, 2004). Feedforward control is used to cancel out the system dynamics as well as the disturbances coming from tire self-aligning moment. Feedback control is used to minimize the steering angle error coming from model uncertainties and real nonlinearities. Yih (2004) studied steering-by-wire, which means replacing the mechanical linkage between the wheels and steering wheel by electric motor, and its implications for handling and safety. Steer-by-wire application could be easily tuned to control a vehicle autonomously.

Cascade control paradigm is particularly useful in control systems when there are significant time delays between the target value and the actual value (Åström et al., 1995). Cascade control means having two or more control loops to control one variable: outer loop, also called primary loop, for controlling the whole process and inner loop, also called secondary loop, for controlling small part of the process. Advantage with using an

inner loop is that it can react much faster to changes in control signal than outer loop, which translates to tighter control of the whole process. However, the acting time in the inner loop should be at least 5 times faster than in the outer loop.

Naranjo et al. (2005) designed a power-steering control architecture for automatic driving using fuzzy control and PID control theories. Control system was cascaded so that fuzzy controller governed the whole steering process by acquiring input data from the sensors (GPS) and generating target steering position. This target steering position was then transferred to the PID controller which was commanding the steering actuator. The purpose of the PID controller was to make sure that the steering position follows the target steering position. The fuzzy controller received input data at a 10 Hz sampling rate and PID controller performed control at 100 Hz rate which shows that the fuzzy controller itself is not enough to control the vehicle effectively.

Milanés et al. (2009) designed an electric power controller for steering wheel management for electric car. Steering controller was cascaded: outer loop consisted of a fuzzy logic controller and inner loop consisted of a PID controller. PID controller was successful in following the fuzzy controller with a small time delay. Authors also measured experimentally that it takes 8 seconds to turn a steering wheel from its leftmost to rightmost position which information was used in building the PID controller.

Al-Mayyahi et al. (2015) studied the performance of a Fractional Order PID (FOPID) for controlling autonomous differential drive vehicle to track a reference path. They used a Particle Swarm Optimization (PSO) algorithm to optimize the FOPID controller's parameters. Fractional order system improves from conventional PID by increasing the speed of response and decreasing the steady-state error and relative stability. Equation 1 presents the FOPID controller's action where u is the control signal, e is the error signal, $K_p$, $K_i$ and $K_d$ are proportional, integral and derivative gains respectively, D is the fractional differentiation operator, λ is the order of integrator and μ is the order of differentiator.

$$u(t) = K_p * e(t) + K_i * D^{-\lambda} * e(t) + K_d * D^{\mu} * e(t) \quad (1)$$

FOPID controller extends from the four control points of the classical PID to a range of control points of the quarter-plane which can be seen in Figure 1.

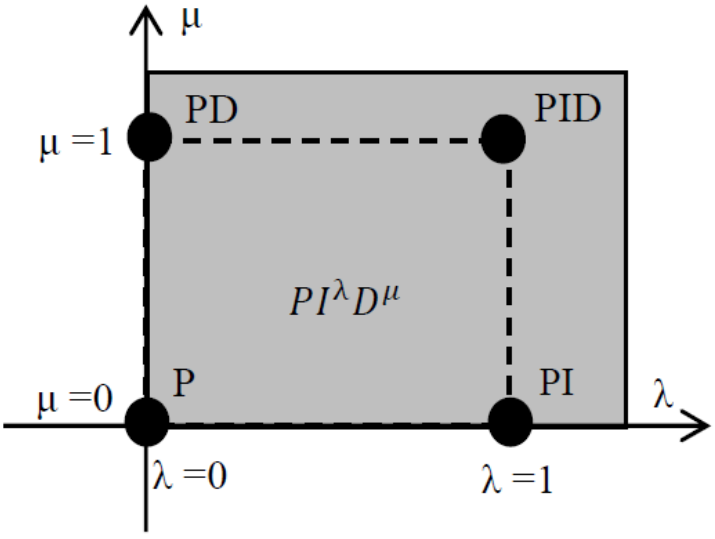


**Figure 1. Graphical illustration of the Fractional Order PID controller. (Al-Mayyahi et al., 2015)**

## 2.4 Lateral control

Lateral control refers to the steering of the vehicle and keeping it on leader vehicle's trajectory. Jansen (2016) distinguishes vehicle following into two main categories: direct vehicle following and vehicle path-following. Direct vehicle-following means that following vehicle steers itself according to its current relative position to the preceding vehicle. This method usually makes follower to cut corners. Vehicle path-following uses the path driven by the preceding vehicle as a reference for the follower's lateral controller.

Vehicle path-following has few advantages over direct vehicle-following. Vehicle's actual goal is to follow the path where as it is not guaranteed with direct vehicle-following. Also, it is easier to construct a feedforward control to improve tracking for vehicle path-following. On the other hand, vehicle path-following approach is a more complex method.

### 2.4.1 Path following

Vehicle path following is applied in two stages: first, the preceding vehicle's path is obtained and second, the controller drives the vehicle to follow the path (Jansen, 2016). Vehicle path following has been studied extensively in the literature.

Elbanhawi et al. (2015) proposed a practical approach for generating motion paths with continuous curvature for car-like vehicles. They addressed two key issues in robot motion planning: path continuity and maximum curvature constraint for non-holonomic robots. Proposed approach uses B-spline curves to generate motion path. Path continuity is achieved by utilizing a single path to present the trajectory. Maximum curvature is satisfied locally using smoothing algorithm if necessary.

Snider (2009) divided path tracking into three categories: geometric, kinematic and dynamic path tracking methods. He compared the performance of different path tracking methods using CarSim-software. Geometric path tracking was divided into Pure Pursuit and Stanley Method. Pure Pursuit consists of calculating the curvature of a circular arc that connects rear axle position to a target location on the path ahead of the vehicle. Equation 2 shows the Pure Pursuit control law where $L_{wb}$ is the length of the wheelbase, α is the angle between heading of the vehicle and the look ahead distance vector and $d_{lad}$ is the look ahead distance.

$$\delta(t) = \tan^{-1}\left(\frac{2*L_{wb}*\sin(\alpha(t))}{d_{lad}}\right) \quad (2)$$

With Pure Pursuit increasing the look ahead distance results in lower precision tracking and eventually stability whereas decreasing it results in higher precision tracking and eventually oscillation. The control law can be tuned by replacing the look ahead distance by the longitudinal velocity of the vehicle v and a gain parameter k. Tuned Pure Pursuit control law can be seen in equation 3. Usually the look ahead distance is saturated at chosen minimum and maximum values.

$$\delta(t) = \tan^{-1}\left(\frac{2*L_{wb}*\sin(\alpha(t))}{k*v(t)}\right) \quad (3)$$

Stanley Method consists of calculating the cross-track error to the desired path measured from the front axle to the nearest path point and heading error. Stanley Method control

law can be seen in equation 4 where $\theta_e$ is the heading error of the vehicle, k is a gain parameter, $e_{fa}$ is cross-track error and $v_f$ is the longitudinal velocity of the front wheels.

$$\delta(t) = \theta_e(t) + \tan^{-1}\left(\frac{k*e_{fa}(t)}{v_f(t)}\right) \quad (4)$$

Stanley Method works better for higher speed driving than Pure Pursuit but has some problems with a discontinuity of a path. Kinematic model path tracking controller showed good results when driving with low velocities. Two dynamic path tracking methods were investigated: optimal controller with feedforward and optimal preview controller. The former showed good tracking performance in smooth high-speed driving and urban driving with lower speeds. The latter performed well in highway driving with relatively constant velocity.

Hoffman et al. (2007) presented a nonlinear control law to track a trajectory. The proposed control law was able to track a predefined trajectory in varying off-road settings with a typical rms cross-track error under 0,1 m. Equation 5 shows the studied control law where two first terms are basically the same as in the Stanley Method control law with the exceptions of added $k_{soft}$ gain parameter to tune the response of the control with slow speeds and $\Psi_{ss}$ which is the controller yaw setpoint. Third term tries to actively damp the yaw rate of the vehicle where $k_{d,yaw}$ is a gain parameter, $r_{meas}$ is the measured yaw rate and $r_{traj}$ is the yaw rate for the trajectory. The last term in the control law was added to account for time delay and overshoot when commanding a steering servo where $k_{d,steer}$ is parameter gain and $\delta_{meas}(i)$ and $\delta_{meas}(i+1)$ are discrete time measurement of the steering angles where i stands for measurement one control period earlier. The output steering command was saturated at $\pm\delta_{max}$.

$$\delta(t) = \left(\Psi(t) - \Psi_{ss}(t)\right) + \tan^{-1}\left(\frac{k*e(t)}{k_{soft}+v(t)}\right) + k_{d,yaw} * \left(r_{meas}(t) - r_{traj}(t)\right) + k_{d,steer} * \left(\delta_{meas}(i) - \delta_{meas}(i+1)\right) \quad (5)$$

$\Psi_{ss}$ can be seen in equation 6 where m is the vehicle mass, $C_y$ is the tire stiffness of the tire pairs, a and b are the distance from the center of gravity to the front and rear wheels, respectively.

$$\Psi_{ss}(t) = \frac{m*v(t)*r_{traj}(t)}{C_y*\left(1+\frac{a}{b}\right)} \quad (6)$$

The proposed control law demonstrated its success by completing the DARPA Grand Challenge 2005 in fastest time on desert and mountainous terrain.

Schnelle et al. (2017) developed a directional control driver model with desired path tracking. Model included a compensatory transfer function, an anticipatory feedforward transfer function and a method to determine the driver's desired path. The proposed driver model parameters were obtained from human subjects performing test tracks in driving simulator. Control law for steering can be seen in equation 7.

$$\delta(t) = (Y_d - Y_L)(t)\frac{G_h}{1+T_h*s} + K_{ff} * \dot{\psi}_d(t) \quad (7)$$

First term expresses the driver model which consists of $Y_d - Y_L$, which is the error between the desired path and the vehicle at look ahead distance, $l_d$, ahead, $G_h$, which is the driver's steering proportional gain and $T_h$, which is driver's lag time constant. Last term reflects human driver's ability to plan path ahead and it consists of $K_{ff}$, which is the driver's feedforward gain, and $\psi_d$, which is the desired yaw rate at look ahead distance ahead. Driver's preview time $T_p$ was also a parameter that was included in the model, because it affected $l_d = T_p$ * constant velocity. The proposed combined driver model was able to effectively predict individual driver's steering wheel angles after model parameters had been identified for each driver individually. Model could capture the differences between drivers for each maneuver which was seen in different parameter combinations.

Zakaria et al. (2013) proposed a stable trajectory tracking control which uses future prediction control. Control system supposed that there is a predefined trajectory path, which was defined in global coordinate system. Path consisted of x- and y-coordinates and vehicle heading direction. Study used steering angle limits which was $-45° \leq \delta \leq 45°$. They also calculated the comfort level using various controller parameter values using ISO 2631-1 standard as a reference. A spike detection algorithm was implemented to reduce high changes in steering angle and handle noisy data. The algorithm acted when the magnitude of derivative of steering angle reached certain value. It was able to reduce errors caused by spikes in trajectory path.

Attia et al. (2014) combined longitudinal and lateral control in their study. Lateral controller was based on nonlinear model predictive control which tries to predict the future states of a dynamic system on a fixed finite time horizon. Lateral position and heading angle errors were admissible in the simulations.

Tan & Huang (2014) explored how bus drivers steer to perform different maneuvers and developed an automatic steering controller based on those findings. They found that, contrary to some conventional driver models, drivers do not plan a trajectory to be followed but instead they use a target and control scheme. That is, drivers identify the angle error between the vehicle's heading and where they would like the vehicle to go and adjust steering accordingly. Authors identified a relationship between the steering rate $\delta$ and the target angle error $\theta_e$ and formed a generic simple control law which can be seen in equation 8.

$$\dot{\delta}(t) = k * \theta_e(t) \tag{8}$$

where $k = k_i$ for $\varepsilon_i \leq |\theta_e| < \varepsilon_{i+1}$ where typically $\varepsilon_0 = 0$ and $i = 0 \ldots 2$ or 3. Gain k was approximately proportional to speed over look ahead distance (v/d) and it increased when target angle error increased or vehicle got close to obstacle. Proportional factor of k was approximately constant which varied from driver to driver. They derived a control law for lane-keeping control which can be seen in equations 9 and 10 where d is look ahead distance, $\rho_{road}$ is road curvature, $y_r$ is vehicle lateral deviation from the center of the lane, v is velocity, $\omega_v$ is yaw rate and $\theta_r$ is vehicle heading angle.

$$\dot{\delta} = k\left(\frac{d}{2}\rho_{road} - \left(\frac{1}{d}y_r + \frac{d}{2v}\omega_v + \theta_r\right)\right) \tag{9}$$

$$\delta = \frac{-k}{v}\left(y_r + \left(\frac{v/d}{s}\right)y_r + \frac{d}{2}\theta_r\right) \tag{10}$$

Authors state that the first control law is usable for an autonomous vehicle that does not need to plan any trajectory to follow. The second and third control laws are usable for trajectory tracking.

Park et al. (2015) developed a steering controller for autonomous vehicle for path tracking problem. Steering controller was based on Pure Pursuit method and was improved by proportional integral controller that tried to reduce the lateral error. Developed control law is seen in equation 11 where first term is the Pure Pursuit part, $e_y$ is the lateral error, P is the proportional gain and Q is the integral gain which is a function of the road curvature κ.

$$\delta(t) = \tan^{-1}\left(\frac{2*L_{wb}*\sin(\alpha(t))}{d_{lad}}\right) + \left(P * e_y(t) + Q\left(\kappa(t)\right) * \int e_y\, dt\right) \quad (11)$$

Maximum lateral error in lane following maneuver was 0,3 m even with high velocities. However, control system encountered problems during double lane change maneuvers.

Hellström & Ringdahl (2006) proposed a path tracking algorithm for autonomous vehicles that uses recorded steering commands to overcome cutting corners phenomenon. Controller used recorded steering commands and heading values and compared those to actual position and heading information achieved by GPS to steer the vehicle accordingly.

Yin et al. (2015) integrated motion planning and model predictive control (MPC) system for autonomous electric vehicle. The control system operated each wheel independently by applying torque and controlled steering to follow the planned trajectory. MPC has the property of considering constraints in computation of the optimal solution, which made it preferred over other control methods. The performance of the control system was validated in CarSim. Proposed planner algorithm and controller achieved requirements of autonomous driving in normal scenarios.

Lam & Katupitiya (2013) designed a control system for a platoon of autonomous buses. Proposed control system consisted of a lateral controller, speed planner and longitudinal controller. Lateral controller was designed to drive the error angle between vehicle's and path's predicted future point and heading down to zero, which can be seen in Figure 2 as angle θ, by using PD controller. They mentioned that increasing the vehicle projection length increases the radius of the actual path and decreasing the path projection length increases the frequency of response.

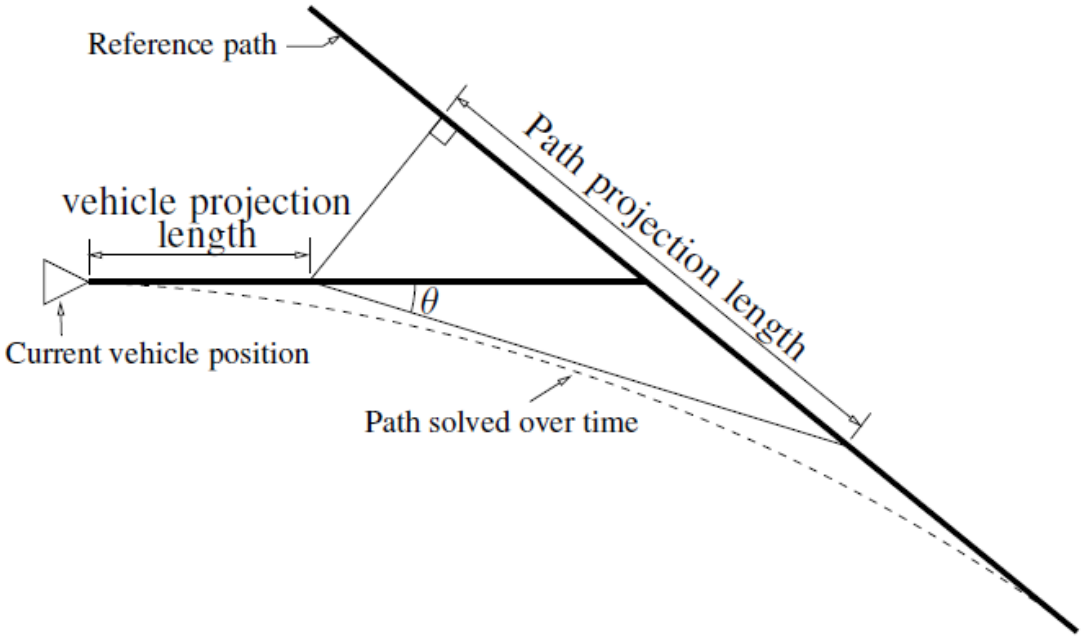


**Figure 2. Geometrical illustration of the lateral controller designed by Lam & Katupitiya. (2013)**

The lateral controller performed well except around gradient discontinuities in the reference path.

Petrov (2009) designed a nonlinear adaptive controller for controlling following vehicle. Controller used inputs from the leader as what could be sensed by the follower i.e. there was no inter-vehicle communication. Controller was designed for constant leader linear and angular velocities and it performed well in simulations.

Kim et al. (2013) proposed a sensor-based motion planning method of robotic vehicle control for path tracking. Method was based on geometric relationships using the Pure Pursuit method. It was effective in reaching static predefined waypoints and avoiding obstacles using limited field of view sensors. However, the proposed method required a set of waypoints defined at a higher level.

Smooth path and speed planning for an automated public transport vehicle was presented in study made by Villagra et al. (2012). Efficiency and comfort are key issues in public transportation. The proposed method considered bounds on lateral and longitudinal accelerations and longitudinal jerk to ensure good comfort level. Method showed better combinations of trip time and comfort than human drivers on two test tracks. Comfort was quantified by computing the whole acceleration affecting passengers.

Matko et al. (2008) proposed a control algorithm for vehicle platoon where controlled vehicle used only on-board sensors. Control algorithm estimated the path of the leading vehicle in a parametric polynomial form after which follower tried to follow that path. Both feedback and feedforward control were used to track the reference path. Control algorithm was designed for one-axle vehicles so it is not directly applicable to two-axle vehicles.

Wirtanen (2017) studied the performance of three different algorithms to control the movements of a bus following another bus: aiming (AIM), line of sight (LOS) and Polynomial algorithms. AIM and LOS algorithms are presented in the next chapter because they are based on direct following method.

Polynomial algorithm showed good tracking results during slow maneuvering. It operated on a relatively small number of inputs: aiming angle, reflector angle and distance between buses. Algorithm was based on path following i.e. it recorded leader vehicle's position into trajectory matrix, fitted a polynomial into the data and tried to follow that trajectory. Author recognizes that even though algorithm performed very well in simulations, it might have some problems with self-location and noise handling. Algorithm also started to oscillate when the simulation time was extended, probably because of accumulated error during the simulation. Equation 12 shows the Polynomial algorithm steering law where $\alpha_{slope}$ is the vehicle heading error, e is the lateral error, $v_f$ is the velocity of the front wheels and $K_p$, $K_i$ and $K_d$ are proportional, integral and derivative gains, respectively. Polynomial algorithm control law resembles Stanley Method control law except that here the lateral error is modified by PID control.

$$\delta(t) = \alpha_{slope}(t) + K_p * \tan^{-1}\left(\frac{e(t)}{v_f(t)}\right) + K_i * \int \tan^{-1}\left(\frac{e(t)}{v_f(t)}\right) dt + K_d \frac{d}{dt} \tan^{-1}\left(\frac{e(t)}{v_f(t)}\right) \quad (12)$$

AIM and LOS algorithms were based on target following method, which resulted them to suffer from phase challenges. Polynomial algorithm performed the best but had fundamental problems with error accumulation.

Soltesz (2008) and his team built a trajectory tracking software and implemented it on test vehicle to compete in 2007 DARPA Urban Challenge. Proposed tracking software was a solution to track a specified trajectory while following a reference velocity profile.

Zakaria et al. (2012) proposed a steering wheel control and lateral control for autonomous vehicle using future prediction. Control law consisted of heading error and lateral error with gain parameter and velocity. They also studied the comfort level of the proposed control law with various gain parameter values by calculating the total acceleration and comparing it to comfort level based on ISO 2631-1 standard (Figure 3). They noticed that by increasing the gain from 0 to 1, increased accuracy and lateral acceleration which resulted to decreased comfort level.

| Overall Acceleration | Consequence |
|---|---|
| $a_w < 0.315$ | Comfortable |
| $0.315 < a_w < 0.63$ | A little uncomfortable |
| $0.5 < a_w < 1$ | Fairly uncomfortable |
| $0.8 < a_w < 1.6$ | Uncomfortable |
| $1.25 < a_w < 2.5$ | Very Uncomfortable |
| $a_w > 2.5$ | Extremely uncomfortable |

**Figure 3. Comfort level based on ISO 2631-1 standard. (Zakaria, 2012)**

### 2.4.2 Direct following

Feng et al. (2013) studied guidance laws for pursuer convoy in three-dimensional case. In two dimensions, the three guidance laws velocity pursuit, deviated pursuit and proportional navigation can be composed into one generic equation (equation 13) where θ is the heading angle, σ is the angle of the line of sight, M is navigation constant ($M \geq 1$) and α is the deviation angle.

$$\theta(t) = M * \sigma(t) + \alpha \tag{13}$$

Guidance laws are specified by following constraints:

- Equation 13 represents velocity pursuit if $M = 1$ and $\alpha = 0$.
- Equation 13 represents deviated pursuit if $M = 1$ and $\alpha \neq 0$.
- Equation 13 represents proportional navigation if $M > 1$ and $\alpha = 0$.

Belkhouche & Belkhouche (2005, August) studied guidance law strategies on controlling a robotic convoy. Guidance laws implemented were velocity pursuit, deviated pursuit and proportional navigation. They were originally designed for missile guidance. Velocity pursuit means forcing the velocity vector of the follower to lie on the line of sight joining the follower and its target. Deviated pursuit implements a non-zero angle between the velocity vector of the follower and line of sight. In proportional navigation, the angular velocity of the follower is proportional to the rate of turn of the line of sight angle. In the study follower robot knew linear and angular velocities of its preceding robot. Studied robots had one axle only.

Belkhouche et al. (2005, November) investigated robot navigation towards a moving object with unknown maneuvers using velocity pursuit and deviated pursuit guidance laws. Studied robot had one axle and its angular velocity was equal to the line of sight angle rate, where line of sight angle was between robots heading and the goal. Velocity pursuit guidance law tries to force the robot's velocity vector to the same direction as the target's velocity vector is. In the case of one-axle robots it means that robot tries to turn its orientation angle to the target's orientation angle. Deviated pursuit guidance law implements a non-zero deviation angle between the line of sight and velocity vector. It means that robot's velocity vector is deviated from the line of sight by a constant angle. Velocity pursuit is actually a special case of deviated pursuit where the deviation angle is zero. This study was done on one-axle vehicle, so it can't be applied directly to two-axle vehicles. The studied guidance laws are meant to reach a target, so they do not necessarily follow target's trajectory very well.

Pham et al. (2004) studied the performance of a unified nonlinear controller for a platoon consisting of two car-like vehicles. Proposed controller used a focus point ahead on the direction of the follower vehicle. Special in this study was that the proposed control law was designed to operate both forward and backward motions of the platoon.

AIM algorithm (Wirtanen, 2017) operated on a small number of inputs: aiming angle and distance between buses. It showed shortcutting behavior and did not adjust to different driving environments. Algorithm used target following method. Command steering value was adjusted by PID-controller to decrease phase error and increase steering angle. Equation 14 shows the AIM algorithm steering law.

$$\delta(t) = K_p(t) * \alpha_{aim}(t) + K_i(t) * \int \alpha_{aim}(t)\, dt + K_d(t) \frac{d}{dt} \alpha_{aim}(t) \quad (14)$$

where PID gains are formed from polynomial function (equation 15) where A, B, C and x were defined separately for each PID gain term:

$$K_{p,i,d}(t) = A((1 + |\alpha_{aim}(t)|)^x - 1) + B|\alpha_{aim}(t)| + C \quad (15)$$

LOS algorithm (Wirtanen, 2017) showed stable results with high velocities but had limitations with large turning angles. However, it required information from the leader vehicle: its steering angle and velocity in addition to aiming angle, reflector angle and distance between buses. Transfer functions were implemented into the algorithm to increase its performance which showed substantial improvements. Algorithm used target following method. Equation 16 shows the LOS algorithm steering law where $K_p$, $K_i$ and $K_d$ are proportional, integral and derivative gains, respectively, $\omega_{los}$ is turning rate of the line of sight, $L_{wb}$ is length of the wheelbase and $v_f$ is the current velocity of the front wheels.

$$\delta(t) = \sin^{-1}\left(\left(K_p * \omega_{los}(t) + K_i * \int \omega_{los}(t)\, dt + K_d * \frac{d}{dt} \omega_{los}(t)\right) \frac{L_{wb}}{v_{f(t)}}\right) \quad (16)$$

Travis & Bevly (2008) presented trajectory duplication methods for controlling of following vehicle to follow leader vehicle's path of travel that is out of sight of following vehicle. The following vehicle received leader vehicle's relative position and relative angles through GPS. The proposed Trailer Method and Extended Hitch Trailer Method are shown in Figure 4. Extended Hitch Trailer Method was originally presented by Ng et al. (2005) as a virtual trailer link model.

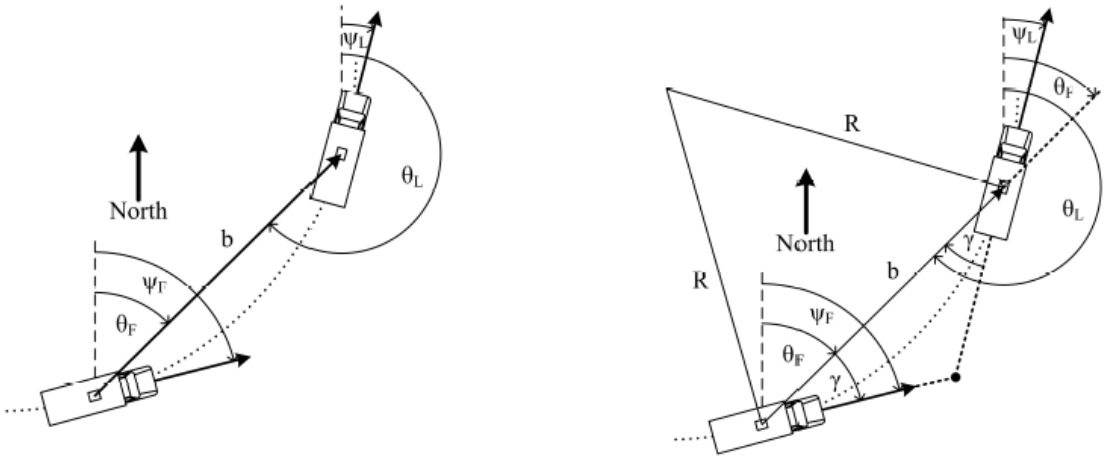


**Figure 4. Geometrical illustration of the Trailer Method and the Extended Hitch Trailer Method. (Travis & Bevly, 2008)**

Trailer Method's target yaw angle was calculated as in equation 17.

$$\psi_F(t) = \theta_F(t) \quad (17)$$

Extended Hitch Trailer Method's target yaw angle was calculated as in equation 18.

$$\psi_F(t) = \theta_F(t) + \gamma(t) \quad (18)$$

The proposed control law for steering included PD and feedforward terms (equation 19). Here $K_p$ and $K_d$ are proportional and derivative gains respectively, $\psi_F - \psi$ is the yaw angle error, $L_{wb}$ is the length of the wheelbase, v is the velocity of the vehicle and $K_{us}$ is vehicle's understeering gradient.

$$\delta(t) = K_p(\psi_F(t) - \psi(t)) + K_d \frac{d}{dt}(\psi_F(t) - \psi(t)) + \left(\frac{L_{wb}}{v(t)} + K_{us} * v(t)\right)\frac{d}{dt}\psi_F(t) \quad (19)$$

From the presented methods, Extended Hitch Trailer Method outperforms the Trailer Method. Trailer Method has the tendency to cut corners and following vehicle's turning radius is smaller than the lead vehicle's which means that larger distances between vehicles increase the tracking error. However, for short distances, natural lags could overcome the tendency to cut corners. Extended Hitch Trailer Method shows good performance when following constant curvature paths. However, it has the tendency to prematurely equalize the turning radius. This action shows when transitioning from straight to curved trajectory the follower turns off the path to the opposite direction than the leader and when transitioning from curved to straight trajectory the follower cuts off the remaining path.

Wit (2000) designed vector pursuit path tracking methods based on screw theory for autonomous ground vehicles. He designed two different methods where the first one did not consider the nonholonomic constraints of the vehicle and the second one considered. Vector pursuit is a geometric path-tracking method that uses the theory of screws. It uses look ahead distance to define a target point and geometry to determine the desired motion of the vehicle. Vector pursuit uses both the location and orientation of the look ahead point to drive the vehicle to the desired state. Method has the same problem with all the other methods that use a look ahead point: vehicle tends to cut corners of a path. To overcome this situation, look ahead distance can be decreased but only to a certain point, otherwise it can lead to instability.

Zhang et al. (2016) designed a path following control system for autonomous agricultural vehicle following another one. Control system obtained information about leading vehicle through camera vision system. Control law designed used longitudinal and heading tracking errors as inputs. The proposed system was able to satisfactorily control the movements of the follower during standard agricultural operations. In addition to direct following, the study also demonstrated parallel tracking of leader movements.

Mariottini et al. (2008) studied vision-based localization and control of a leader-follower formation of one-axle mobile robots. System consisted of a follower, which measured the relative angle between its heading and line of sight through a panoramic camera, and a leader, which measured follower's relative angles to it and controlled the follower i.e. the control system was centralized to the leader.

## 2.5 Longitudinal control

Longitudinal control refers to the acceleration and deceleration of a vehicle. For vehicle following, the role of longitudinal control is to keep proper distance to preceding vehicle and avoid collisions (Khodayari, 2010).

Longitudinal control of autonomous vehicle can be implemented by using two different methods: constant and variable spacing. Constant spacing method implements very short inter-vehicular distances but it requires V2V communication. For variable spacing V2V communication is not necessary but distance between vehicles can be very large, especially with high velocities. (Ali et al., 2013, July)

### 2.5.1 Constant spacing

Constant spacing method implements a fixed distance between vehicles. With constant spacing, distance between vehicles can be very small but it requires inter-vehicle communication with the preceding vehicle. (Ali et al., 2013, July)

### 2.5.2 Variable spacing

Variable spacing means having a varying inter-vehicular distance that can change according to velocity, dynamics or road condition. For variable spacing V2V communication is not necessary. However, distance between vehicles can be very large, especially with high velocities. (Ali et al., 2013, July)
Ali et al. (2013, July) minimized the inter-vehicle distance of the time headway policy for platoon control on highways. Variable spacing can be implemented by using two different methods: constant or variable time headway. Constant time headway (CTH) policy is the simplest and most common among variable spacing policies and it can be seen in equation 20 where e is the spacing error, d is the current distance between vehicles, $d_0$ is the minimum target distance, h is the time headway and v is the velocity of the vehicle. Variable time headway (VTH) can vary linearly with velocity, relative velocity, vehicle dynamics or road condition.

$$e(t) = d(t) - d_0 - h * v(t) \tag{20}$$

Ali et al. (2013, July) proposed a modification to CTH policy to decrease the distance between vehicles which is seen in equation 21 where V is a same velocity value shared between all the vehicles in the platoon at the same sampling time (for ordinary CTH policy V = 0). The proposed modification makes the inter-vehicle distance become equal to constant spacing policy at equilibrium ($d = d_0$).

$$e(t) = d(t) - d_0 - h * (v(t) - V) \tag{21}$$

The proposed policy is string stable, it decreases inter-vehicle distances when compared to CTH policy and it does not require as frequent communication between vehicles as constant spacing method. However, if connection between vehicles is lost, it can switch to fully autonomous mode by forcing V = 0. Authors also mention that for system to be stable the time headway h in presence of lags $\tau$ should be:

$$h \geq 2\tau \tag{22}$$

where $\tau$ is the sum of all the lags in the system.

Ali et al. (2013, October) generalized the results they obtained in previous work (Ali et al., 2013, July) to be applicable in urban environment by using decoupled longitudinal and lateral control.

Adaptive Cruise Control (ACC) system is an enhancement to the conventional Cruise Control (CC), which regulates only vehicle's speed. ACC maintains a desired cruise speed and following gap to the preceding vehicle. Desired time headway must be at least 1,0 s according to standards and it can be as high as 3,6 s for commercial road vehicles equipped with ACC. (Eskandarian, 2012)

ACC uses CTH policy to determine desired velocity. However, if the vehicle reaches cruise velocity, because the preceding vehicle is so far away, ACC works like an ordinary CC.

# 3 Methods

## *3.1 Simulation model overview*

Simulations were conducted in MATLAB Simulink environment. Simscape Multibody First Generation blocks were used to build the simulation model, which allows reliable modelling of the dynamics of buses. Figure 5 represents the overall architecture of the simulation model. It consists of a simulation input block that determines movements of the leader bus. Vehicle models block includes both buses, road and their interaction. Lateral control block includes steering control laws and steering controller. Longitudinal control block includes target distance algorithm and distance controller.

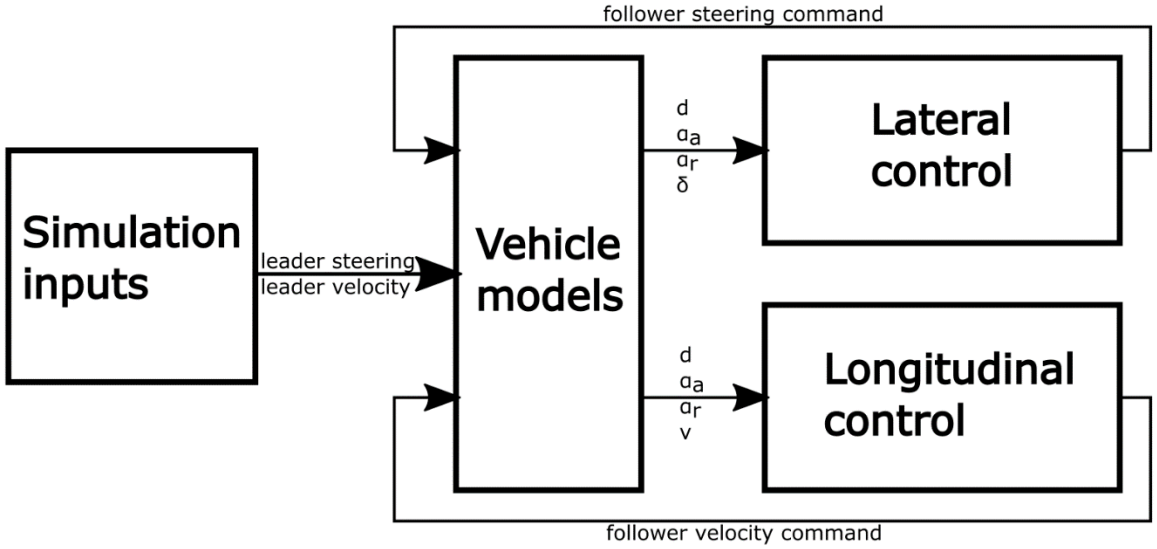


**Figure 5. The overall architecture of the simulation model.**

Figure 6 shows the geometry of the bus. Parameters for simulation model are gathered from Linkker 12+ datasheet, shown in Table 1.

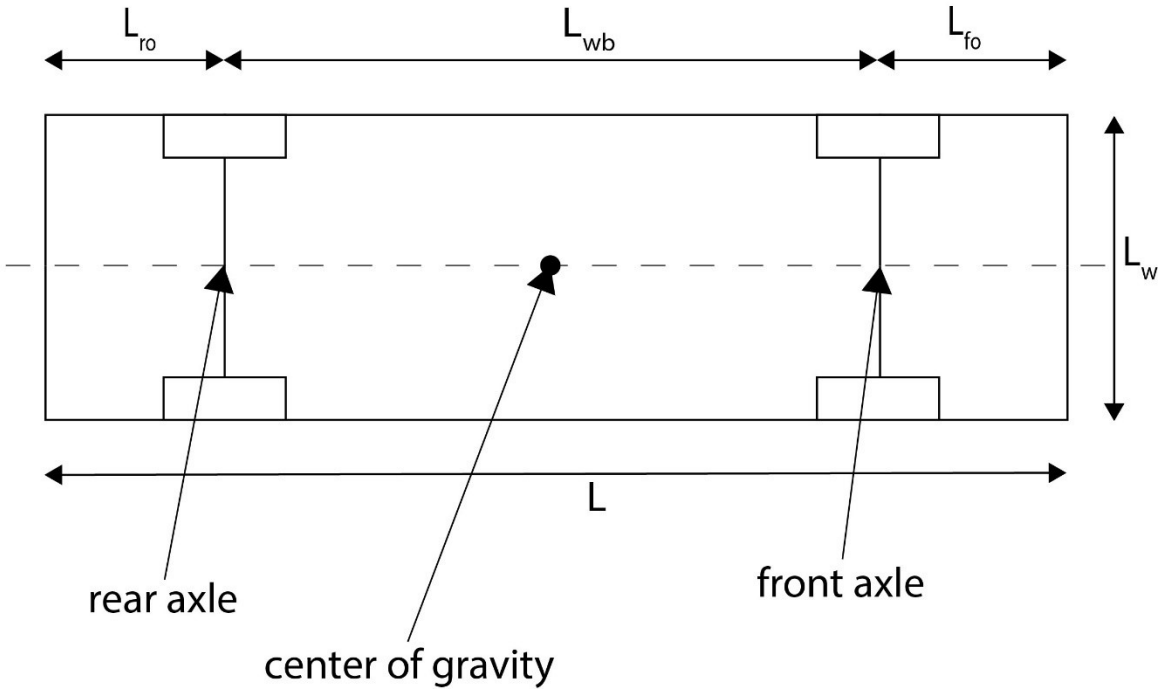


**Figure 6. Geometry of the bus, where L is the length of the bus, $L_w$ is the width of the bus, $L_{ro}$ is the length of the rear overhang, $L_{wb}$ is the length of the wheelbase and $L_{fo}$ is the length of the front overhang.**

**Table 1. Properties of Linkker 12+ bus. (Linkker, 2017)**

| | |
|---|---|
| length | 12818 mm |
| width | 2550 mm |
| wheelbase | 6750 mm |
| front overhang | 2754 mm |
| rear overhang | 3314 mm |
| empty weight | 10500 kg |
| payload | 5500 kg |
| tires | 285/70 R 19,5 |
| max power | 180 kW |
| max torque at rear wheels | 7824 Nm |

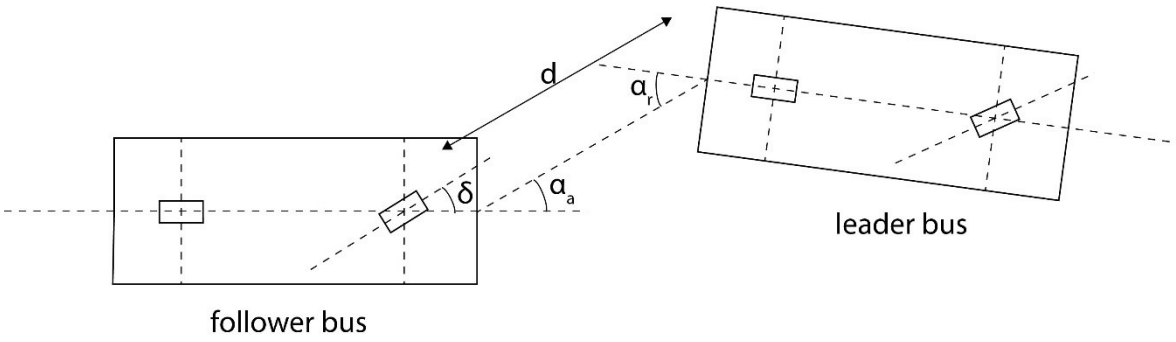


**Figure 7. Geometry of the bus platoon, where d is the distance between the buses (from center of the follower's front to center of the leader's rear), $\alpha_a$ is the aiming angle (positive direction shown), $\alpha_r$ is the reflector angle (positive direction shown) and $\delta$ is the steering angle of the follower bus (positive direction shown).**

Geometry of the bus platoon and important variables are shown in Figure 7. Bicycle models of the buses were used in the simulation model. Simulation model did not include the model for friction. Therefore, cornering stiffness of the tires was not modelled. Tires were also modelled to perfectly translate rotational movements into translational movements. This simplification is valid to represent a good tire-road-interaction. It obviously does not represent the case in rainy weather or when there is snow or ice present.

Buses have identical performance characteristics. Therefore, it is safe to assume that they perform similarly with given weather conditions. For instance, if there is snow and ice present, the performance of both buses will be decreased similarly. When assuming that buses are driving almost the same path, this assumption holds true. The only special case would be when the weather conditions vary longitudinally for instance leader bus could be on pavement and follower on ice momentarily. In this special case, the performance of the buses could vary. However, if this kind of weather would be present, one could assume that the professional bus driver driving the leader bus would take it into account and drive carefully and smoothly.

Buses could be connected either wirelessly or by a mechanical link. Mechanical link could be either rigid or flexible i.e. it could change its length. Mechanical link, whether it be flexible or not, poses physical constraints to the bus platoon: the link must not deviate more than 90 ° from position where the buses are lined up, otherwise it will hit the leader or the follower bus. In practice, the constraint would be probably tighter. Figure 9 presents a tight turn performed by the follower bus. The arrow in red represents the ultimate deviation direction without mechanical link hitting the follower bus. However, the arrow in blue shows where the link should actually point in order to buses be connected by it assuming buses are driving on circles whose center points coincide. Therefore, it is not possible to use a mechanical link between the buses if buses are capable of performing as tight turns as shown in the Figure 8.

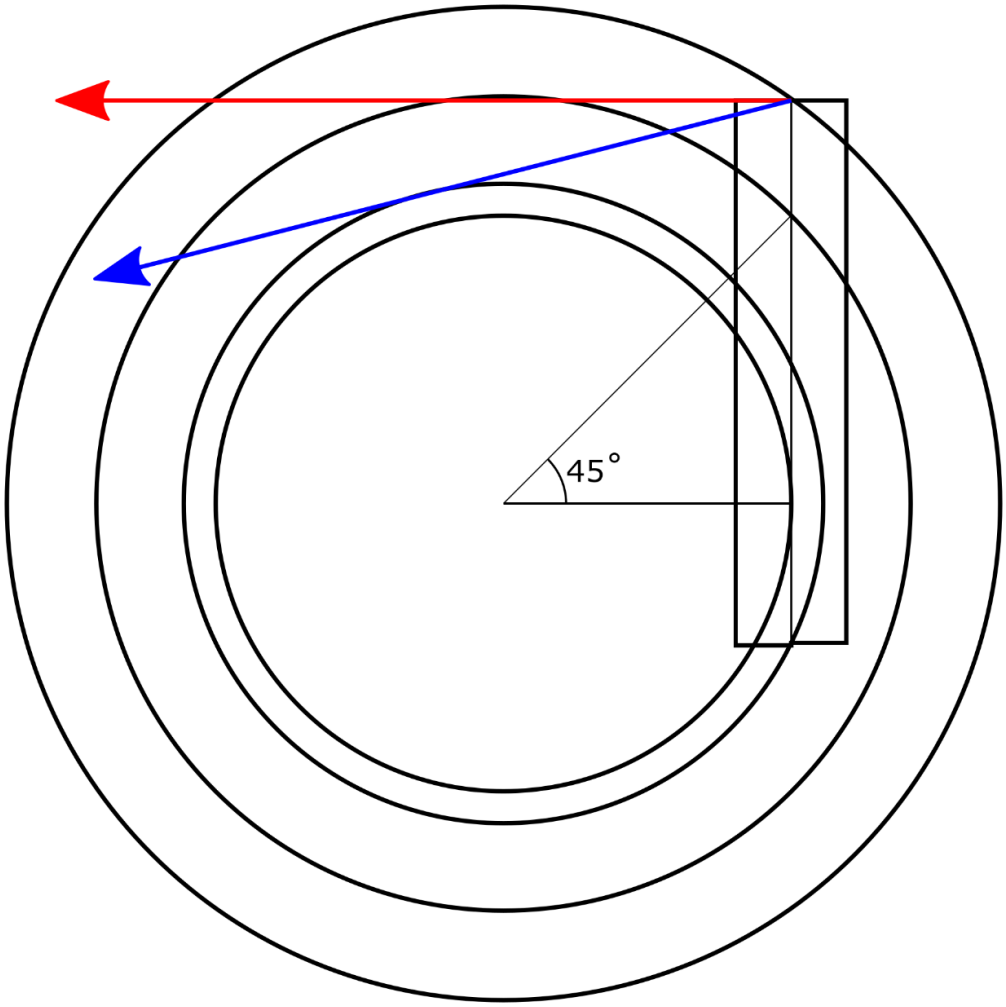


**Figure 8. Follower bus performing a tight turn (45 ° steering angle) where red arrow indicates the farthest direction where physical link could point and blue arrow indicates where it should be able to point at least.**

Distance between the buses could be measured through radar and lidar using sensor fusion techniques. This method gathers the advantages of both sensors together: the speed of radar signals and the measuring range of lidar. Lidar can measure up to 360 ° so it would not cause any physical constraints if it would be mounted on top on follower buses front. Radar can only measure in small range but it could benefit control system when driving on relatively straight roads with high speeds.

Aiming angle could be measured directly by lidar. Lidar could be also used to measure $d_r$ (distance to the right rear corner of leader bus) to calculate the reflector angle as seen in Figure 9.

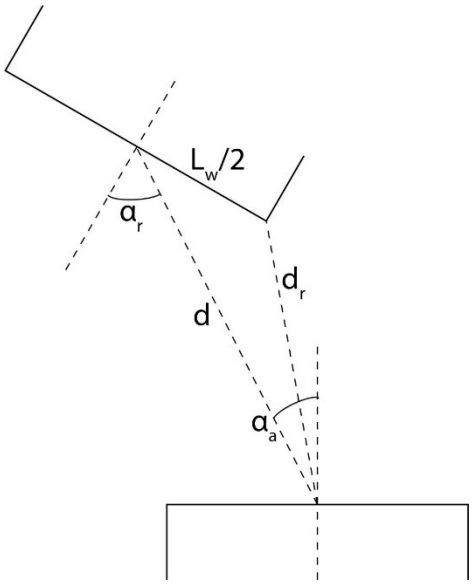


**Figure 9. Calculation of the reflector angle, where $d_r$ is the distance from the follower bus to the right rear corner of the leader bus.**

The reflector angle could then be calculated by using law of cosines:

$$\alpha_r = 90\,° - \cos^{-1}\left(\frac{d^2+\left(\frac{L_w}{2}\right)^2-{d_r}^2}{d*L_w}\right) \tag{23}$$

## *3.2 Longitudinal controller*

As the purpose of this study is to test the performance of a control system that has no information coming from the leader bus, the longitudinal controller implemented must be based on variable spacing policy. Constant time headway policy has proven to be an effective method to drive the velocity of a vehicle in situations similar to this. It is also a method that is implemented in commercial applications successfully. However, commercial applications use very high values for time headway term, which is not wanted when operating a bus platoon. The distance between buses should be large enough to avoid collisions in all situations but small enough to indicate that buses are driving as a platoon, which would further avoid other traffic to move between the buses.

CTH policy requires two parameters to be defined: $d_0$ which is the minimum target distance and h which is the time headway. Minimum target distance is related to the geometry of the vehicles. Time headway is related to the lags present in the system. These lags come from distance measurement and velocity control.

When considering two commercially available sensors (Table 2 and Table 3) a lag of distance measurement of 100 ms should be achievable.

**Table 2. Properties of Continental Short Range Radar. (Continental, 2016)**

| | | |
|---|---|---|
| distance | range: 1-50 m | accuracy: 0,2 m |
| speed | range: ±146 km/h | accuracy: 0,2 km/h |
| cycle time | >= 33 ms (typical 38 ms) | |

**Table 3. Properties of Götting Laser Scanner HG 43600-A. (Götting, 2014)**

| | | |
|---|---|---|
| distance | range: 1-30 m | accuracy: ±5 mm |
| angle | range: 360° | resolution: up to 65536 increments/360° |
| measuring rate | 6-18 1/s | |

Lags coming from the velocity controller come from actuator and sensor. Linkker 12+ electric bus uses permanent magnet motor for actuating the velocity of the bus (Linkker, 2017). The lag of electric motor composes of electrical and mechanical time constant. If treated as one lag, electric motors in general should be capable of achieving a lag of 50 ms. (Wu, 2012) Rotational velocity of rear axle in vehicles is usually measured by an encoder. The raw encoder data is usually filtered out to reduce noise. This filtering introduces the lag that comes from the encoder. A lag of 10 ms for filter is chosen for the simulation model.

The magnitude of lags present in the system indicates that it is not reasonable to use cascaded control i.e. two control loops. Therefore, it is better to use one controller for controlling the distance. PID-controller is chosen, as it is easy to implement and tune it. Also, a feedforward control is added to better tune the response of the controller. When calculating above mentioned lags together, the sum of all the lags present in the longitudinal control system becomes:

$$\tau = 160\ ms$$

These lags are rough estimates of what could be possible to achieve. Therefore, it is better to oversize the time headway term which can be calculated using equation 22. When using parameter values $d_0$ = 1 m and h = 0,4 s, for a bus driving between 0 and 80 km/h the distance varies between 1 and 9,89 m.

However, buses need to be able to perform tight turns. Tight turns must increase the minimum target distance, otherwise buses would collide. On the other hand, tight turns do not affect the time headway, because it is not a function of geometry. If we suppose buses have steering angle limits of $-45° \leq \delta \leq 45°$, which was also used in Zakaria et al. (2013) study, the geometry of the platoon can be calculated assuming buses are driving on circles whose center points coincide, shown in Figure 10.

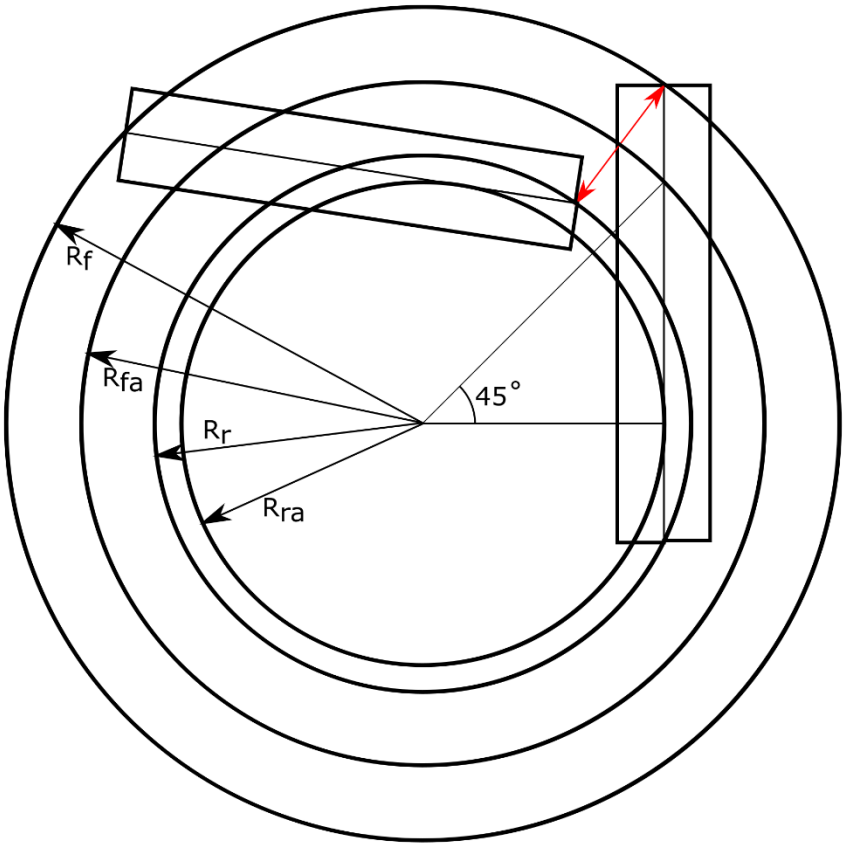


**Figure 10. Geometry of the bus platoon during a tight turn. Red arrow indicates the absolute minimum for the distance.**

When driving with maximum steering angle δ = 45 ° the following turning radius for different parts of the bus are achieved:

$$R_{ra} = \frac{L_{wb}}{\tan\delta} = 6{,}75\ m$$

$$R_{fa} = \sqrt{{R_{ra}}^2 + {L_{wb}}^2} \approx 9{,}55\ m$$

$$R_f = \sqrt{{R_{ra}}^2 + \left(L_{wb} + L_{fo}\right)^2} \approx 11{,}66\ m$$

$$R_r = \sqrt{{R_{ra}}^2 + {L_{ro}}^2} \approx 7{,}52\ m$$

where $R_f$, $R_{fa}$, $R_{ra}$ and $R_r$ are the turning radius of the front, the front axle, the rear axle and the rear, respectively. Because the distance between the buses is measured from the front of the follower bus to the rear of the leader bus, it creates geometrical constraint during tight turning. The absolute minimum for the distance, if driving minimum radius turns and with the assumption that buses are turning around the same center point with same turning radius, must be:

$$R_f - R_r \approx 4{,}14\ m$$

If the distance reaches this value during 45 ° steering angle turn, the longitudinal controller does not know what direction to drive. That is, because from that point the distance grows in both directions. Therefore, this distance must never be reached during tight turning.

There exists even more extreme situation when the follower drives with maximum steering angle and the leader turns its steering angle to the opposite maximum i.e. for instance $\delta_{leader}$ = -45 ° and $\delta_{follower}$ = 45 ° as seen in Figure 11.

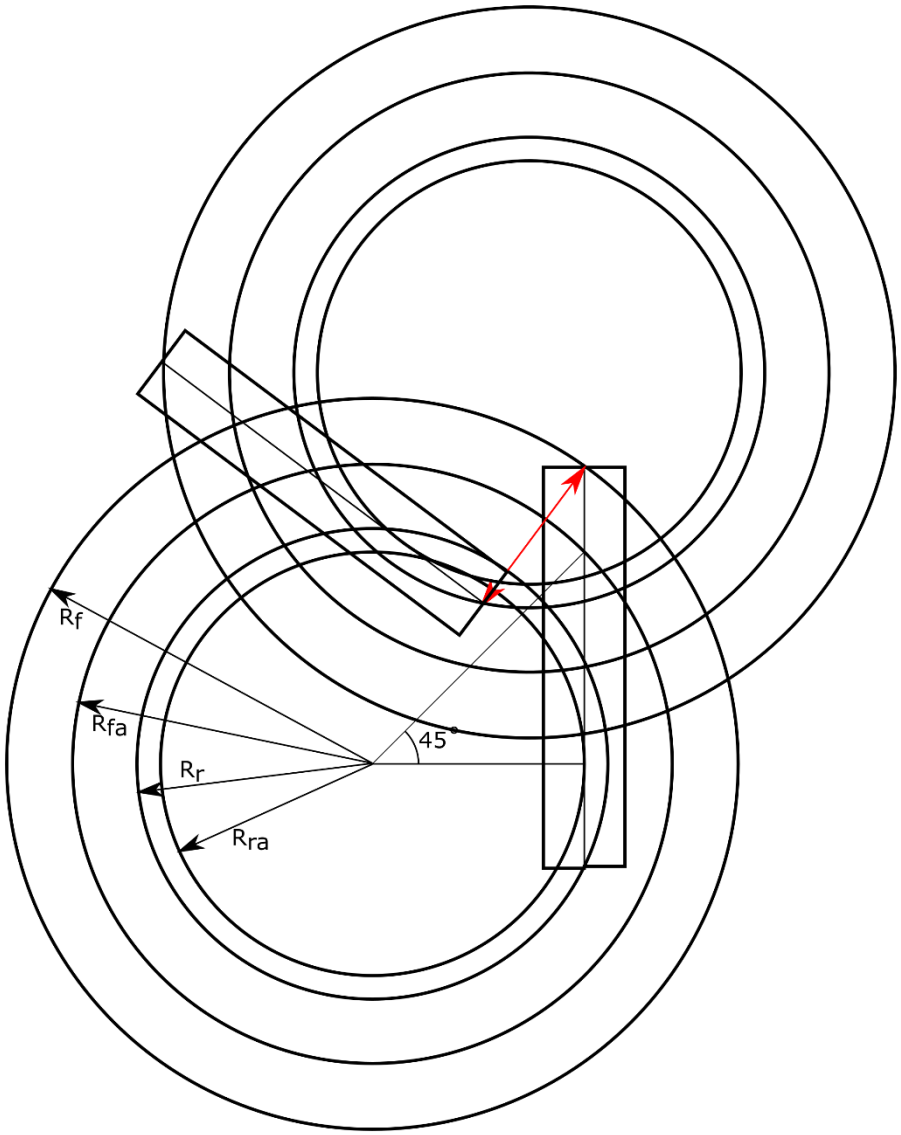


**Figure 11. Extreme case of tight turning. Red arrow indicates the absolute minimum for the distance.**

Now, the absolute minimum for the distance is:

$$R_f - R_r + 2 * (R_r - R_{ra}) \approx 5{,}68\, m$$

This corresponds to an aiming angle of:

$$\alpha_a = 180\,° - (90\,° - \tan^{-1}\left(\frac{L_{wb} + L_{fo}}{R_{ra}}\right) \approx 144{,}62\,°$$

The other extreme case to be considered is when the reflector angle is large. This brings the rear corner of the leader bus closer to the follower by $L_w/2$ (half of the width of the bus) when the reflector angle is 90 °. As a side note, the reflector angle barely ever exceeds 90 ° so there is no interest of accounting for that.

However, distance must not reach the absolute minimum distance, which is taken into account by off-setting the minimum target distance by 1 m. Therefore, the following equation to determine the target distance is proposed:

$$d_{target}(t) = d_0(t) + h * v(t) \quad (24)$$

where the minimum target distance, which is off-set by 1 m from the absolute limit, is:

$$d_0(t) = 1\ m + 5{,}68\ m * \frac{|\alpha_a(t)|}{144{,}62\,^\circ} + \frac{L_w}{2} * \frac{|\alpha_r(t)|}{90\,^\circ} \quad (25)$$

and the time headway is:

$$h = 0{,}4\ s$$

and v is the velocity of the follower bus. Figure 12 represents the architecture of the longitudinal controller.

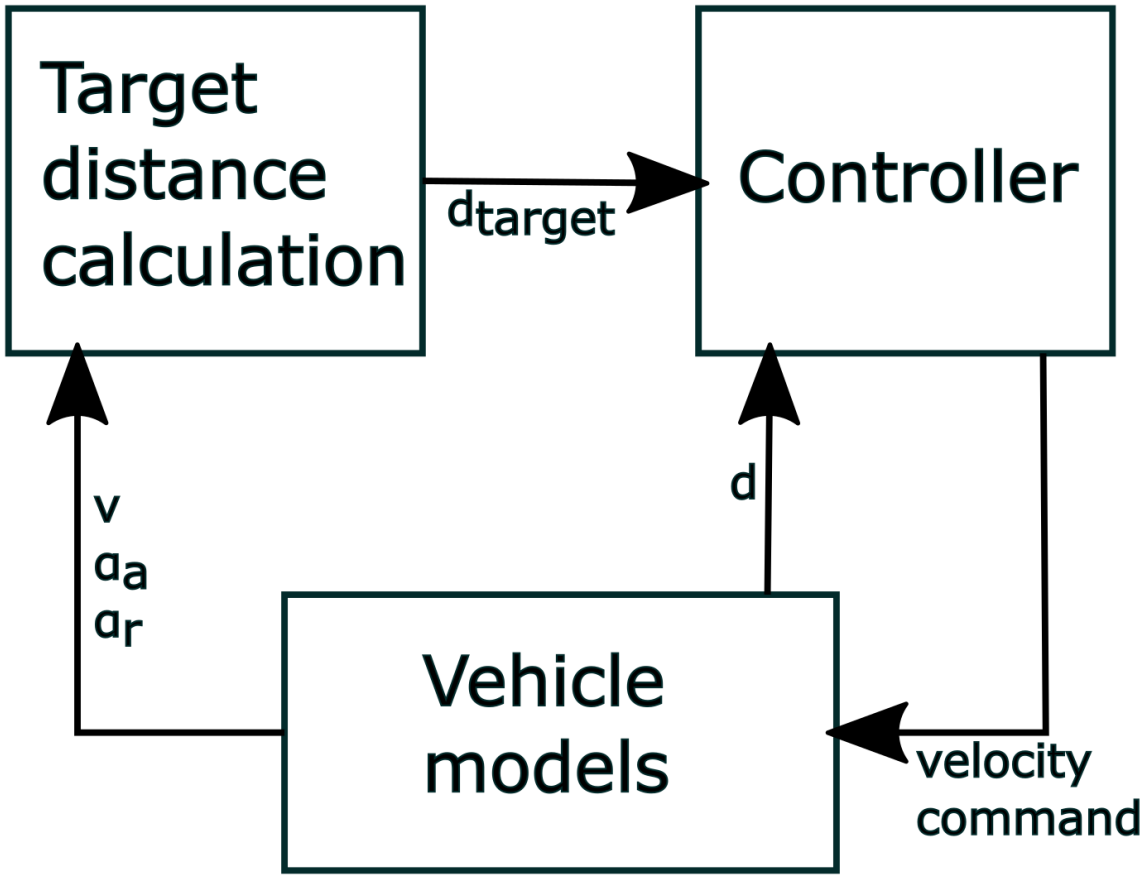


**Figure 12. The architecture of the longitudinal control.**

## *3.3 Lateral controller*

The simulation model assumes that lateral forces acting on the wheels are negligible and maneuvering of the vehicle can be done by pure rolling of the wheels if we neglect tire

turn slip (Pauwelussen, 2014). Therefore, Ackermann steering is used. Ackermann steering using bicycle model define steering angle δ as following (equation 26):

$$\delta = \tan^{-1}\left(\frac{L_{wb}}{R_{ra}}\right) = \tan^{-1}(\kappa * L_{wb}) \quad (26)$$

where $L_{wb}$ is the length of the wheelbase, $R_{ra}$ is the turning radius of the rear axle and κ is the corresponding curvature of the path.

Lateral control of the follower bus happens in two stages. First, the tested control law calculates target steering angle. Last, the target steering angle is compared to the measured steering angle and the error is fed to the controller which adjusts the steering wheel accordingly.

If we suppose using Ackerman steering, for Linkker 12+ bus it is reasonable to assume steering limits of -45 ° ≤ δ ≤ 45 °, which was also used in Zakaria et al. (2013) study. PID-controller is used with a feedforward term for lateral control. Figure 13 represents the working principle of the lateral control.

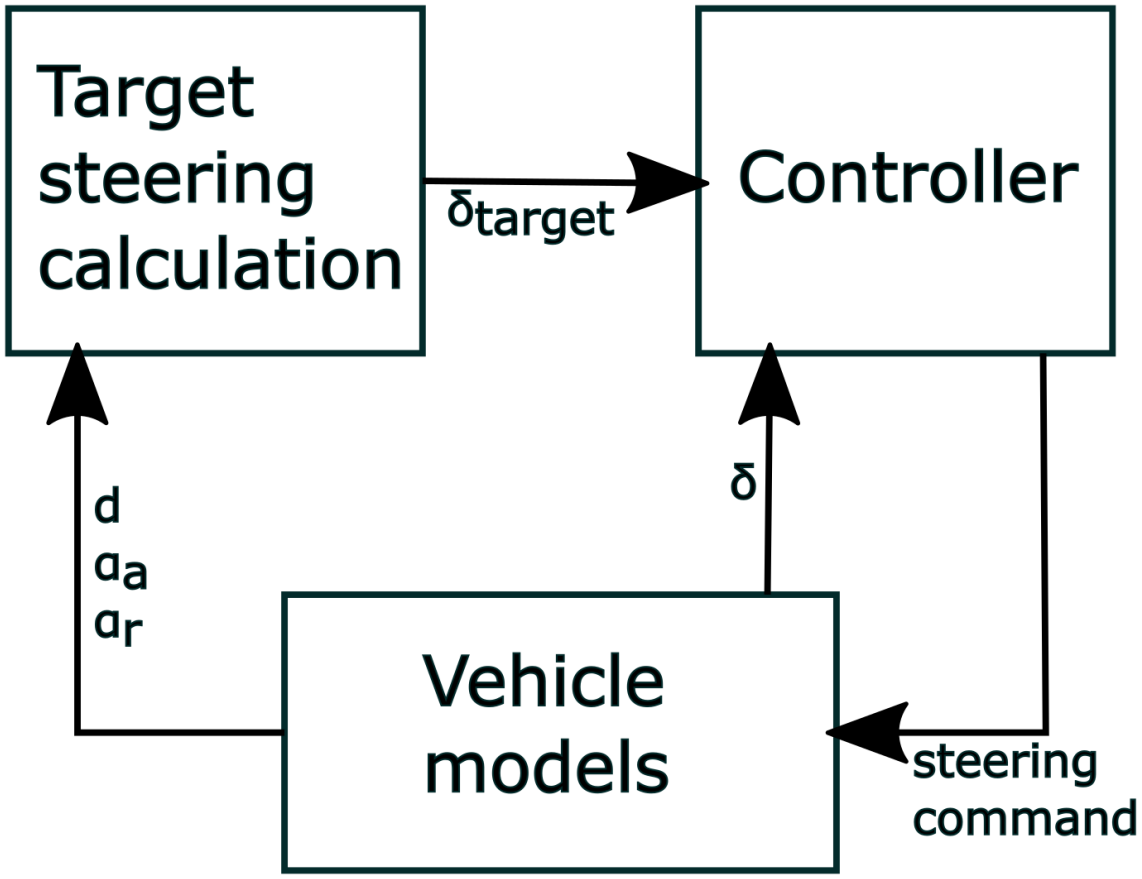


**Figure 13. The architecture of the lateral control.**

### 3.3.1 Pure Pursuit method

The Pure Pursuit method is utilized here but using direct target following. Usually the look ahead point is chosen to be on a predefined trajectory. Here the look ahead point is chosen to be on the middle of the rear axle of the leader bus. The proposed control law

tries to drive the following bus on a circular arc so that the center of follower's rear axle will coincide with the position where the center of the rear axle of the leader bus was. Figure 14 shows the geometrical relationship of buses and the Pure Pursuit method.

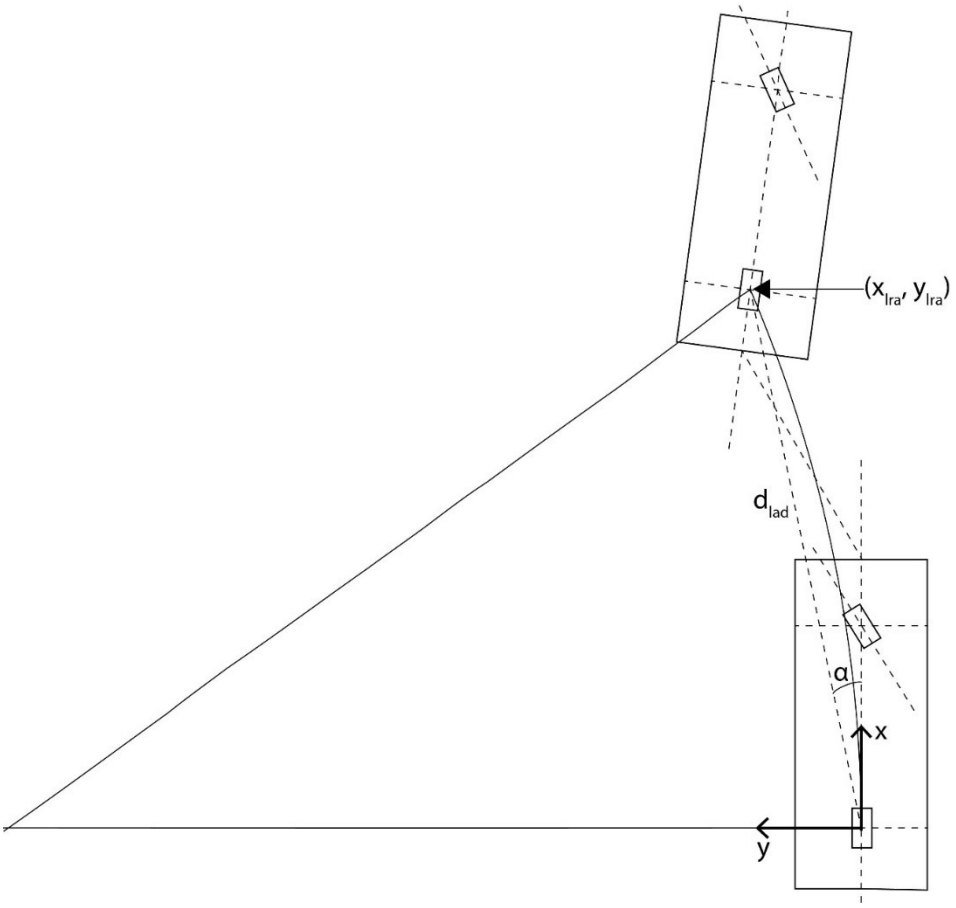


**Figure 14. Geometry of the Pure Pursuit method.**

The origin of coordinate system is chosen to be on the center of the rear axle of follower bus. The position of the look ahead point ($x_{lra}$, $y_{lra}$) in follower's coordinate system and leader's relative heading γ can be calculated as following:

$$\begin{bmatrix} x_{lra}(t) \\ y_{lra}(t) \\ \gamma(t) \end{bmatrix} = \begin{bmatrix} L_{wb} + L_{fo} + d(t) * \cos\alpha_a(t) + L_{ro} * \cos\gamma(t) \\ d(t) * \sin\alpha_a(t) + L_{ro} * \sin\gamma(t) \\ \alpha_a(t) - \alpha_r(t) \end{bmatrix} \quad (27)$$

The proposed Pure Pursuit control law uses look ahead distance. Because it is already a function of the velocity there is no need to account for velocity anymore. Look ahead distance $d_{lad}$ and angle α can be calculated as following:

$$d_{lad}(t) = \sqrt{x_{lra}(t)^2 + y_{lra}(t)^2} \quad (28)$$

$$\alpha(t) = \tan^{-1}\left(\frac{y_{lra}(t)}{x_{lra}(t)}\right) \quad (29)$$

The Pure Pursuit control law can be defined as:

$$\delta_{target}(t) = \tan^{-1}\left(\frac{2*L_{wb}*\sin(\alpha(t))}{K*d_{lad}(t)}\right) \quad (30)$$

where K is a gain parameter for tuning the look ahead distance.

Figure 15 and Figure 16 show the preliminary performance of the Pure Pursuit control law when using value of K = 1 and leader bus is moving with velocities of 5 m/s and 10 m/s. Follower bus seems to follow leader's path quite well. However, steering angle of the follower does not perfectly match with the leader's. With higher velocity, follower does not seem to follow leader's path as precisely as with lower velocity.

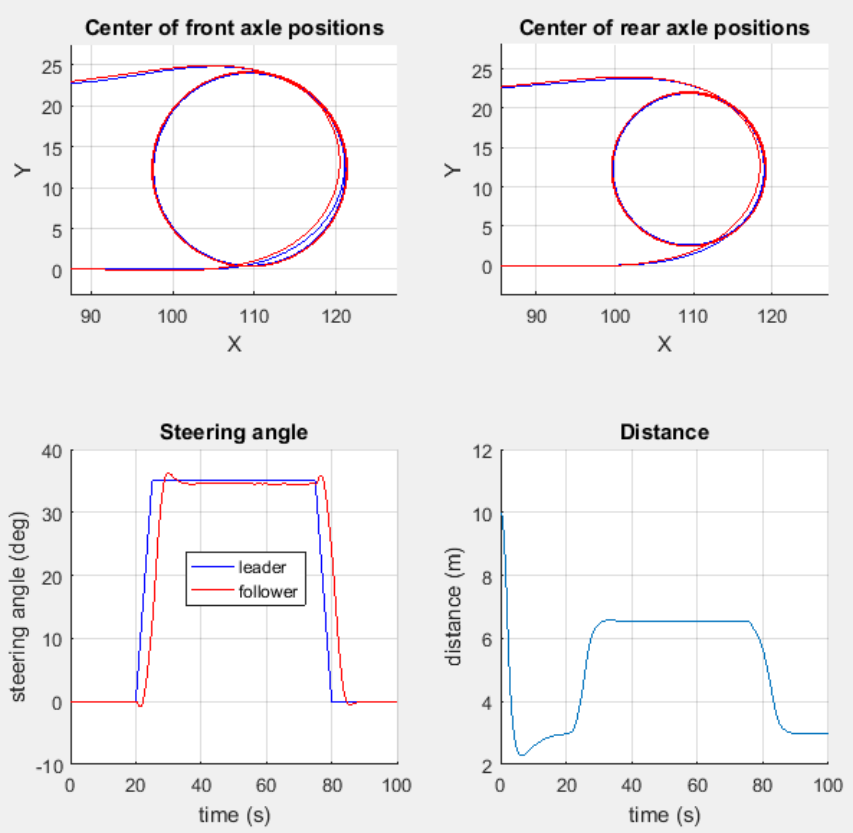


**Figure 15. Performance of the Pure Pursuit control law, when $v_{leader}$ = 5 m/s and K = 1.**

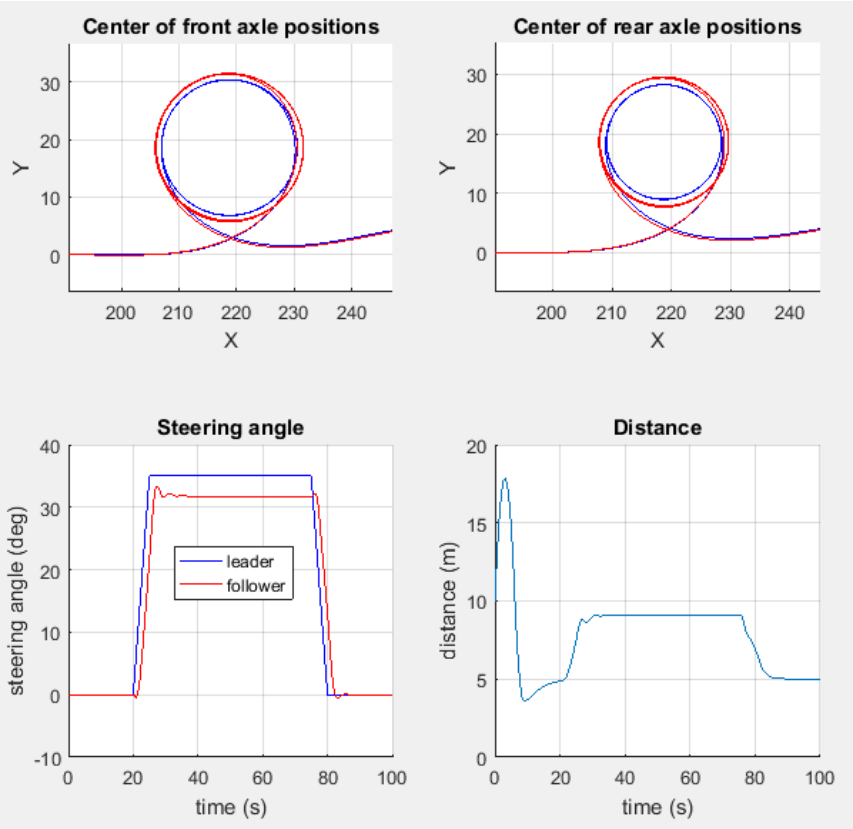


**Figure 16. Performance of the Pure Pursuit control law, when $v_{leader}$ = 10 m/s and K = 1.**

### 3.3.2 Spline Pursuit method

Spline Pursuit method is based on the idea to take into account the heading of the leader in relation to the follower. The idea here is to form a function for a cubic spline between the rear axles of the buses. The origin of the coordinate system is located on the follower bus as seen in Figure 17. The position of the target point is defined the same way as in Pure Pursuit method. After that, the curvature of the spline in the origin is calculated. Curvature itself can be directly used to calculate the target steering angle.

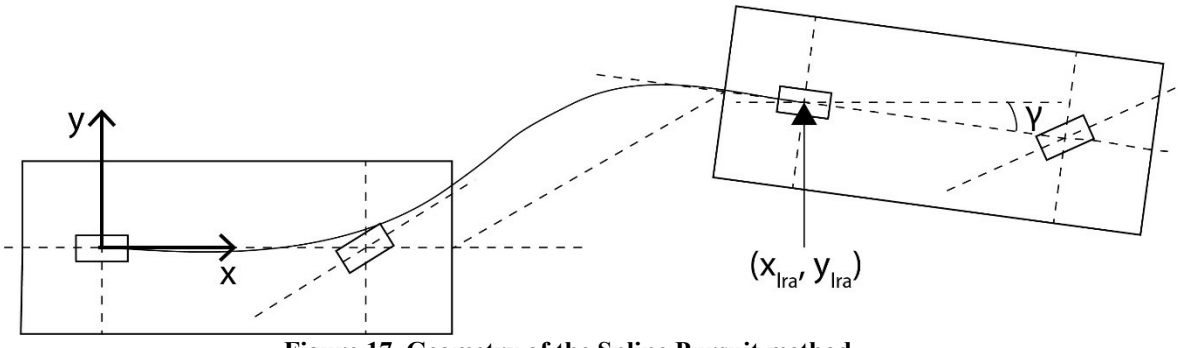


**Figure 17. Geometry of the Spline Pursuit method.**

A general cubic polynomial function can be presented as following:

$$f(x) = a * x^3 + b * x^2 + c * x + d \quad (31)$$

The first derivative of the polynomial function is:

$$f'(x) = 3a * x^2 + 2b * x + c \quad (32)$$

Next, boundary conditions are applied to solve unknown parameters a, b, c and d. The boundary conditions are:

$$f(0) = 0$$
$$f'(0) = 0$$
$$f(x_{lra}) = y_{lra}$$
$$f'(x_{lra}) = \tan\gamma$$

These conditions produce the following parameter values for a, b, c and d:

$$a = \frac{x_{lra} * \tan\gamma - 2 * y_{lra}}{{x_{lra}}^3}$$
$$b = \frac{3 * y_{lra} - x_{lra} * \tan\gamma}{{x_{lra}}^2}$$
$$c = 0$$
$$d = 0$$

The effect of relative heading on the shape of the spline can be seen in Figure 18.

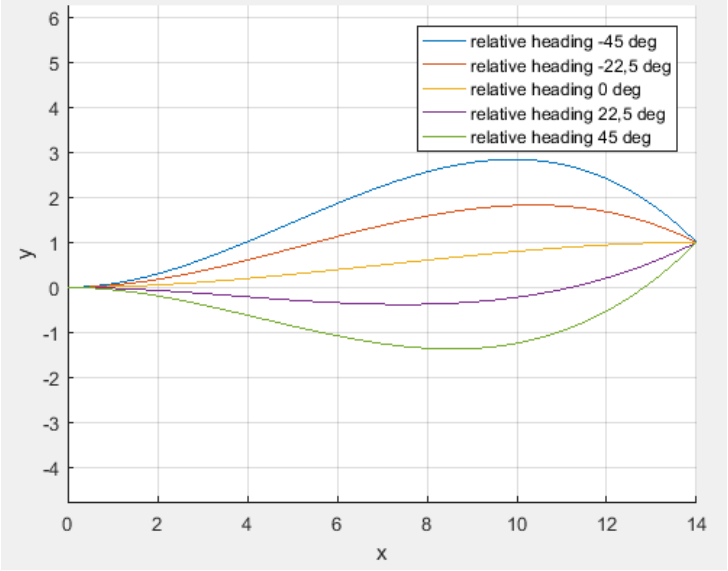


**Figure 18. Effect of relative heading on the shape of the spline.**

The curvature κ of a curve can be calculated by following equation:

$$\kappa(x) = \frac{f''(x)}{(1+f'(x)^2)^{3/2}} \quad (33)$$

Next, the curvature in the origin can be calculated and it simplifies to the following:

$$\kappa(t) = \frac{6y_{lra}(t) - 2x_{lra}(t) * \tan\gamma(t)}{(x_{lra}(t))^2} \quad (34)$$

From the last equation can be seen that:

- When $x_{lra}$ increases, the magnitude of κ decreases.
- When $y_{lra}$ increases, κ increases.
- When γ increases, κ decreases.

The Spline Pursuit control law can now be defined as:

$$\delta_{target}(t) = \tan^{-1}(\kappa(t) * L_{wb}) \tag{35}$$

Figure 19 and Figure 20 show the preliminary performance of the Spline Pursuit control law. As can be seen, the method is inherently oscillatory.

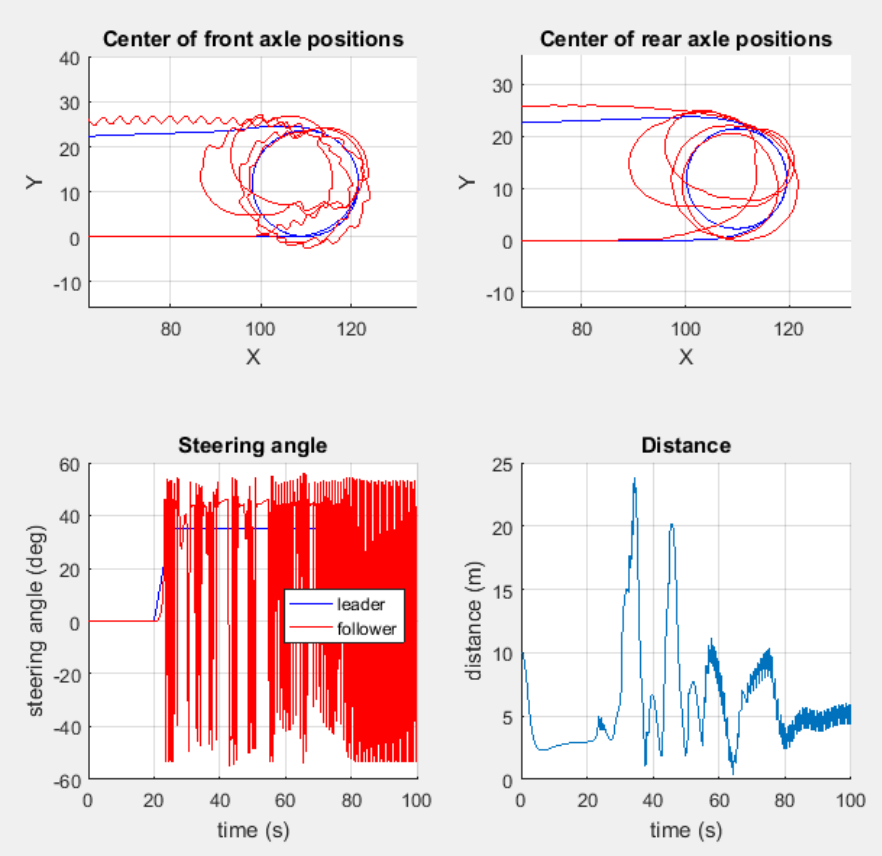


**Figure 19. Performance of the Spline Pursuit control law, when $v_{leader}$ = 5 m/s.**

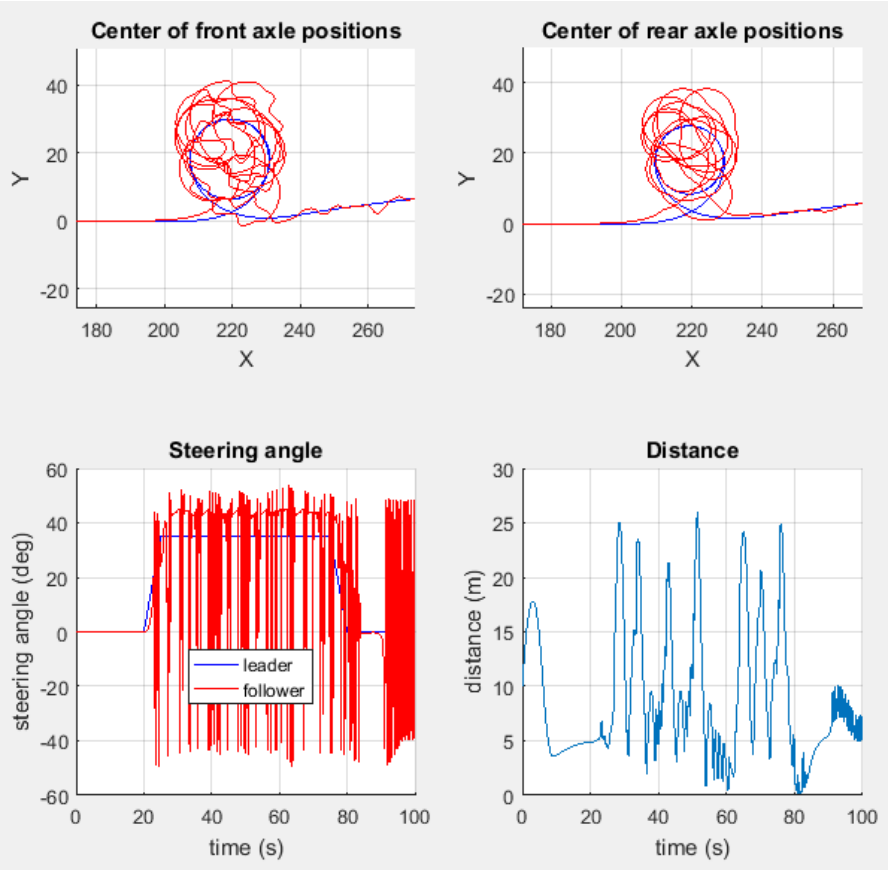


**Figure 20. Performance of the Spline Pursuit control law, when $v_{leader}$ = 10 m/s.**

### 3.3.3 Circular Pursuit method

In Circular Pursuit method, the steering angle tries to follow a circular arc which coincides with the leader vehicle's front axle and is tangential to leader vehicle's heading. Control law tries to drive the follower's center of the front axle on a circular arc to the position where the center of the leader's front axle was. The geometry of the bus platoon and idea behind Circular Pursuit method can be seen in Figure 21. The circular arc goes through the center of follower's front axle and the center of leader's front axle and is tangential to leader's heading at leader's front axle location. This was the arc is completely defined.

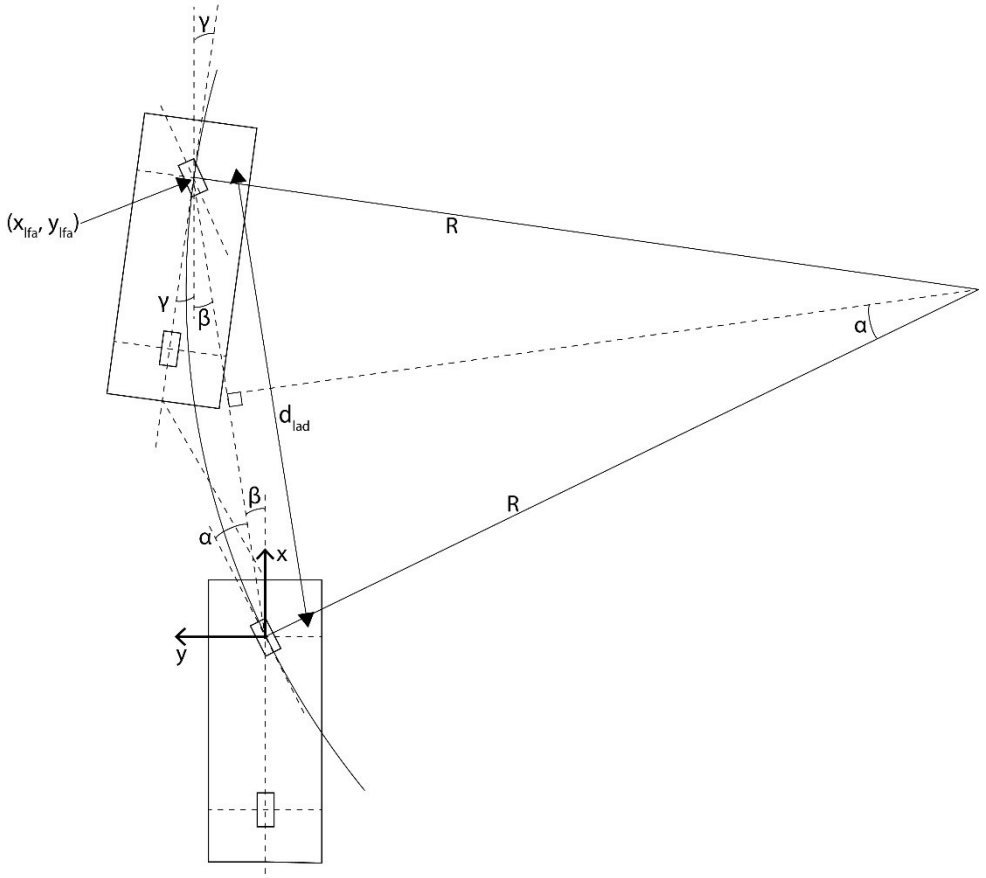


**Figure 21. Geometry of the Circular Pursuit method.**

In the proposed control law, the coordinate system is placed so that its origin lies on the center of follower bus's front axle. The position on leader bus's front axle ($x_{lfa}$, $y_{lfa}$) and leader's relative heading γ is calculated as following:

$$\begin{bmatrix} x_{lfa}(t) \\ y_{lfa}(t) \\ \gamma(t) \end{bmatrix} = \begin{bmatrix} L_{fo} + d(t) * \cos\alpha_a(t) + (L_{ro} + L_{wb}) * \cos\gamma(t) \\ d(t) * \sin\alpha_a(t) + (L_{ro} + L_{wb}) * \sin\gamma(t) \\ \alpha_a(t) - \alpha_r(t) \end{bmatrix} \quad (36)$$

Next, the look ahead distance is calculated:

$$d_{lad}(t) = \sqrt{x_{lfa}(t)^2 + y_{lfa}(t)^2} \quad (37)$$

The angle β which is between the heading of the follower bus and the look ahead vector is calculated as following:

$$\beta(t) = \tan^{-1}\left(\frac{y_{lfa}(t)}{x_{lfa}(t)}\right) \quad (38)$$

Next, the radius R of the circle is calculated:

$$\cos\big(90° - (\beta + \gamma)\big) = \frac{d_{lad}/2}{R} \quad (39)$$

$$\sin(\beta + \gamma) = \frac{d_{lad}}{2R} \quad (40)$$

$$R(t) = \frac{d_{lad}(t)}{2\sin(\beta(t)+\gamma(t))} \tag{41}$$

Using the law of sines, the following equation is formed:

$$\frac{d_{lad}}{\sin(2\alpha)} = \frac{R}{\sin(90°-\alpha)} \tag{42}$$

$$\frac{d_{lad}}{2\sin\alpha*\cos\alpha} = \frac{R}{\cos\alpha} \tag{43}$$

$$\frac{d_{lad}}{\sin\alpha} = 2R \tag{44}$$

$$\alpha(t) = \sin^{-1}\left(\frac{d_{lad}(t)}{2R(t)}\right) \tag{45}$$

The Circular Pursuit control law is expressed as following:

$$\delta_{target}(t) = \alpha(t) + \beta(t) \tag{46}$$

Figure 22 and Figure 23 show preliminary performance of the Circular Pursuit control law. The control law seems to be quite oscillatory. With $v_{leader}$ = 5 m/s, the control law completely fails to follow the leader.

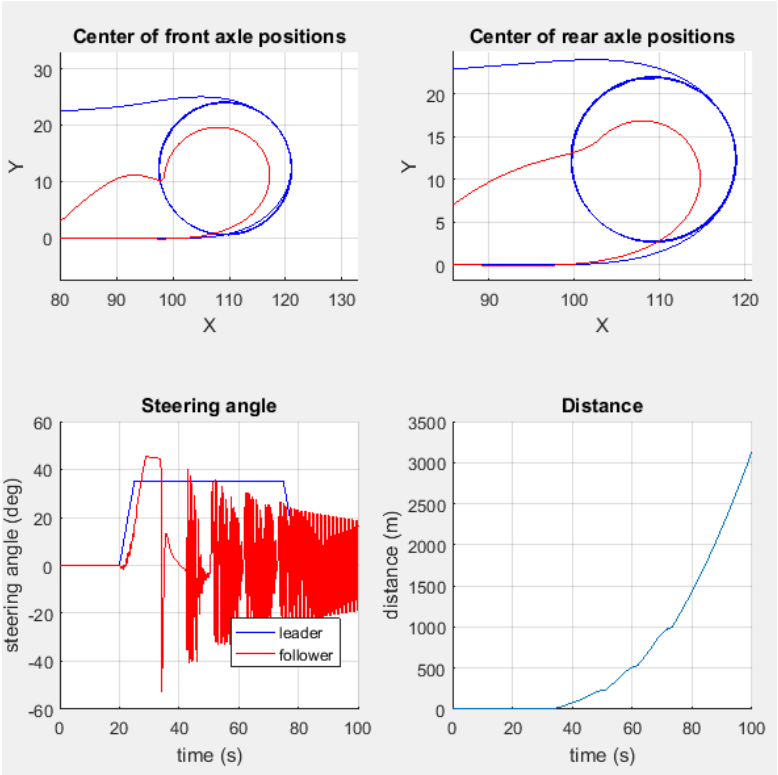


**Figure 22. Performance of the Circular Pursuit control law, when $v_{leader}$ = 5 m/s.**

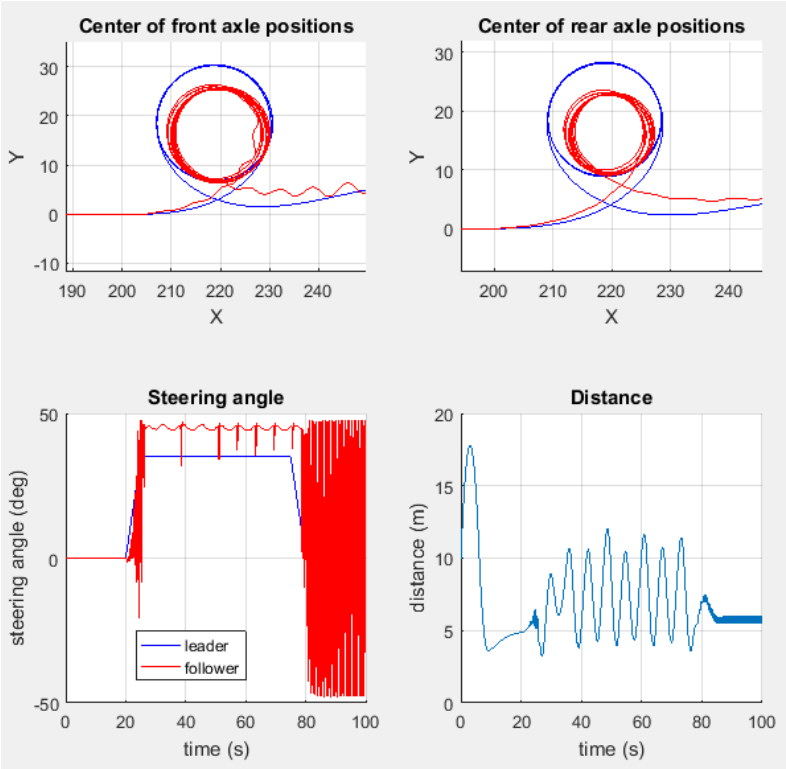


**Figure 23. Performance of the Circular Pursuit control law, when $v_{leader}$ = 10 m/s.**

### 3.3.4 Modified Pure Pursuit method

Modified Pure Pursuit method is an extension to the studied Pure Pursuit method. It tries to take into account the relative heading of the leader bus, which is not considered in Pure Pursuit. Figure 24 represents the geometry of the method. The idea here is to define Pure Pursuit geometry for a virtual position of the follower so that virtual heading is tangential to a circle defined by positions of center of follower's and leader's rear axles and tangential to leader's heading.

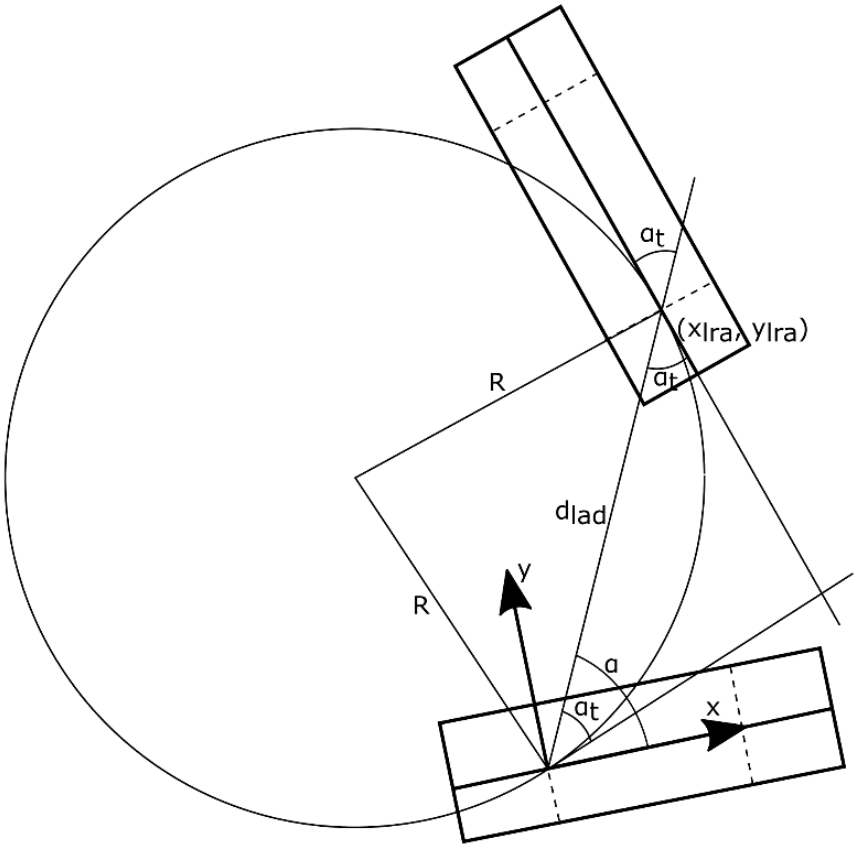


**Figure 24. Geometry of the Modified Pure Pursuit method, where $\alpha_t$ is the angle between the virtual heading of the follower and the look ahead vector.**

The position and heading of the leader's rear axle are defined the same way as in Pure Pursuit. The look ahead distance and the angle α between follower's heading and the look ahead vector are defined also the same way.
The angle between the virtual follower's heading and the look ahead vector $\alpha_t$ is defined by the following equation:

$$\alpha_t(t) = \gamma(t) - \alpha(t) \tag{47}$$

However, follower bus has different heading than virtual follower has. Only in steady-state situation they coincide. Therefore, there has to be a term to drive the follower bus into the same heading than the virtual follower is. This can be seen in the following equation which describes the Modified Pure Pursuit control law:

$$\delta_{target}(t) = \tan^{-1}\left(\frac{2*L_{wb}*\sin(\alpha_t(t))}{K*d_{lad}(\mathrm{t})}\right) + M\big(\alpha(t) - \alpha_t(t)\big) \tag{48}$$

where the first term expresses the Pure Pursuit control law with added modification and the second term expresses transient behavior which tries to drive α -> $\alpha_t$ and K and M are gain parameters.

Preliminary performance of the Modified Pure Pursuit control law can be seen in Figure 25 and Figure 26. Method seems to follow the leader's path more precisely with lower velocity.

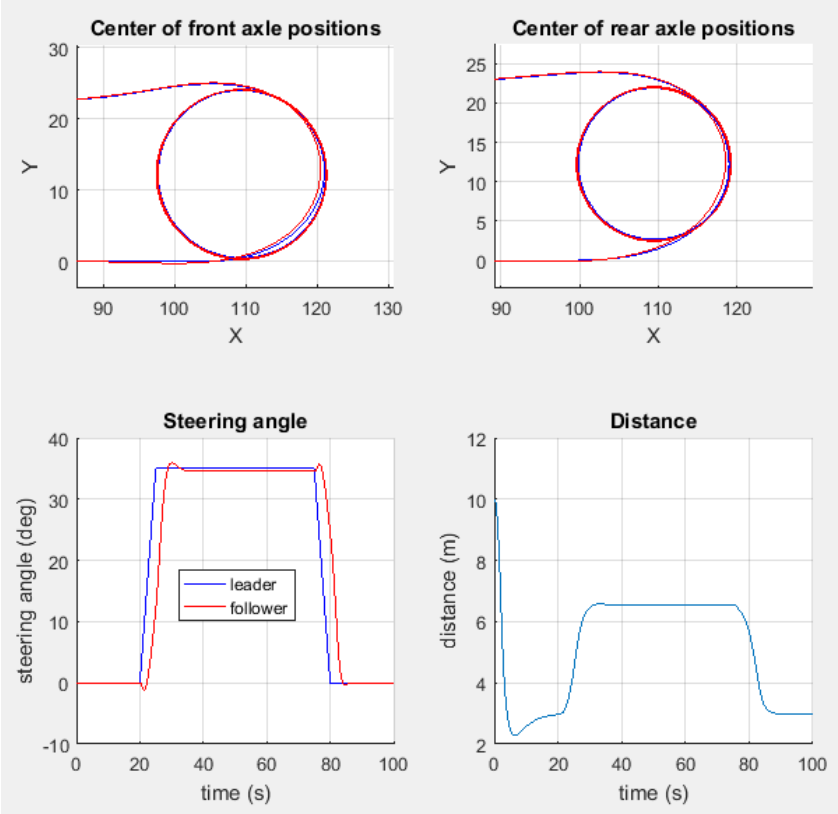


**Figure 25. Performance of the Modified Pure Pursuit control law, when $v_{leader}$ = 5 m/s, K = 1 and M = 0,5.**

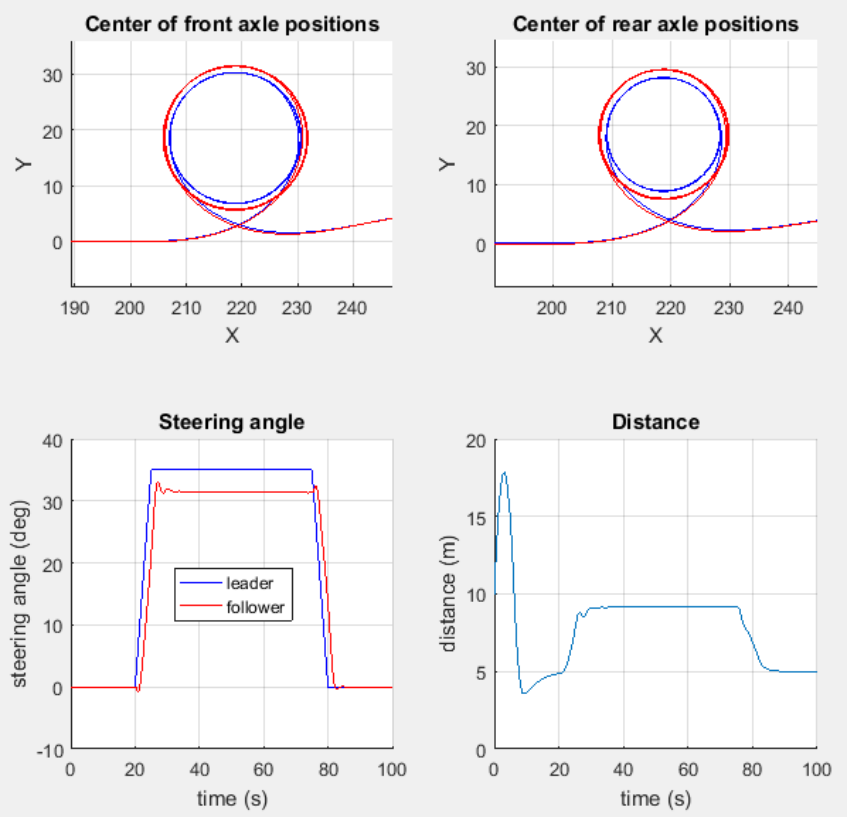


**Figure 26. Performance of the Modified Pure Pursuit control law, when $v_{leader}$ = 10 m/s, K = 1 and M = 0,5.**

# 4 Results and analysis

## 4.1 Longitudinal controller

The performance of the longitudinal controller is evaluated here. There are three different types of tests performed: initialization, acceleration and deceleration.

### 4.1.1 Set-up with initial distance

Following tests relate to the situation when the whole controller system is initialized. At the time of initialization, buses are probably not exactly at right distance from each other. Therefore, it is necessary to study the performance of the longitudinal controller when buses have varying inter-vehicular distances.

In tests, the leader bus is stationary and so is the follower bus initially. Buses are lined-up, so the effects of aiming and reflector angles are not studied. Tests were performed with initial distance of 2, 5 and 10 m. Figure 27, Figure 28 and Figure 29 show performance of the controller. Controller corrects large errors quite fast. After that it slowly drives the follower bus to the proper distance.

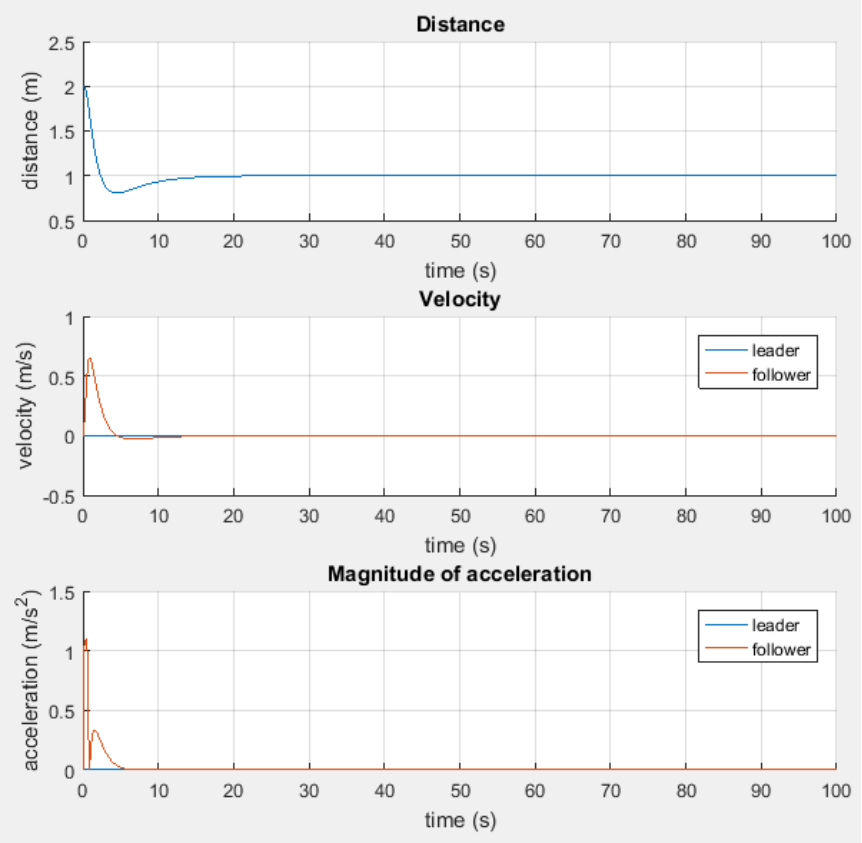


**Figure 27. System initialization with initial distance of 2 m.**

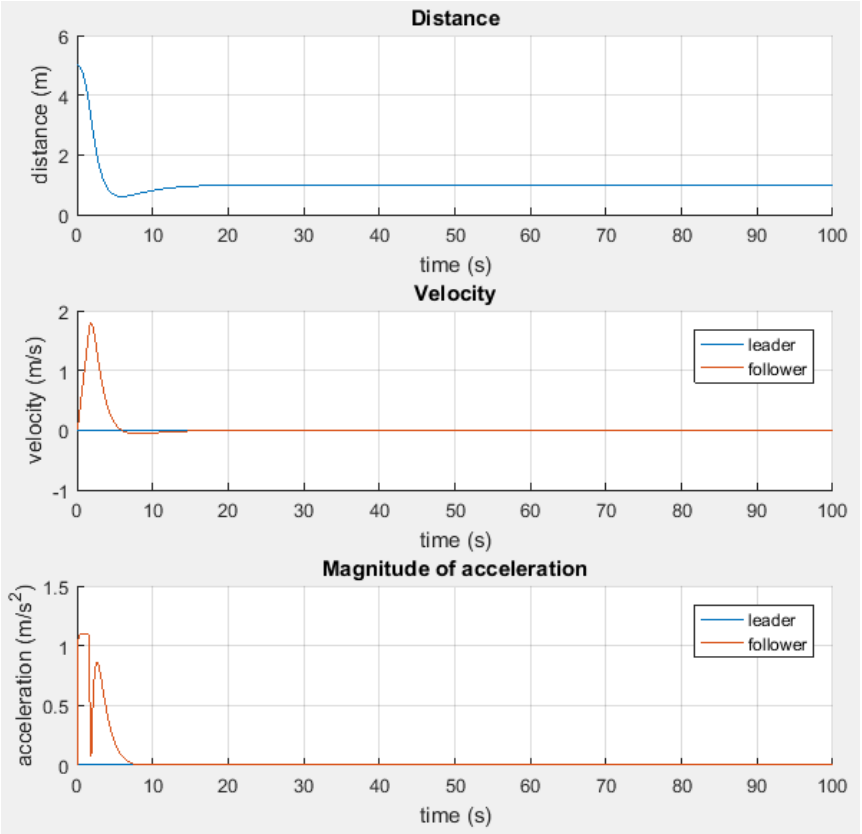


**Figure 28. System initialization with initial distance of 5 m.**

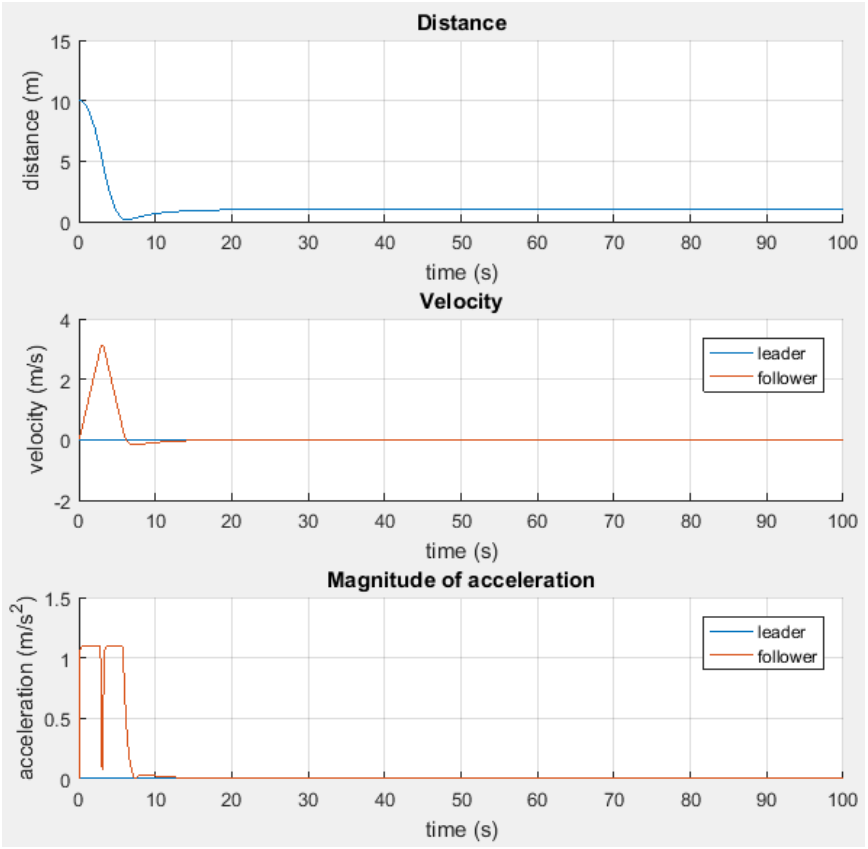


**Figure 29. System initialization with initial distance of 10 m.**

It can be concluded that the longitudinal controller works in initialization for inter-vehicular distances ranging from 2 to 10 m.

### 4.1.2 Acceleration and deceleration

Following tests were performed the following way. A PID-controller was implemented to control the velocity of the leader bus in order to take dynamics of the leader bus into account. A step input of 10 m/s at simulation time of 10 s was added to control the leader. A step input of -10 m/s was added at simulation time of 60 s. Three tests were performed. In the first test buses had no additional payload i.e. they were empty. In the second test both buses carried full payload (5500 kg). In the third test leader bus was empty and follower bus carried full payload.

Figure 30, Figure 31 and Figure 32 show the performance of the longitudinal controller in acceleration and deceleration tests. First test shows that the follower is able to follow leader very rapidly. Second test shows some overshooting in distance. Third test shows that follower is unable to maintain safe distance to the leader and crashes. Second and third tests show the reduced acceleration and deceleration capabilities of the buses when compared to the first test.

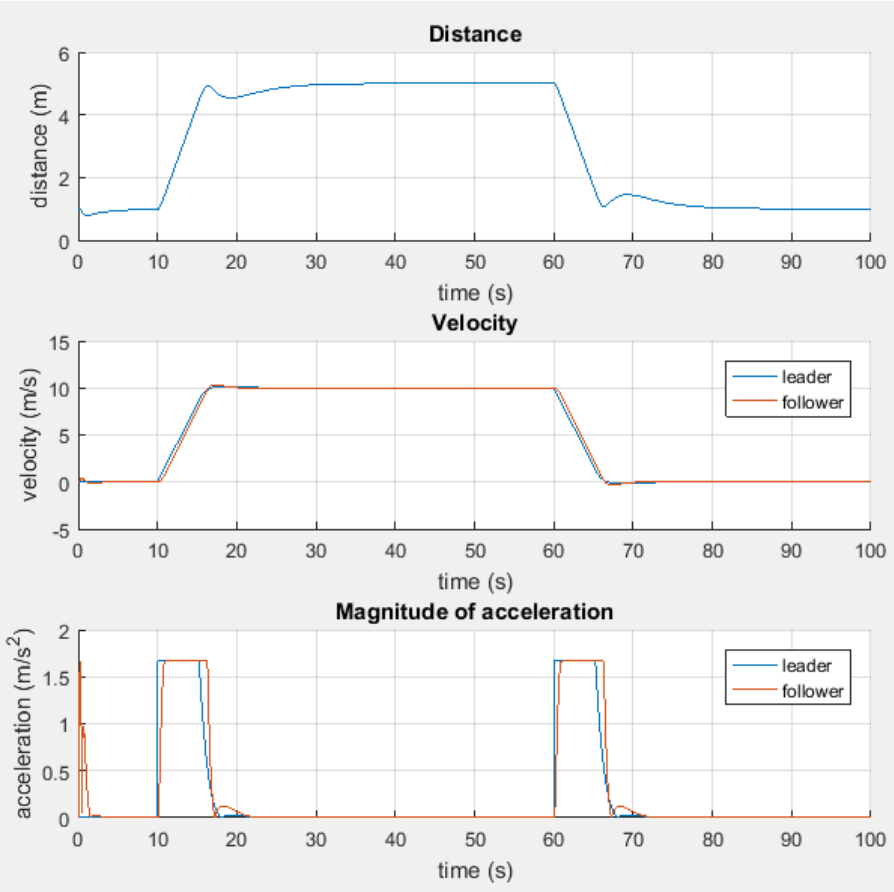


**Figure 30. Acceleration and deceleration test with target velocity of 10 m/s. Payloads of both buses 0 kg.**

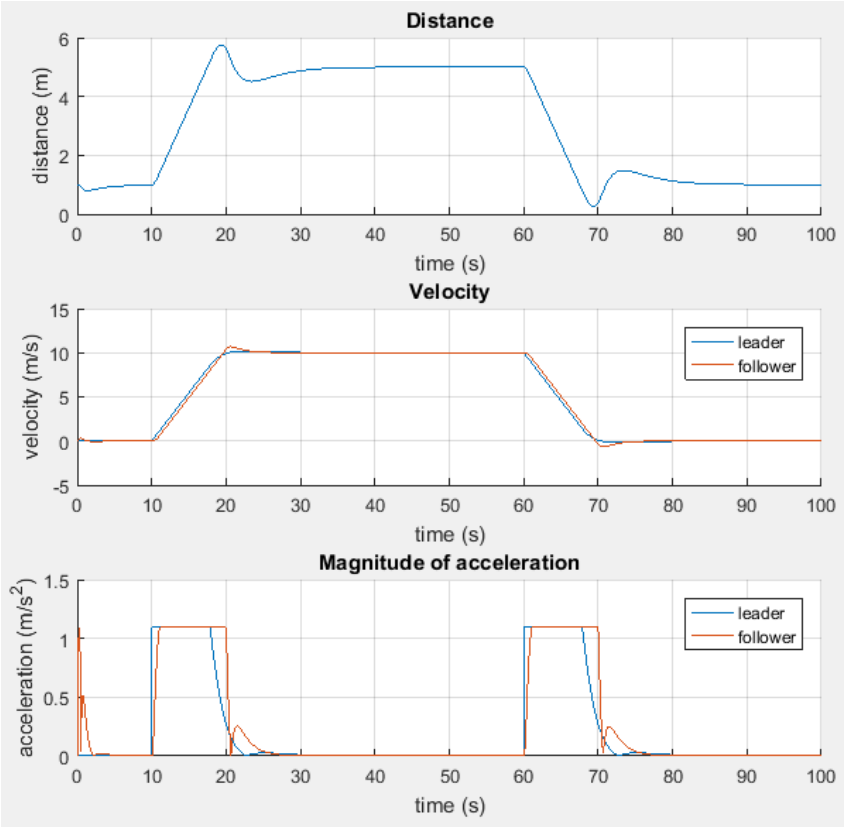


**Figure 31. Acceleration and deceleration test with target velocity of 10 m/s. Payloads of both buses 5500 kg.**

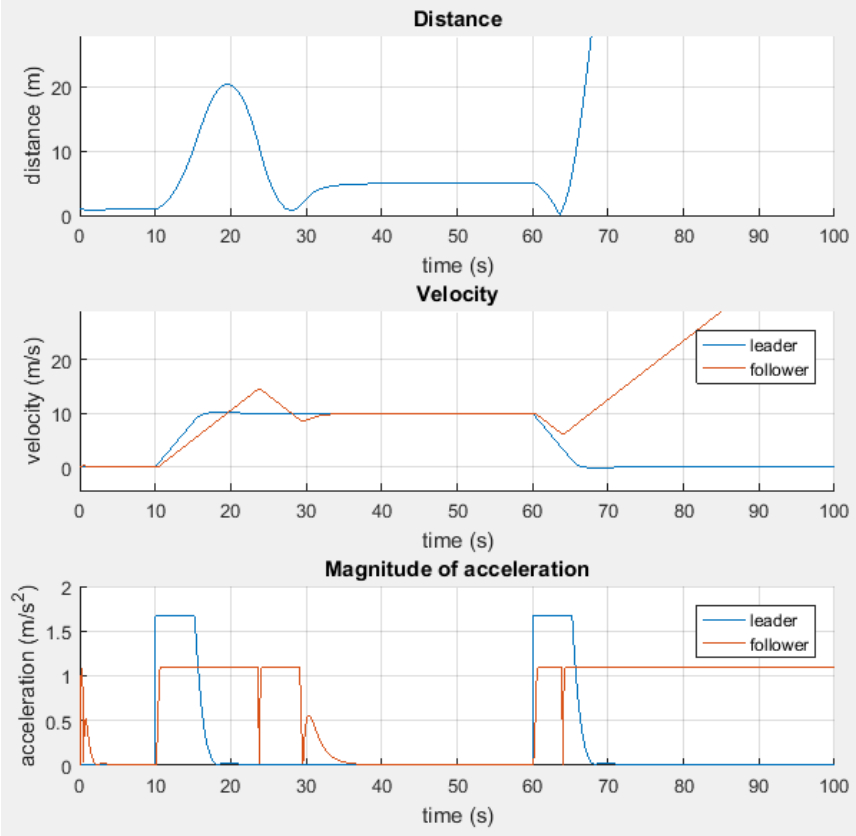


**Figure 32. Acceleration and deceleration test with target velocity of 10 m/s. Payload of leader bus 0 kg and follower bus 5500 kg.**

Longitudinal controller seems to work well, when both buses are loaded with same amounts of payload. However, when the follower is loaded more than the leader, controller might not be able to prevent collision. Therefore, this situation must be considered separately or parameters of the longitudinal controller must be adjusted.

## 4.2 Lateral controller

Performance of the lateral controller will be studied in two different scenarios: when following constant curvature paths (steady-state behavior) and varying curvature paths (transient behavior) measured from the rear axle. On constant curvature path, the steering angle of the vehicle stays the same. On varying curvature path, the steering angle either increases or decreases. Because the distance between the buses changes according to the driving velocity, tests must be done on various driving velocities, because it might change the performance of the lateral controller.

### 4.2.1 Steady-state behavior

Test were performed by the following way. Leader bus drives into a circle of constant curvature (constant steering angle) and follower's behavior is measured. Steering angles experimented were 5, 10, 20, 30 and 40 °. Straight driving was not studied i.e. steering angle of 0 °. Only positive steering angles were studied because all of the designed lateral controllers are symmetrical in that sense. Driving velocities of 0,1 to 25 m/s were to be tested.

Even though it would be interesting to see the performance of the controllers in cases where both steering angle and velocity are high, it is by no means reasonable. When driving on circles with constant speed, there is lateral acceleration present. This is due to the change of the direction of the velocity. The amount of lateral i.e. centripetal acceleration (denoted as $a_c$) at the center of rear axle of the bus can be calculated as following:

$$a_c = \frac{v^2}{R_{ra}} = \frac{v^2 * \tan\delta}{L_{wb}} \tag{49}$$

This centripetal acceleration, even when driving with constant velocity, is experienced as uncomfortability by the passengers. According to ISO 2631-1 standard, the border of extremely uncomfortable overall acceleration is 2,5 m/s$^2$ (section 2.4.1, figure 4). It is reasonable to assume that a professional bus driver will not reach that limit. Therefore, velocity in tests is limited according to the following equation:

$$v_{max} = \sqrt{\frac{L_{wb} * a_{c,max}}{\tan\delta}} \tag{50}$$

where:

$$a_{c,max} = 2{,}5\ m/s^2$$

This limit results in following maximum test velocities:

$$v_{max,5°} \approx 13{,}89\ m/s$$
$$v_{max,10°} \approx 9{,}78\ m/s$$
$$v_{max,20°} \approx 6{,}81\ m/s$$
$$v_{max,30°} \approx 5{,}41\ m/s$$

$$v_{max,40^\circ} \approx 4{,}48\ m/s$$

However, it is better to test the performance of the controllers to the next integer of velocity.

Tests were performed so that leader bus was driven to a constant velocity and some time was spent on that velocity for the follower bus to settle the distance to the target value. This was done to minimize the effects of varying velocities on the performance of the lateral controllers.

After the distance had settled down, the steering angle of the leader was increased to the target value linearly in 5 seconds. When the follower's steering angle had settled down, the value was collected with precision of 2 decimals.

Table 4, Table 5, Table 6 and Table 7 show steady-state test results using different control laws. For Pure Pursuit and Modified Pure Pursuit the effect of gain parameter K was also investigated. Gathered follower's steering angles were gathered using value of K = 1. After that, follower's steering angle was investigated using different values of K and the value of K was gathered with precision of 2 decimals to best match the follower's steering to the leader's.

**Table 4. Steady-state tests using Pure Pursuit control law.**

| v leader (m/s) | δ leader (°) | δ follower (°) | K | δ leader (°) | δ follower (°) | K | δ leader (°) | δ follower (°) | K | δ leader (°) | δ follower (°) | K | δ leader (°) | δ follower (°) | K |
|---|---|---|---|---|---|---|---|---|---|---|---|---|---|---|---|
| 0,1 | 5 | 5,02 | 1,92 | 10 | 10,15 | 1,6 | 20 | 20,88 | 1,36 | 30 | 31,93 | 1,25 | 40 | 42,48 | 1,17 |
| 1 | 5 | 5,02 | 1,73 | 10 | 10,14 | 1,5 | 20 | 20,77 | 1,29 | 30 | 31,58 | 1,19 | 40 | 41,77 | 1,11 |
| 2 | 5 | 5,02 | 1,6 | 10 | 10,12 | 1,4 | 20 | 20,65 | 1,23 | 30 | 31,2 | 1,13 | 40 | 40,96 | 1,06 |
| 3 | 5 | 5,02 | 1,5 | 10 | 10,11 | 1,31 | 20 | 20,53 | 1,17 | 30 | 30,83 | 1,09 | 40 | 40,16 | 1,01 |
| 4 | 5 | 5,01 | 1,38 | 10 | 10,09 | 1,25 | 20 | 20,41 | 1,12 | 30 | 30,47 | 1,04 | 40 | 39,27 | 0,96 |
| 5 | 5 | 5,01 | 1,3 | 10 | 10,07 | 1,19 | 20 | 20,29 | 1,08 | 30 | 30,11 | 1,01 | 40 | 38,35 | 0,92 |
| 6 | 5 | 5,01 | 1,2 | 10 | 10,06 | 1,14 | 20 | 20,18 | 1,05 | 30 | 29,72 | 0,98 | | | |
| 7 | 5 | 5,01 | 1,15 | 10 | 10,05 | 1,1 | 20 | 20,07 | 1,02 | | | | | | |
| 8 | 5 | 5,01 | 1,1 | 10 | 10,03 | 1,06 | | | | | | | | | |
| 9 | 5 | 5 | 1,08 | 10 | 10,02 | 1,03 | | | | | | | | | |
| 10 | 5 | 5 | 1,06 | 10 | 10 | 1 | | | | | | | | | |
| 11 | 5 | 5 | 1,01 | | | | | | | | | | | | |
| 12 | 5 | 5 | 0,99 | | | | | | | | | | | | |
| 13 | 5 | 5 | 0,97 | | | | | | | | | | | | |
| 14 | 5 | 5 | 0,95 | | | | | | | | | | | | |

**Table 5. Steady-state tests using Spline Pursuit control law, where o indicates oscillation and f indicates failing to follow.**

| v leader (m/s) | δ leader (°) | δ follower (°) | δ leader (°) | δ follower (°) | δ leader (°) | δ follower (°) | δ leader (°) | δ follower (°) | δ leader (°) | δ follower (°) |
|---|---|---|---|---|---|---|---|---|---|---|
| 0,1 | 5 | o | 10 | o | 20 | o | 30 | o | 40 | o |
| 1 | 5 | o | 10 | o | 20 | o | 30 | o | 40 | f |
| 2 | 5 | o | 10 | o | 20 | o | 30 | o | 40 | 45 |
| 3 | 5 | o | 10 | o | 20 | o | 30 | o | 40 | o |
| 4 | 5 | o | 10 | o | 20 | o | 30 | o | 40 | f |
| 5 | 5 | o | 10 | o | 20 | o | 30 | f | 40 | f |
| 6 | 5 | o | 10 | o | 20 | o | 30 | f | | |
| 7 | 5 | o | 10 | o | 20 | o | | | | |
| 8 | 5 | o | 10 | o | | | | | | |
| 9 | 5 | o | 10 | o | | | | | | |
| 10 | 5 | o | 10 | o | | | | | | |
| 11 | 5 | o | | | | | | | | |
| 12 | 5 | 5,02 | | | | | | | | |
| 13 | 5 | 5,06 | | | | | | | | |
| 14 | 5 | o | | | | | | | | |

**Table 6. Steady-state tests using Circular Pursuit control law, where o indicates oscillation and f indicates failing to follow.**

| v leader (m/s) | δ leader (°) | δ follower (°) | δ leader (°) | δ follower (°) | δ leader (°) | δ follower (°) | δ leader (°) | δ follower (°) | δ leader (°) | δ follower (°) |
|---|---|---|---|---|---|---|---|---|---|---|
| 0,1 | 5 | 5,04 | 10 | 10,3 | 20 | 22,98 | 30 | 45 | 40 | f |
| 1 | 5 | 5,04 | 10 | 10,31 | 20 | 23,07 | 30 | 45 | 40 | f |
| 2 | 5 | 5,04 | 10 | 10,32 | 20 | 23,16 | 30 | 45 | 40 | f |
| 3 | 5 | 5,04 | 10 | 10,32 | 20 | 23,26 | 30 | 45 | 40 | f |
| 4 | 5 | o | 10 | 10,33 | 20 | 23,37 | 30 | 45 | 40 | f |
| 5 | 5 | o | 10 | o | 20 | 23,48 | 30 | 45 | 40 | f |
| 6 | 5 | o | 10 | o | 20 | 23,6 | 30 | 45 | | |
| 7 | 5 | o | 10 | o | 20 | o | | | | |
| 8 | 5 | o | 10 | o | | | | | | |
| 9 | 5 | o | 10 | o | | | | | | |
| 10 | 5 | o | 10 | o | | | | | | |
| 11 | 5 | o | | | | | | | | |
| 12 | 5 | o | | | | | | | | |
| 13 | 5 | o | | | | | | | | |
| 14 | 5 | o | | | | | | | | |

**Table 7. Steady-state tests using Modified Pure Pursuit control law, where M = 0,5.**

| v leader (m/s) | δ leader (°) | δ follower (°) | K | δ leader (°) | δ follower (°) | K | δ leader (°) | δ follower (°) | K | δ leader (°) | δ follower (°) | K | δ leader (°) | δ follower (°) | K |
|---|---|---|---|---|---|---|---|---|---|---|---|---|---|---|---|
| 0,1 | 5 | 5,03 | 1,83 | 10 | 10,21 | 1,59 | 20 | 21,24 | 1,31 | 30 | 31,9 | 1,15 | 40 | 41,23 | 1,06 |
| 1 | 5 | 5,03 | 1,74 | 10 | 10,19 | 1,53 | 20 | 21,09 | 1,28 | 30 | 31,6 | 1,13 | 40 | 41 | 1,05 |
| 2 | 5 | 5,02 | 1,64 | 10 | 10,18 | 1,46 | 20 | 20,92 | 1,24 | 30 | 31,26 | 1,11 | 40 | 40,61 | 1,03 |
| 3 | 5 | 5,02 | 1,55 | 10 | 10,16 | 1,39 | 20 | 20,76 | 1,19 | 30 | 30,89 | 1,08 | 40 | 40,11 | 1,01 |
| 4 | 5 | 5,02 | 1,47 | 10 | 10,14 | 1,33 | 20 | 20,59 | 1,15 | 30 | 30,51 | 1,04 | 40 | 39,43 | 0,97 |
| 5 | 5 | 5,02 | 1,39 | 10 | 10,11 | 1,27 | 20 | 20,43 | 1,11 | 30 | 30,12 | 1,01 | 40 | 38,62 | 0,93 |
| 6 | 5 | 5,02 | 1,32 | 10 | 10,09 | 1,21 | 20 | 20,26 | 1,07 | 30 | 29,69 | 0,97 | | | |
| 7 | 5 | 5,01 | 1,26 | 10 | 10,07 | 1,16 | 20 | 20,1 | 1,03 | | | | | | |
| 8 | 5 | 5,01 | 1,2 | 10 | 10,05 | 1,1 | | | | | | | | | |
| 9 | 5 | 5,01 | 1,13 | 10 | 10,03 | 1,06 | | | | | | | | | |
| 10 | 5 | 5 | 1,07 | 10 | 10,01 | 1,01 | | | | | | | | | |
| 11 | 5 | 5 | 1,02 | | | | | | | | | | | | |
| 12 | 5 | 5 | 0,98 | | | | | | | | | | | | |
| 13 | 5 | 5 | 0,95 | | | | | | | | | | | | |
| 14 | 5 | 4,99 | 0,9 | | | | | | | | | | | | |

Tables show that Spline Pursuit is inherently oscillatory. It also fails to follow the leader bus at tight turns.

Circular Pursuit seems to work at small velocities and at turns from large to medium radius circles. Otherwise, it becomes oscillatory and even fails to follow at tight turns.

Pure Pursuit control law is able to follow the leader bus in all tests. It shows small deviations from leader's steering angle at large radius turns and larger deviations at small radius turns. It tends to use higher steering angles at small velocities and lower steering angles at higher velocities. Using gathered values of follower's steering angle, the radius of circle performed by follower can be calculated and compared to the leader's. The maximum error in circle radius, which represents the lateral error, can be calculated. The results can be seen in Table 8.

**Table 8. Turning radius and lateral errors in steady-state tests when using Pure Pursuit.**

| test (°) | R_fa leader (m) | R_fa follower min (m) | R_fa follower max (m) | R_fa error max (m) | R_ra leader (m) | R_ra follower min (m) | R_ra follower max (m) | R_ra error max (m) |
|---|---|---|---|---|---|---|---|---|
| 5 | 77,45 | 77,14 | 77,45 | 0,31 | 77,15 | 76,84 | 77,15 | 0,31 |
| 10 | 38,87 | 38,30 | 38,87 | 0,57 | 38,28 | 37,70 | 38,28 | 0,58 |
| 20 | 19,74 | 18,94 | 19,67 | 0,80 | 18,55 | 17,70 | 18,48 | 0,85 |
| 30 | 13,50 | 12,76 | 13,62 | 0,74 | 11,69 | 10,83 | 11,82 | 0,86 |
| 40 | 10,50 | 10,00 | 10,88 | 0,51 | 8,04 | 7,37 | 8,53 | 0,67 |

The maximum lateral error when combining all tests is 0,8 m for front axle and 0,86 m for rear axle. The maximum lateral error for front axle seems to happen when driving 20 ° steering angle turns.

The effect of gain parameter K was investigated as seen in Table 4. The point of it was to identify if it is possible to tune the response of the algorithm by adding a speed dependent

gain parameter. Figure 33 shows the optimal values of K with different driving velocities and steering angle values.

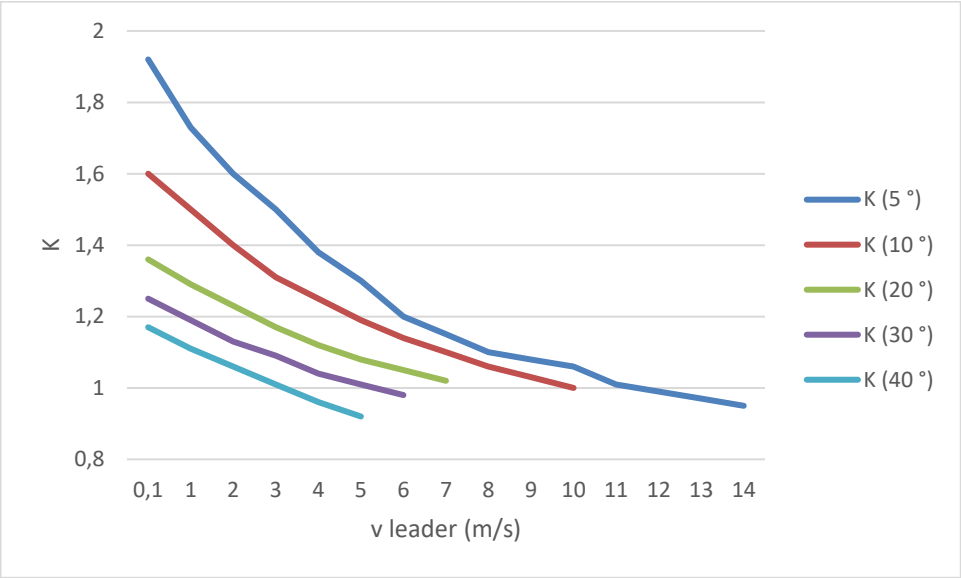


**Figure 33. Optimal values of gain parameter K in different driving scenarios for Pure Pursuit.**

As can be seen, the response of the algorithm cannot be tuned by a speed dependent gain parameter.

Modified Pure Pursuit control law is able to follow the leader bus in all tests. It shows small deviations from leader's steering angle at large radius turns and larger deviations at small radius turns. It tends to use higher steering angles at small velocities and lower steering angles at higher velocities. Using gathered values of follower's steering angle, the radius of circle performed by follower can be calculated and compared to the leader's. The maximum error in circle radius, which represents the lateral error, can be calculated. The results can be seen in Table 9.

**Table 9. Turning radius and lateral errors in steady-state tests when using Modified Pure Pursuit**

| test (°) | R_fa leader (m) | R_fa follower min (m) | R_fa follower max (m) | R_fa error max (m) | R_ra leader (m) | R_ra follower min (m) | R_ra follower max (m) | R_ra error max (m) |
|---|---|---|---|---|---|---|---|---|
| 5 | 77,45 | 76,99 | 77,60 | 0,46 | 77,15 | 76,69 | 77,31 | 0,46 |
| 10 | 38,87 | 38,08 | 38,83 | 0,79 | 38,28 | 37,48 | 38,24 | 0,80 |
| 20 | 19,74 | 18,63 | 19,64 | 1,10 | 18,55 | 17,37 | 18,45 | 1,18 |
| 30 | 13,50 | 12,77 | 13,63 | 0,73 | 11,69 | 10,84 | 11,84 | 0,85 |
| 40 | 10,50 | 10,24 | 10,81 | 0,31 | 8,04 | 7,70 | 8,45 | 0,41 |

The maximum lateral error when combining all tests is 1,1 m for front axle and 1,18 m for rear axle. The maximum lateral error seems to happen when driving 20 ° steering angle turns.

The effect of gain parameter K was investigated as seen in Table 7. The point of it was to identify if it is possible to tune the response of the algorithm by adding a speed dependent gain parameter. Figure 34 shows the optimal values of K with different driving velocities and steering angle values.

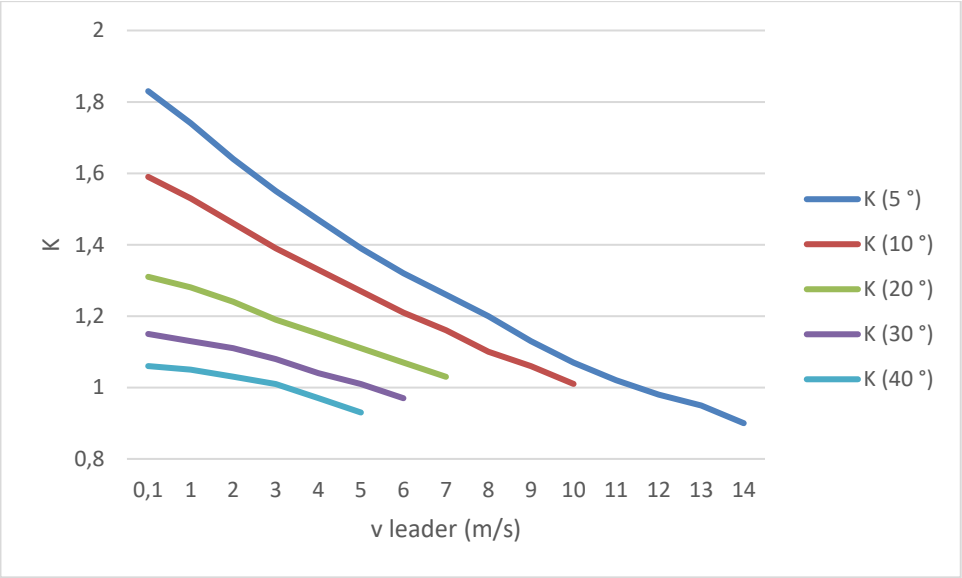


**Figure 34. Optimal values of gain parameter K in different driving scenarios for Modified Pure Pursuit.**

As can be seen, the response of the algorithm cannot be tuned by a speed dependent gain parameter.

Steady-state tests show the performance of studied control laws when following a vehicle that drives on a constant curvature path. Spline Pursuit and Circular Pursuit do not perform well at all. Pure Pursuit method out-performs the Modified Pure Pursuit method by a small margin.

Pure Pursuit and Modified Pure Pursuit were not able to follow the leader vehicle perfectly, which should be the case in theory. This inaccuracy in probably due to the lags present in the lateral control system and errors present in simulations.

### 4.2.2 Transient behavior

Transient behavior of the lateral controller means the case when the leader vehicle changes its steering angle. This can be studied by examining the paths of the leader and the follower in following cases: driving from straight path to curve i.e. increasing the steering angle and driving from curve to straight path i.e. decreasing the steering angle. Transient behavior is studied in two common maneuvers performed in traffic: u-turn and double lane change.

#### 4.2.2.1 U-turn maneuver

U-turn maneuver is a great real-world example of how vehicles really move in traffic. It requires a lot of accuracy from the lateral controller. According to Suomen Paikallisliikenneliitto (2010) a two-axle bus should achieve a turning radius of 12 m measured from the middle of the front axle. To achieve a 12-m turning radius measured from the middle of the front axle the corresponding steering angle is:

$$\delta = \sin^{-1}\left(\frac{L_{wb}}{R_{fa}}\right) \approx 34{,}23°$$

This is used as a basis for constructing the movements of the leader bus. Leader bus is driven with a constant velocity of 5 m/s into a u-turn to the left. A slow velocity of 5 m/s is chosen because in reality such an extreme maneuver would be performed slowly. Also, higher velocity would increase centripetal acceleration into extremely uncomfortable levels. After the u-turn maneuver, the leader continues its path to the direction where it originally came from.

U-turn maneuver includes both increasing and decreasing of the steering angle i.e. path curvature. Therefore, both transient behavior aspects can be studied.

Figure 35 shows the results of u-turn maneuver tests. Pure Pursuit and Modified Pure Pursuit follow the leader bus quite well. Spline Pursuit and Circular Pursuit do not follow well and they start to oscillate after the maneuver. Furthermore, Spline Pursuit fails to get into the same lane after the maneuver.

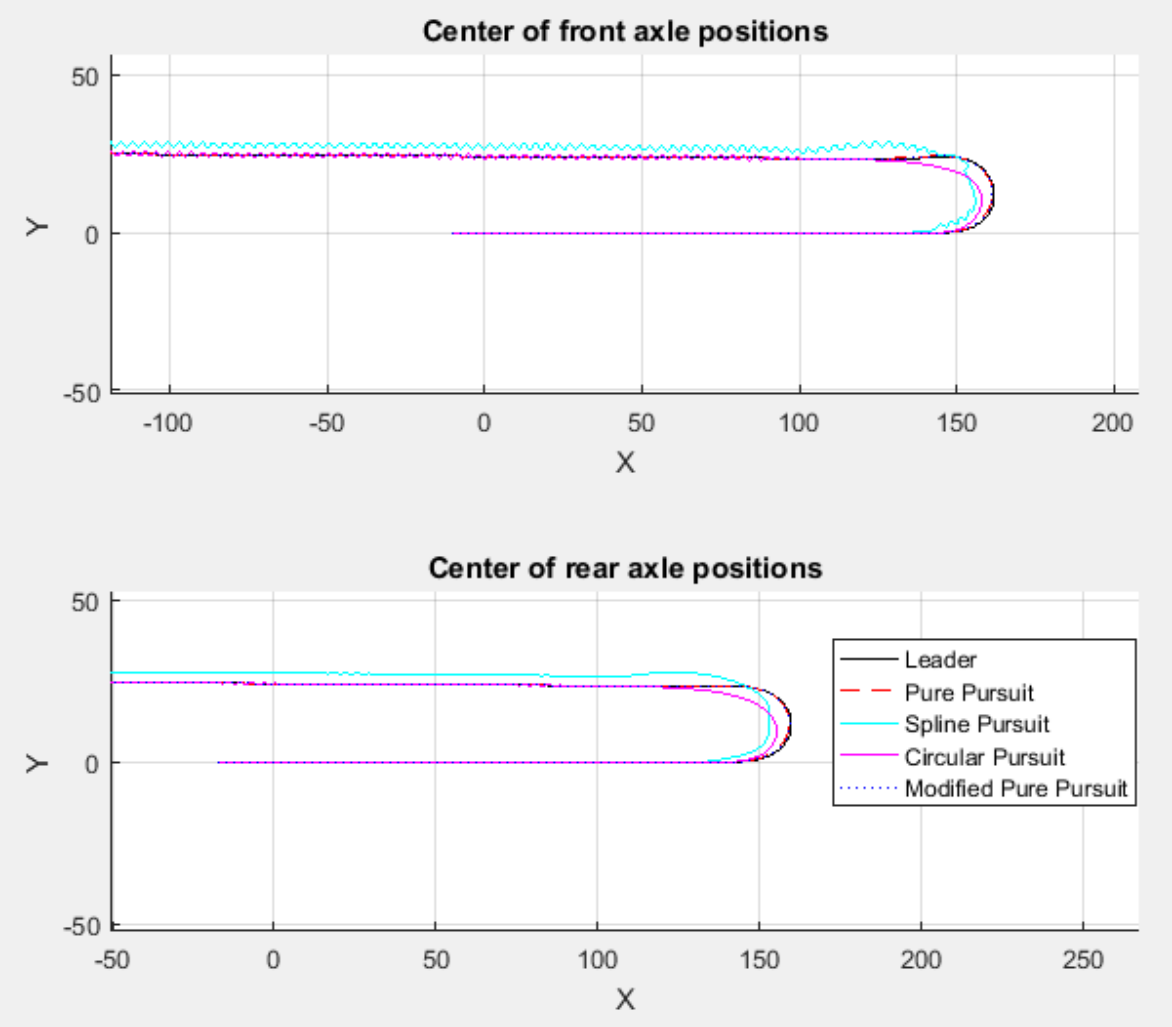


**Figure 35. U-turn maneuver test results.**

Close-up of u-turn maneuver test results (Figure 36) shows that Pure Pursuit and Modified Pure Pursuit turn follower bus at the start of the turn to the other direction than the direction of the turn. They also make the largest lateral error slightly after start of turn and cut the remainder path short at the end of turn.

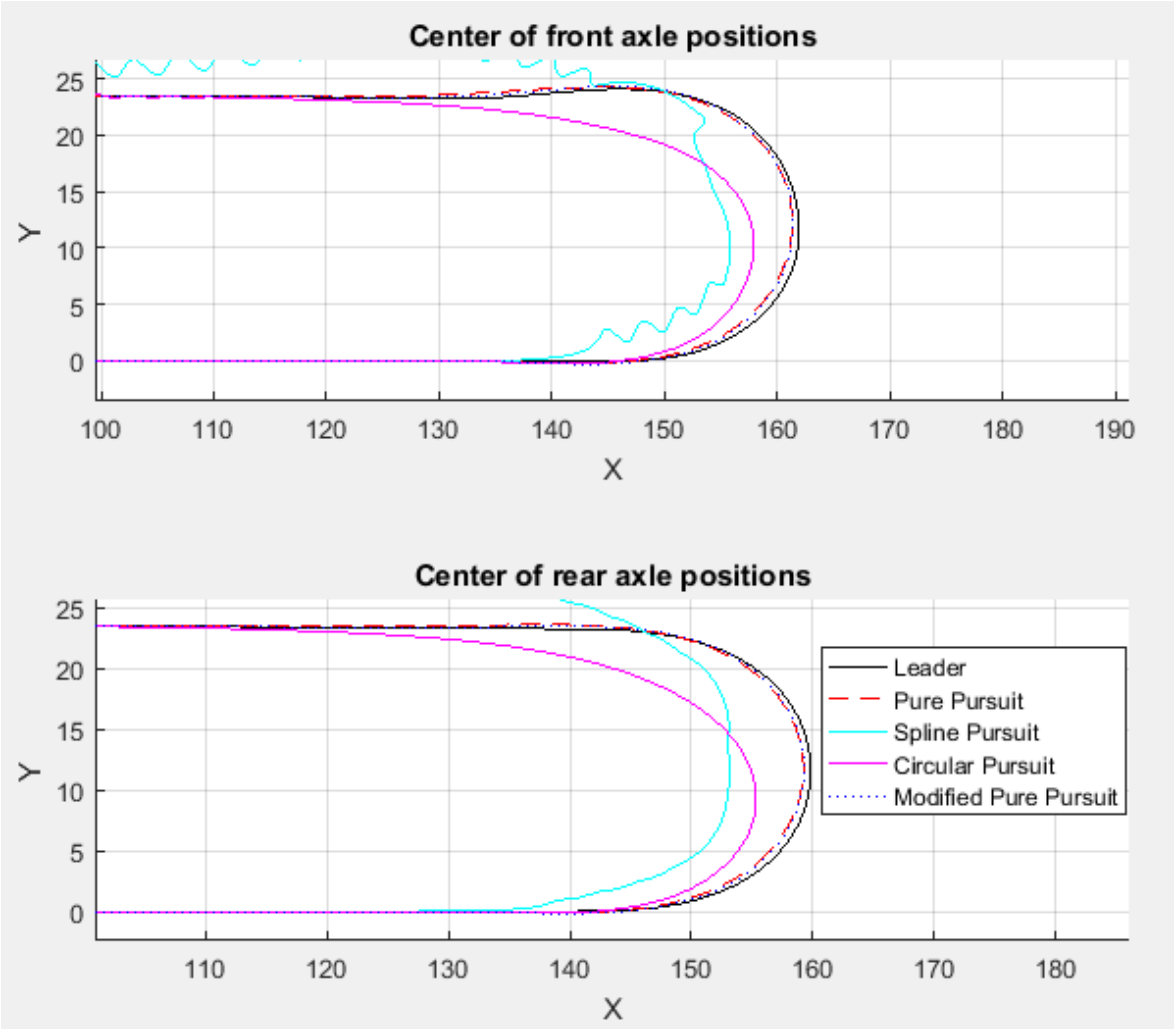


**Figure 36. Close-up of u-turn maneuver test results.**

Figure 37 shows close-up from the start of the maneuver. When measured from the middle of the front axle, Pure Pursuit makes maximum lateral error of under 0,2 m and Modified Pure Pursuit under 0,3 m.

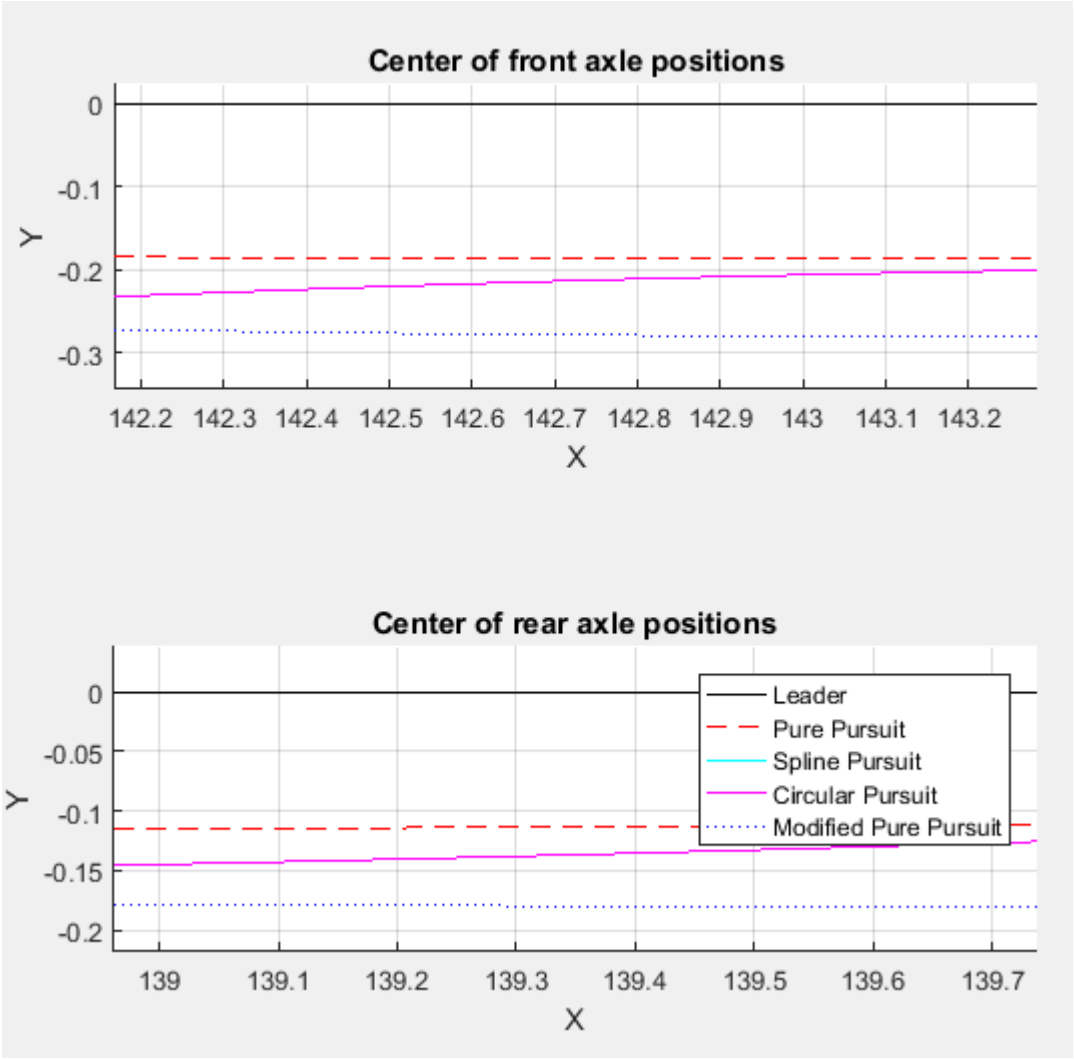


**Figure 37. Close-up of u-turn maneuver test results, start of turn.**

Figure 38 shows close-up of the turn where the largest lateral error occurs by Pure Pursuit and Modified Pure Pursuit. When measured from the middle of the front axle, Pure Pursuit makes maximum lateral error of about 0,8 m and Modified Pure Pursuit under 0,7 m.

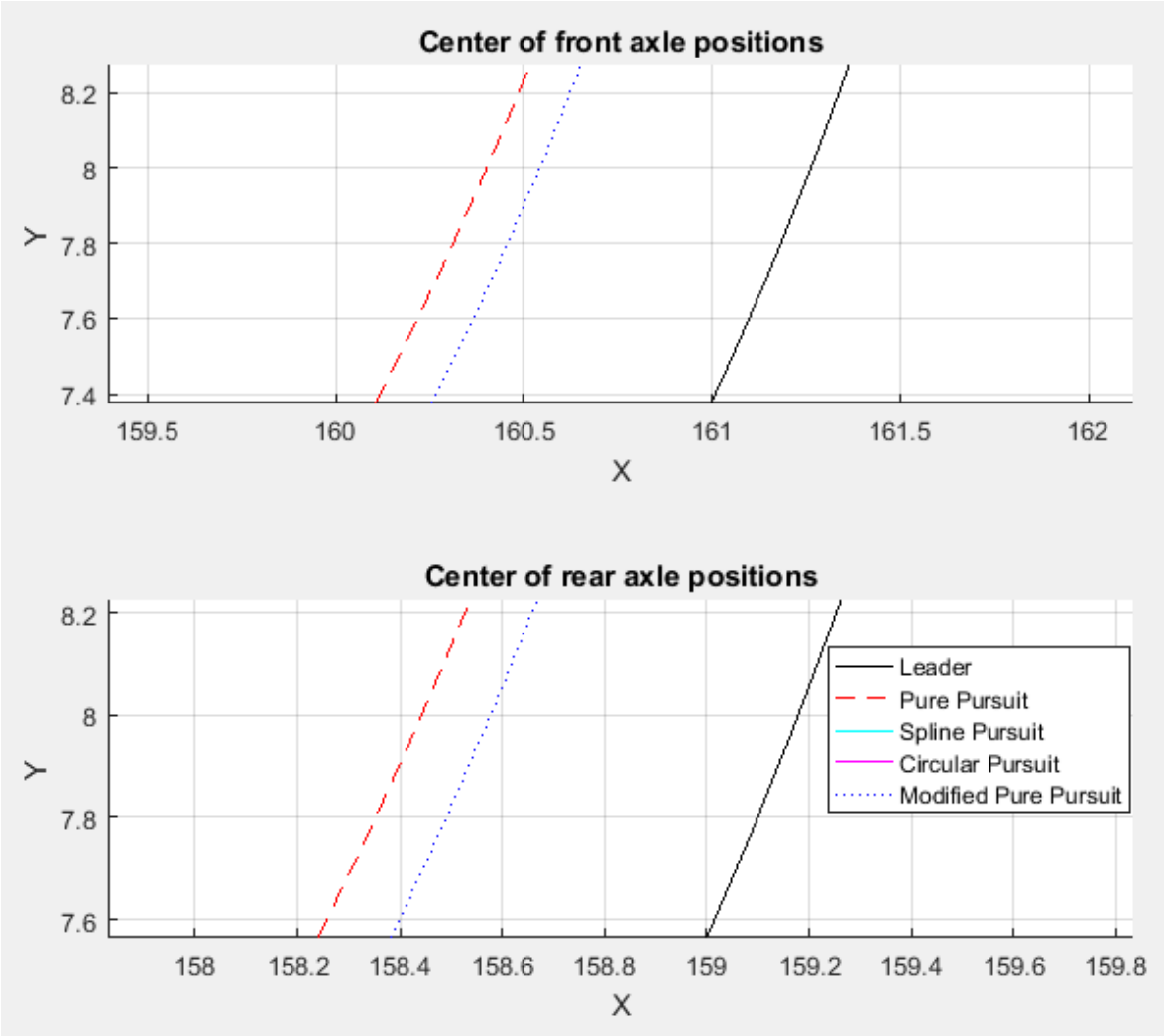


**Figure 38. Close-up of u-turn maneuver test results, largest lateral error.**

Figure 39 shows close-up from the end of the maneuver. When measured from the middle of the front axle, Pure Pursuit makes maximum lateral error of under 0,5 m and Modified Pure Pursuit under 0,3 m.

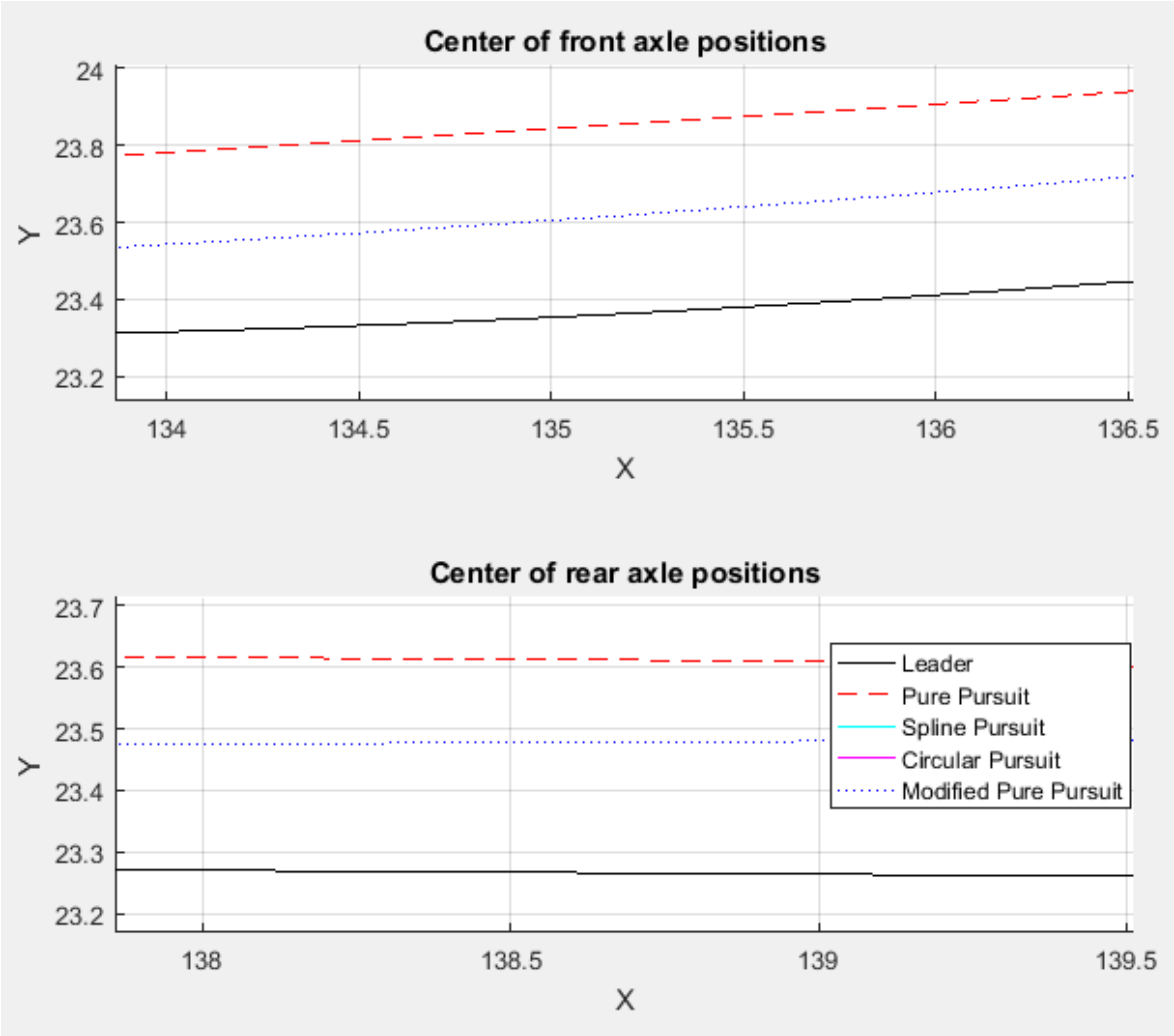


**Figure 39. Close-up of u-turn maneuver test results, end of turn.**

Spline Pursuit and Circular Pursuit fail to follow movements of the leader bus precisely. Pure Pursuit and Modified Pure Pursuit follow movements of the leader bus quite well. However, they both make similar errors at the start of the maneuver, slightly after start and when returning to straight driving. If measured by the maximum lateral error present, Modified Pure Pursuit performs the best of the studied methods in u-turn maneuver.

#### 4.2.2.2 Double lane change maneuver

Double lane change (DLC) maneuver represents regular traffic behavior when a vehicle tries to evade an obstacle on the road. The maneuver also resembles bus behavior when bus drives into a bus stop and leaves it. Figure 40 shows dimensions of Finnish bus stops. It can be seen that the width of a bus stop is similar to the width of a road line. Therefore, it is enough to study the behavior of the bus platoon only in double lane change maneuver because the results can be probably extrapolated into bus stop action.

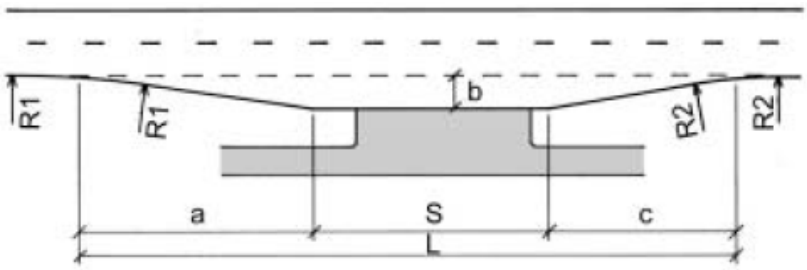


| Tyyppi | Nopeusrajoitus v (km/h) | a (m) | b (m) | c (m) | L [1] (m) | Pyöristyssäde | |
|---|---|---|---|---|---|---|---|
| | | | | | | $R_1$ (m) | $R_2$ (m) |
| $A_1$ | 30 - 50 | 20 | 3,0 | 15 | 60 | 40 | 20 |
| $A_2$ | 50 - 60 | 25 | 3,5 | 20 | 70 | 50 | 25 |
| $A_3$ | 80 - 100 | 35 | 4,0 | 25 | 85 | 60 | 30 |

*Taulukko: Seisontatilan S ohjearvot haja-asutusaleella ja taajamissa.*[2)]

HAJA-ASUTUSALUEELLA

| Linja-autoja samanaikaisesti pysäkillä | Seisontatila $S_{min}$ [m] |
|---|---|
| 1 | 25 |
| 2 | 43 |
| 3 | 61 |

TAAJAMISSA

| Linja-autoja samanaikaisesti | Mitoittava liikennetilanne | | | Seisontatila S [m] |
|---|---|---|---|---|
| | 2-akseliset | Teliautot | Nivelautot | |
| 1 | 1 | | | 16 |
| | | 1 | | 20 |
| | | | 1 | 23 |
| 2 | 2 | | | 33 |
| | | 2 | | 38 |
| | 1 | | 1 | 39 |
| | | | 2 | 45 |

[2)] Taulukoiden seisontatilan ohjearvot on määritetty 3 metrin ajoneuvovälillä. Jos pysäkki on tarve mitoittaa useammalle linja-autolle tai tarvetta on tehdä mahdolliseksi linja-autojen tulo ja lähtö toisistaan riippumatta sovelletaan tällöin seisontatilan mitoituksessa *liitteen 2* laskentakaavaa.

**Figure 40. Dimensions of Finnish bus stops. (Tiehallinto, 2003)**

Double lane change maneuver includes both increasing and decreasing of steering angle i.e. path curvature. It also includes maneuver (single lane change) after maneuver performed without settling time between which increases challenge to control laws. This action is not present in u-turn maneuver. Therefore, DLC maneuver is essential in studying the performance of the proposed control laws.

Double lane change maneuver simulations are driven with velocities of 5 m/s and 10 m/s. Higher velocities are not studied because it would increase the centripetal acceleration into extremely uncomfortable levels or otherwise the length of the maneuver would be very long and it would be performed with low steering angles. Low steering angle driving is not interesting to study anymore because steady-state behavior tests showed that largest lateral errors are happening with higher steering angle turns.

Figure 41 shows the results of double lane change maneuver tests with driving velocity of 5 m/s. Pure Pursuit and Modified Pure Pursuit follow the leader bus quite well. Spline Pursuit and Circular Pursuit do not follow well and they start to oscillate. Furthermore, Spline Pursuit fails to get into the same lane after the maneuver.

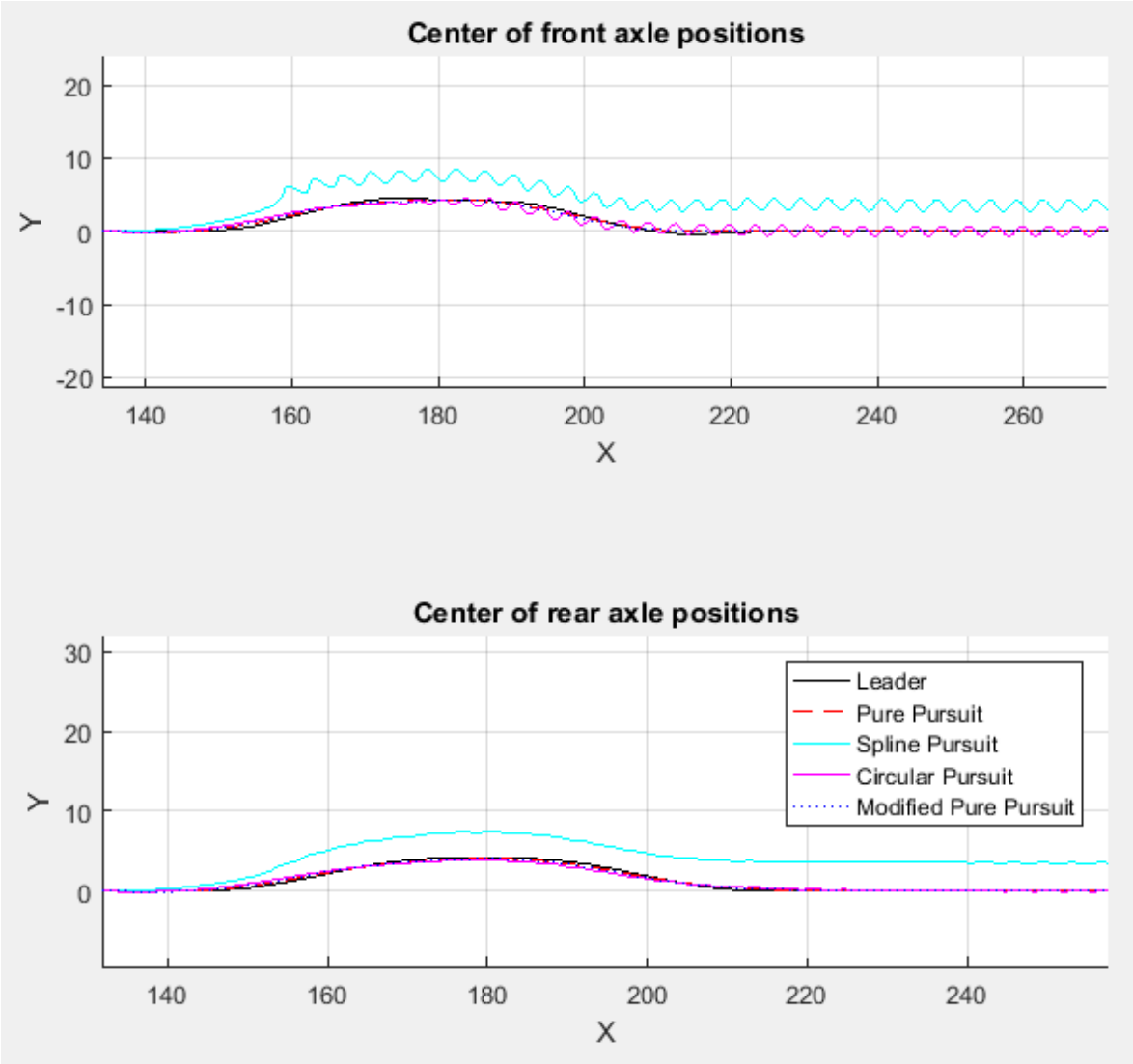


**Figure 41. Double lane change maneuver tests with driving velocity of 5 m/s.**

Figure 42 shows lateral errors performed by Pure Pursuit and Modified Pure Pursuit at the start of the maneuver. They visit the next lane slightly before turning to the direction of the leader bus. When measured from the middle of the front axle Pure Pursuit makes maximum lateral error of under 0,1 m and Modified Pure Pursuit under 0,15 m.

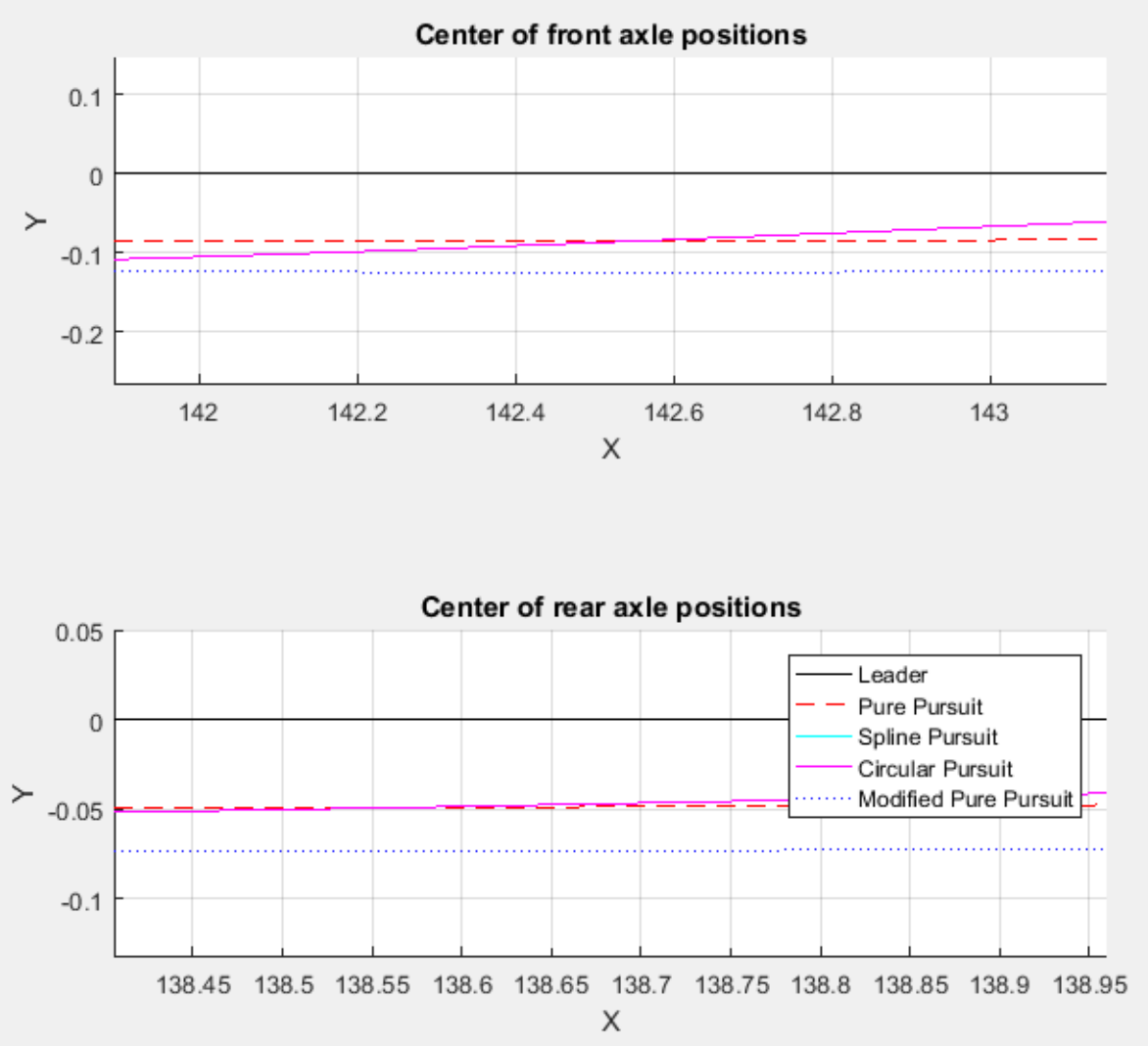


**Figure 42. Close-up of double lane change maneuver tests with driving velocity of 5 m/s, start of the maneuver.**

Figure 43 shows lateral errors performed by Pure Pursuit and Modified Pure Pursuit at after the start of the maneuver. When measured from the middle of the front axle Pure Pursuit makes maximum lateral error of about 0,4 m and Modified Pure Pursuit about 0,5 m.

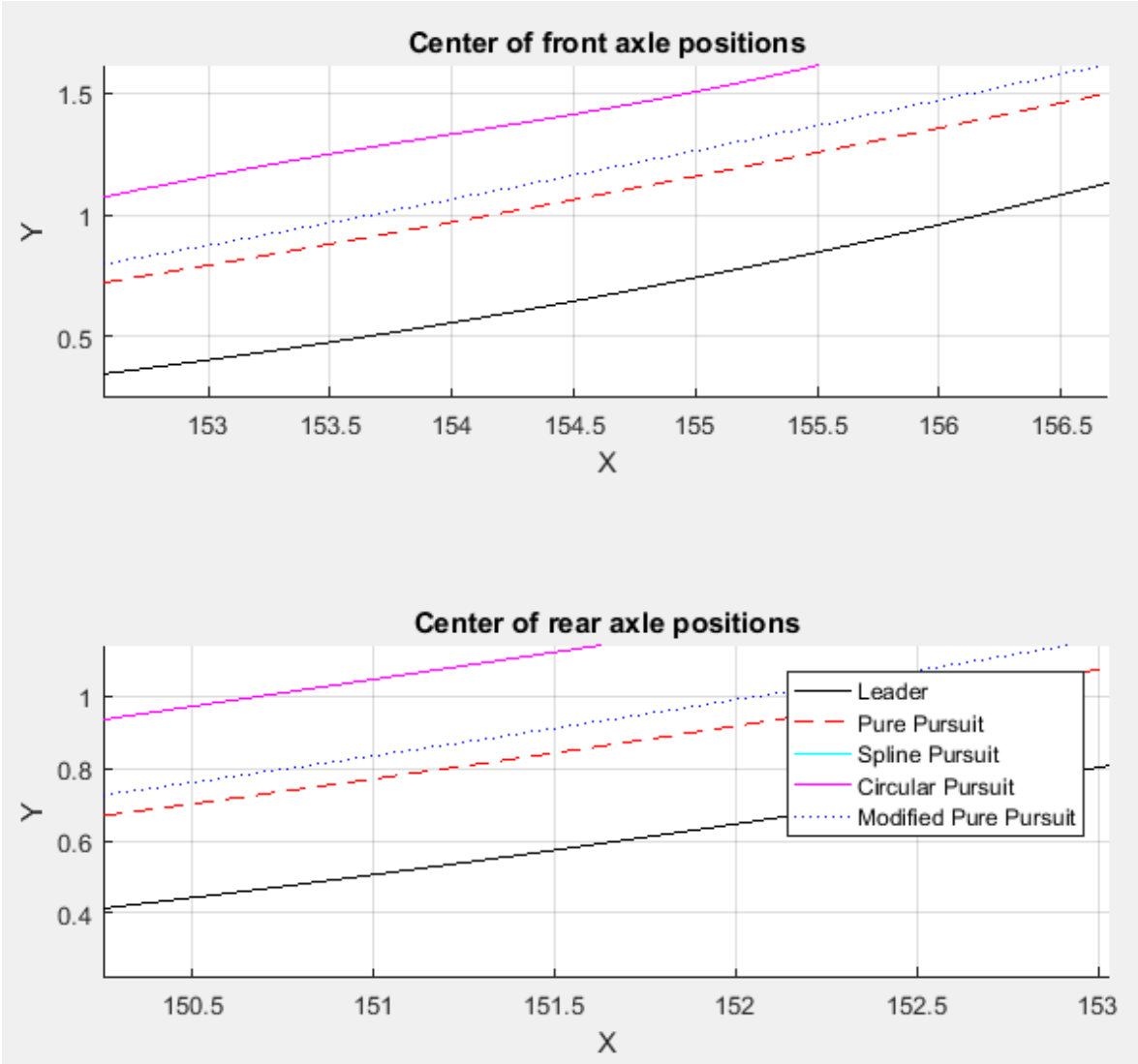


**Figure 43. Close-up of double lane change maneuver tests with driving velocity of 5 m/s, after start of the maneuver.**

Figure 44 shows lateral errors performed by Pure Pursuit and Modified Pure Pursuit at the middle of the maneuver. When measured from the middle of the front axle Pure Pursuit makes maximum lateral error of about 0,4 m and Modified Pure Pursuit under 0,5 m.

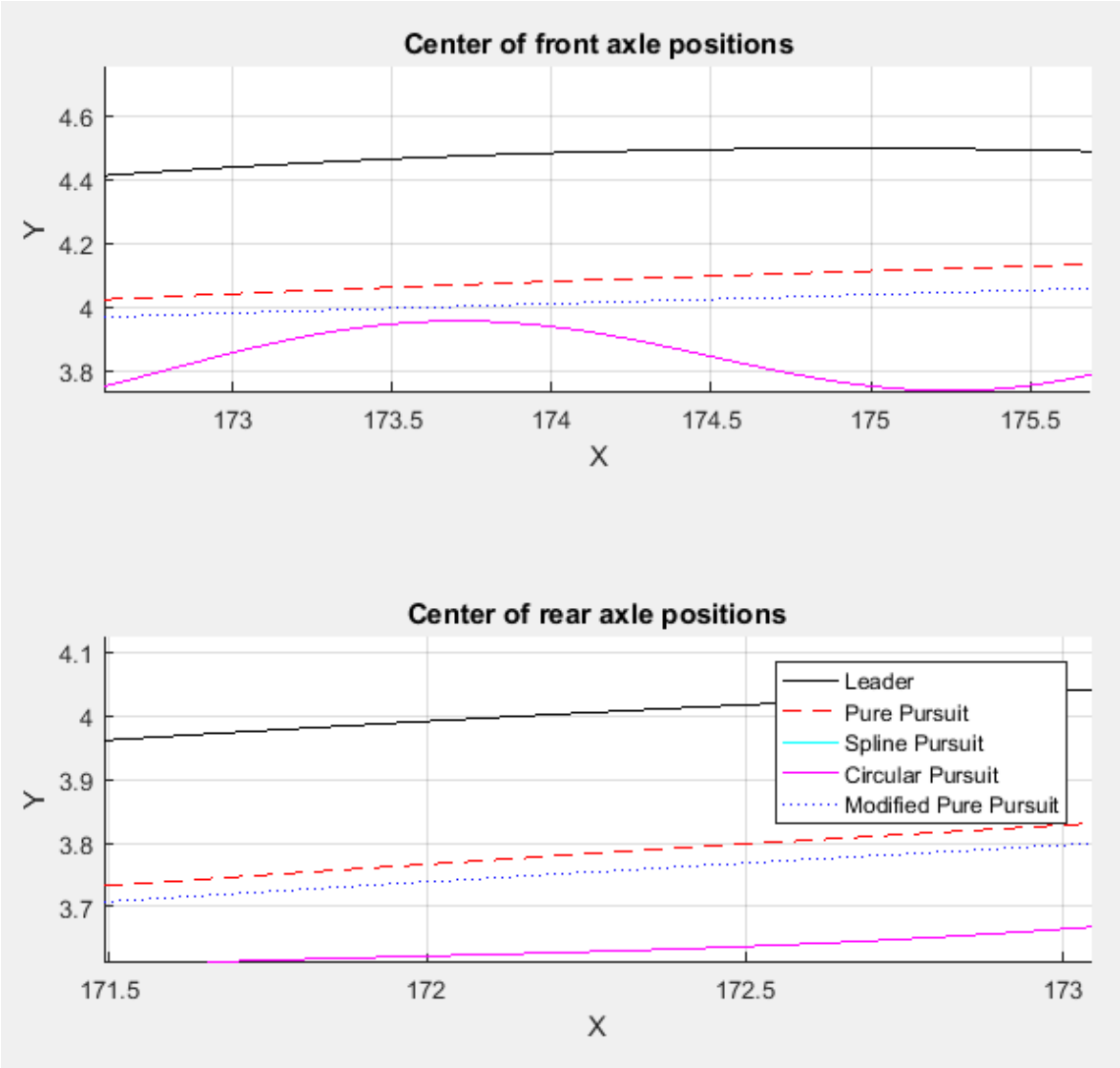


**Figure 44. Close-up of double lane change maneuver tests with driving velocity of 5 m/s, middle of the maneuver.**

Figure 45 shows lateral errors performed by Pure Pursuit and Modified Pure Pursuit at after the middle of the maneuver. When measured from the middle of the front axle Pure Pursuit makes maximum lateral error of about 0,4 m and Modified Pure Pursuit about 0,5 m.

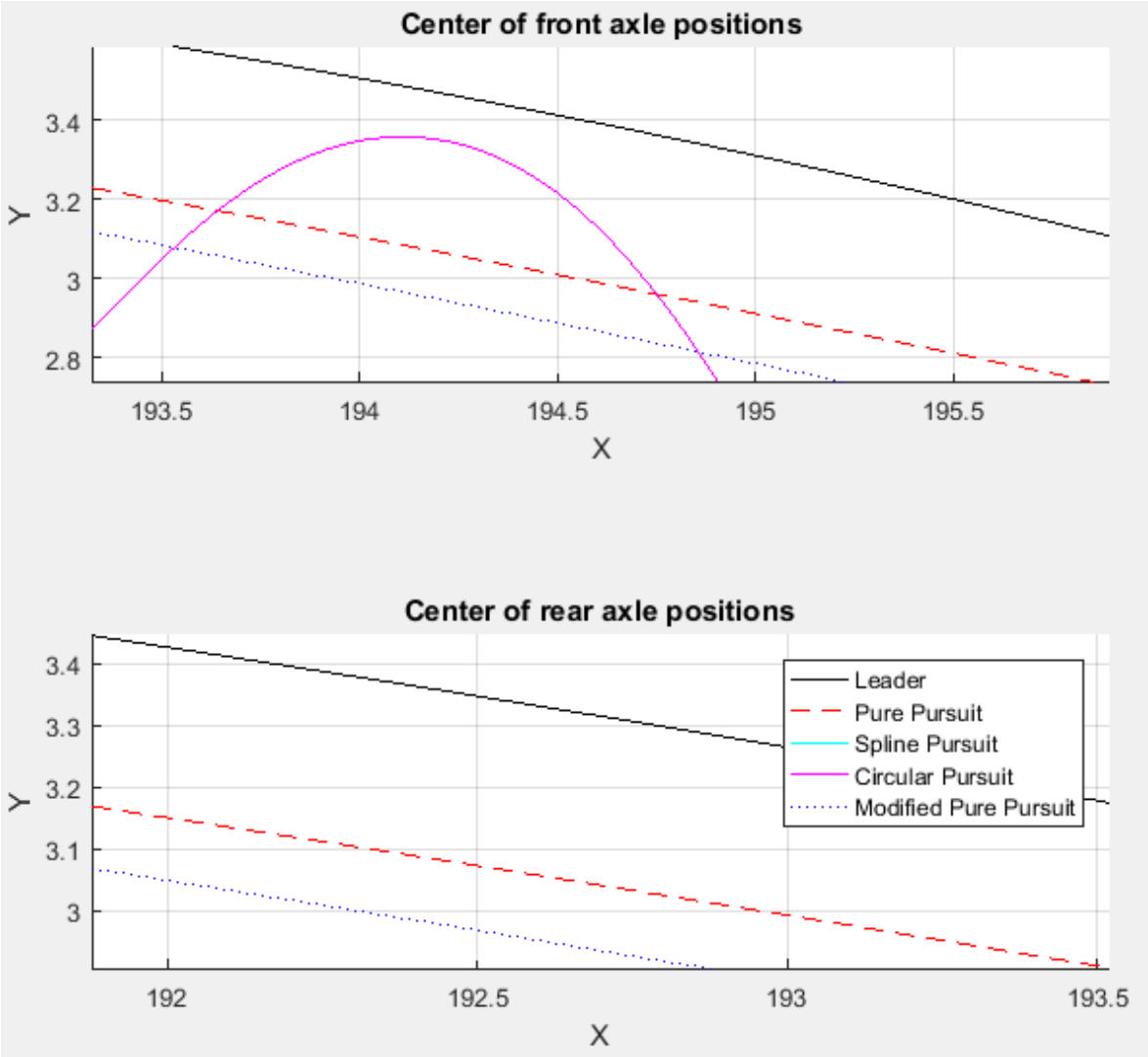


**Figure 45. Close-up of double lane change maneuver tests with driving velocity of 5 m/s, returning to the original lane.**

Figure 46 shows lateral errors performed by Pure Pursuit and Modified Pure Pursuit at the end of the maneuver. When measured from the middle of the front axle Pure Pursuit makes maximum lateral error of about 0,4 m and Modified Pure Pursuit under 0,5 m.

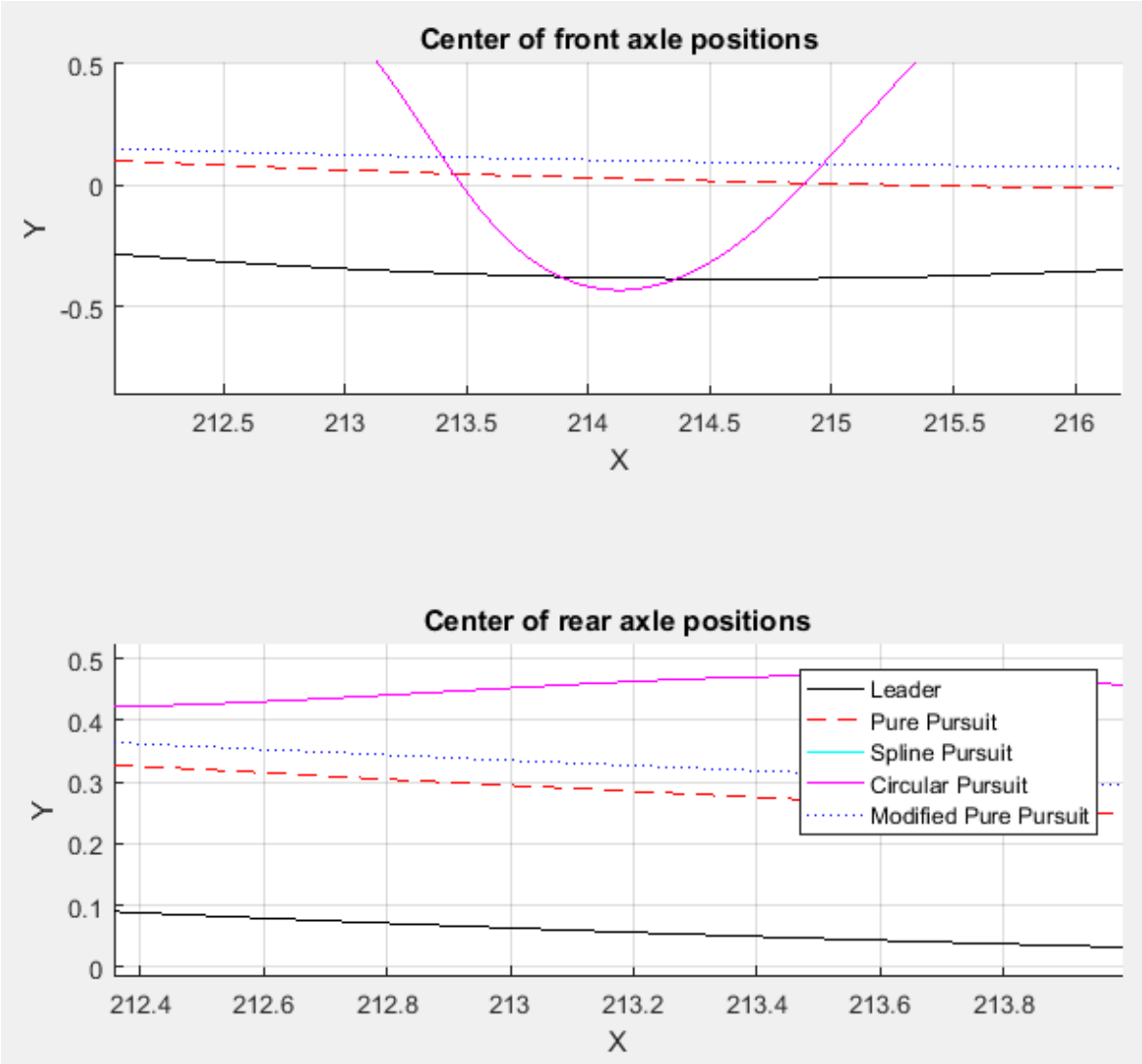


**Figure 46. Close-up of double lane change maneuver tests with driving velocity of 5 m/s, end of the maneuver.**

Figure 47 shows the results of double lane change maneuver tests with driving velocity of 10 m/s. Pure Pursuit and Modified Pure Pursuit follow the leader bus quite well. Spline Pursuit and Circular Pursuit do not follow well and they start to oscillate. Furthermore, Spline Pursuit fails to get into the same lane after the maneuver.

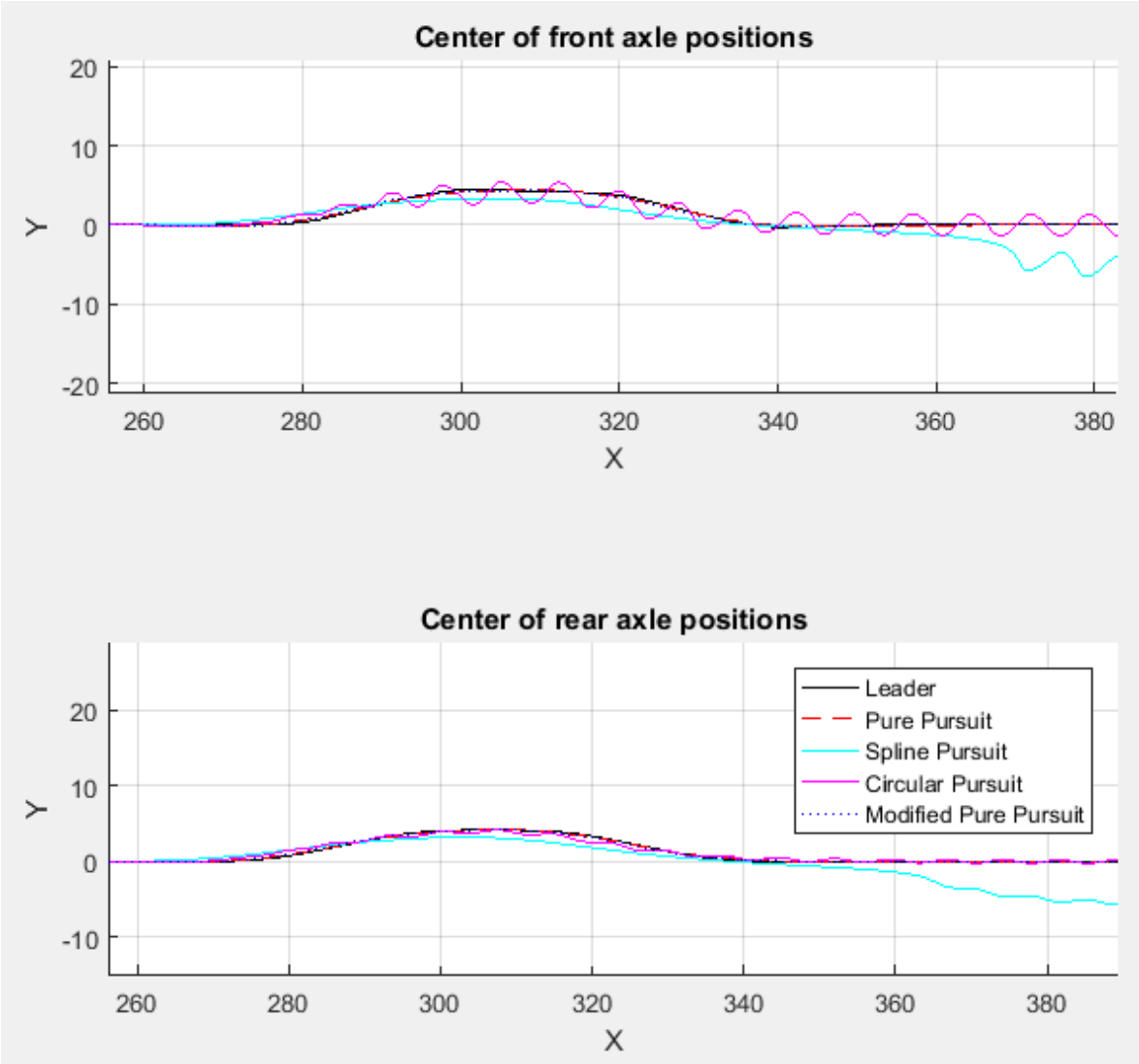


**Figure 47. Double lane change maneuver tests with driving velocity of 10 m/s.**

Figure 48 shows lateral errors performed by Pure Pursuit and Modified Pure Pursuit at the start of the maneuver. They visit the next lane slightly before turning to the direction of the leader bus. When measured from the middle of the front axle Pure Pursuit makes maximum lateral error of under 0,1 m and Modified Pure Pursuit under 0,2 m.

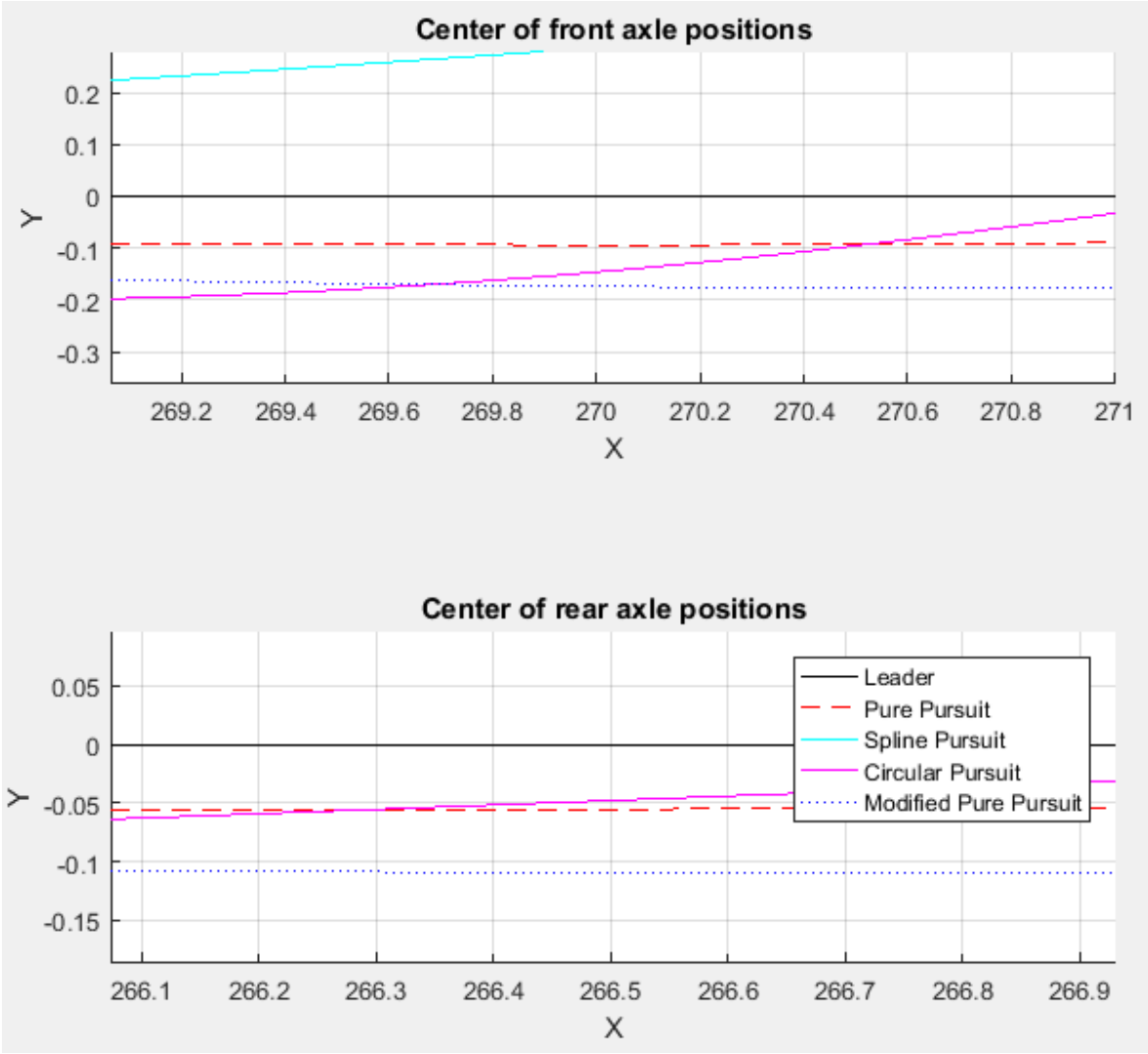


**Figure 48. Close-up of double lane change maneuver tests with driving velocity of 10 m/s, start of the maneuver.**

Figure 49 shows lateral errors performed by Pure Pursuit and Modified Pure Pursuit at after the start of the maneuver. When measured from the middle of the front axle Pure Pursuit makes maximum lateral error of about 0,3 m and Modified Pure Pursuit under 0,4 m.

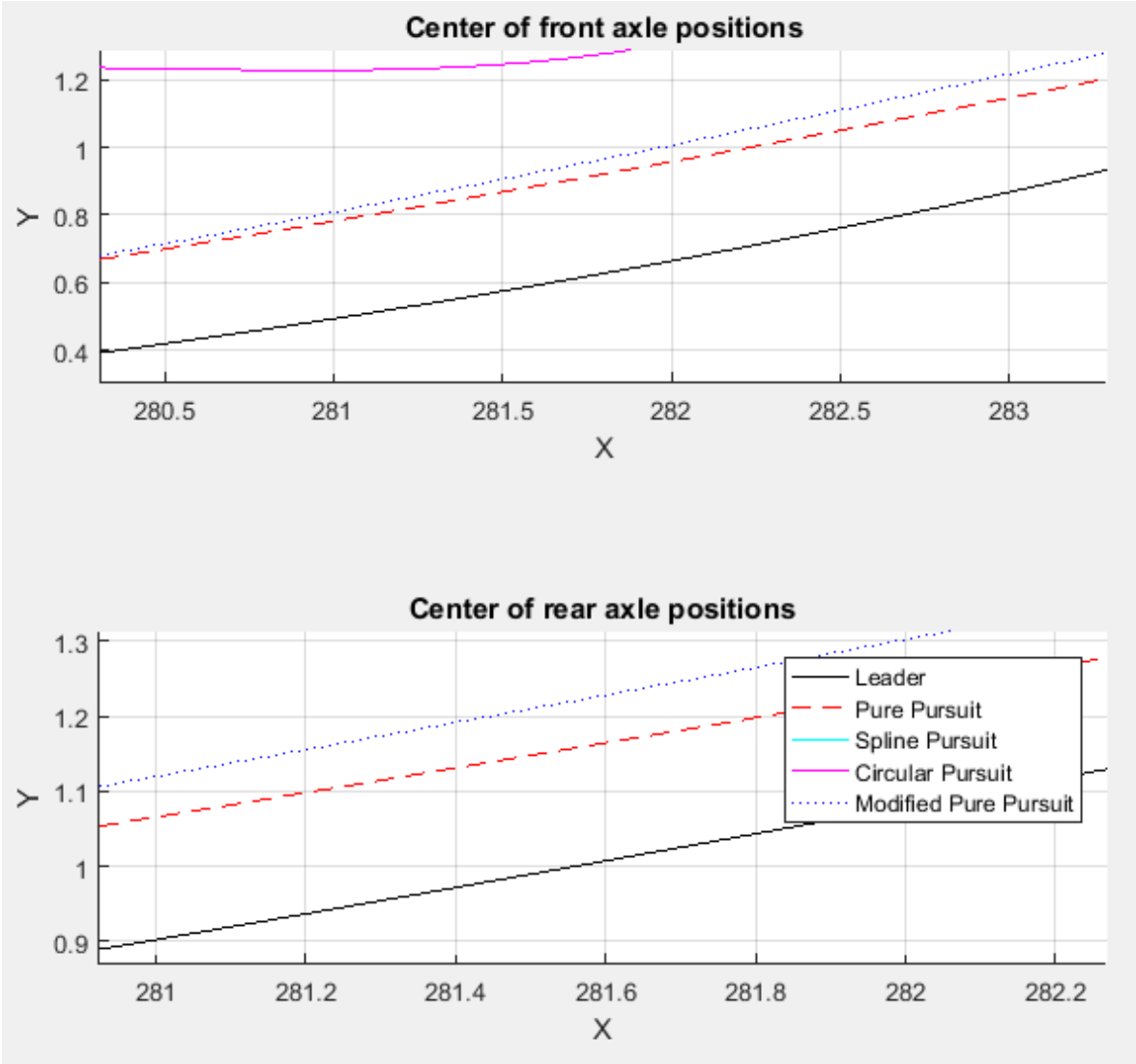


**Figure 49. Close-up of double lane change maneuver tests with driving velocity of 10 m/s, after start of the maneuver.**

Figure 50 shows lateral errors performed by Pure Pursuit and Modified Pure Pursuit at the middle of the maneuver. When measured from the middle of the front axle Pure Pursuit makes maximum lateral error of about 0,3 m and Modified Pure Pursuit under 0,3 m.

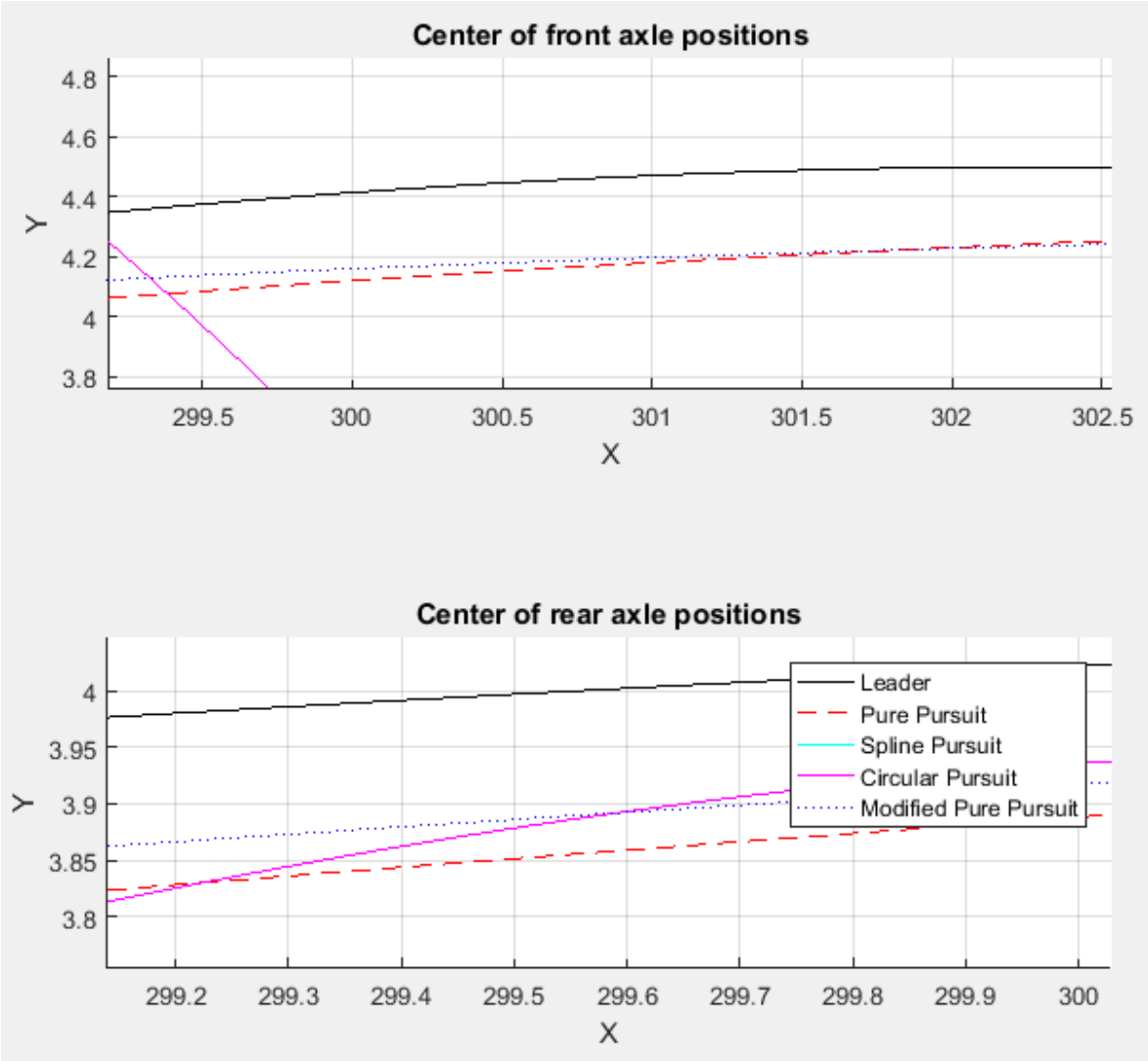


**Figure 50. Close-up of double lane change maneuver tests with driving velocity of 10 m/s, middle of the maneuver.**

Figure 51 shows lateral errors performed by Pure Pursuit and Modified Pure Pursuit at after the middle of the maneuver. When measured from the middle of the front axle Pure Pursuit makes maximum lateral error of under 0,3 m and Modified Pure Pursuit under 0,4 m.

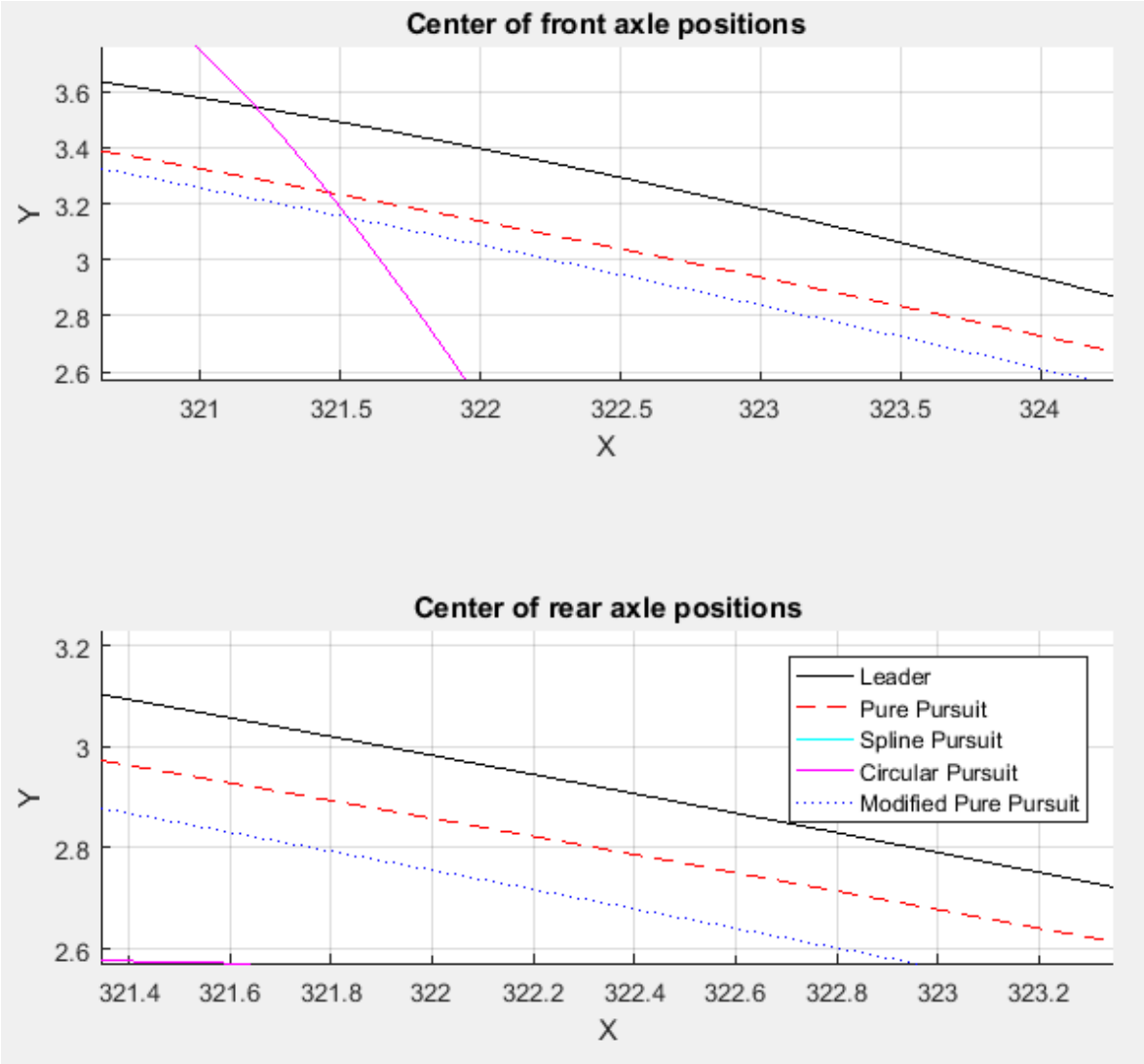


**Figure 51. Close-up of double lane change maneuver tests with driving velocity of 10 m/s, returning to the original lane.**

Figure 52 shows lateral errors performed by Pure Pursuit and Modified Pure Pursuit at the end of the maneuver. When measured from the middle of the front axle Pure Pursuit makes maximum lateral error of under 0,3 m and Modified Pure Pursuit under 0,3 m.

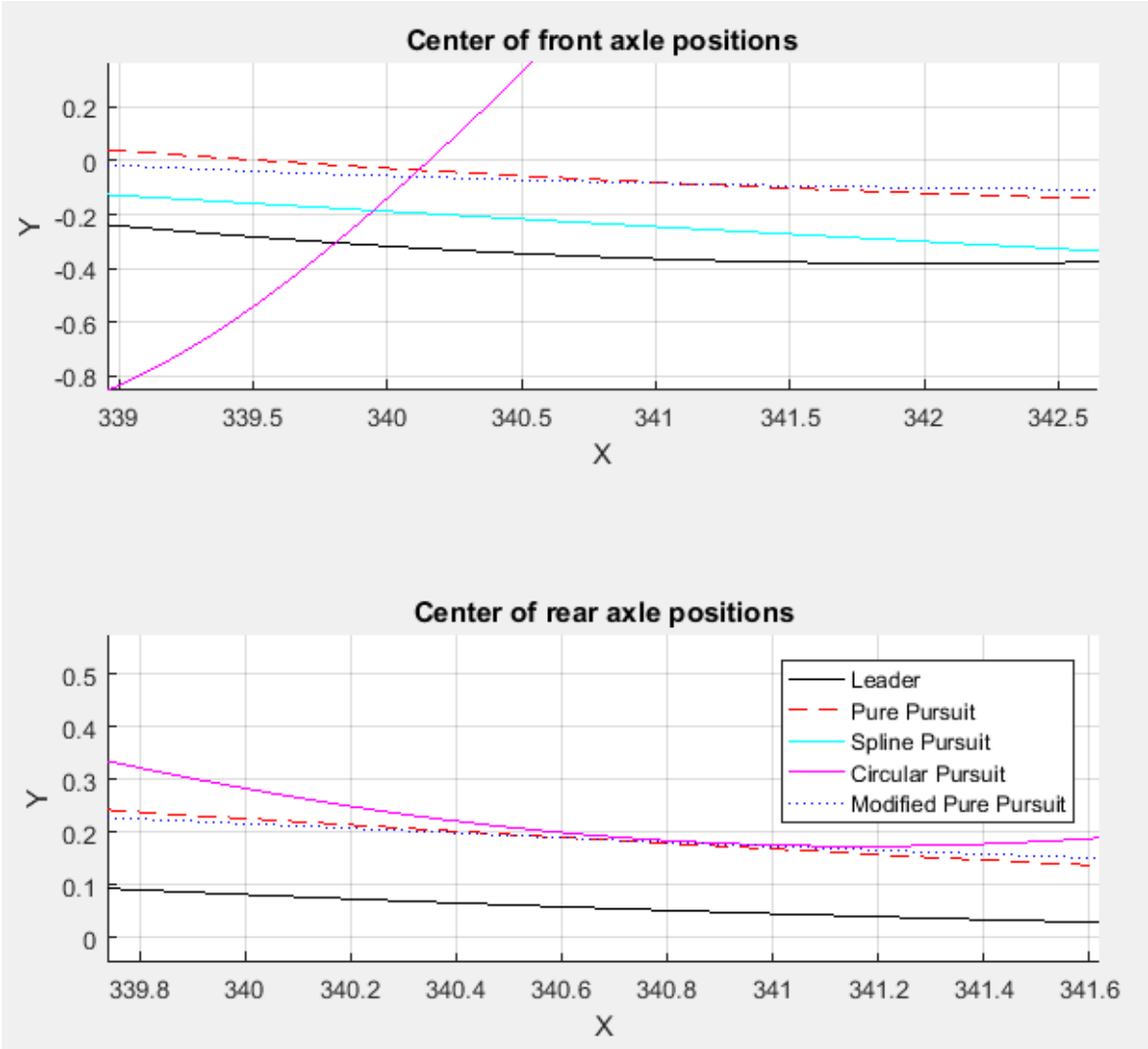


**Figure 52. Close-up of double lane change maneuver tests with driving velocity of 10 m/s, end of the maneuver.**

Spline Pursuit and Circular Pursuit fail to follow movements of the leader bus precisely. Pure Pursuit and Modified Pure Pursuit follow movements of the leader bus quite well. However, they both make similar errors during the maneuver. If measured by the maximum lateral error performed, Pure Pursuit performs the best of the studied methods in double lane change maneuver. Both Pure Pursuit and Modified Pure Pursuit perform better in terms of lateral error with driving velocity of 10 m/s than with 5 m/s.

# 5 Discussion

## 5.1 Conclusion

Longitudinal and lateral control of a vehicle have been studied extensively in the literature. Longitudinal control has also been implemented in commercial applications. Cruise Control and Adaptive Cruise Control are applications of that. However, commercial applications of ACC use very long inter-vehicular distances, which are not suitable for platoons.

Most lateral control research has concentrated on vehicle path following problem: how to control a vehicle to force it to follow a predefined path precisely. This control method must include a path generation procedure for it to be suitable for control of a platoon. This two-part hierarchy increases its computational complexity. Some lateral control research has concentrated on a direct vehicle following methods. They are computationally easy but are not as precise as path following methods. This is probably due to the fact that they are not designed to follow a given path.

A simulation model consisting of two identical buses was built to test proposed lateral and longitudinal controllers. One longitudinal controller and four lateral control laws were designed. More effort was put into lateral control because longitudinal control is already very thoroughly investigated. However, longitudinal control in extreme turning maneuvers was studied more precisely because buses must be able to perform routinely extreme maneuvers when compared to their physical size. Lateral control laws proposed for direct vehicle following were Pure Pursuit, Spline Pursuit, Circular Pursuit and Modified Pure Pursuit. They were all geometrical methods by nature and were based on direct vehicle following.

The performance of the longitudinal controller was studied in two stages: set-up with initial distance and acceleration and deceleration tests. Longitudinal controller performed well with initial distance ranging from 2 to 10 m. It also did well in acceleration and deceleration tests when both buses were loaded with same payloads. However, it failed when the follower was loaded much more with additional mass than the leader.

The performance of proposed lateral controllers was studied in two stages: first their steady-state behavior and second their transient behavior was tested. In steady-state tests, Pure Pursuit slightly out-performed Modified Pure Pursuit by corresponding maximum lateral errors of 0,8 m and 1,1 m measured from the middle of the front axle. Spline Pursuit showed very oscillatory behavior and sometimes failed to follow the leader bus. Circular Pursuit was able to follow the leader with small to medium steering angles with small driving velocities. Otherwise, it became oscillatory and even failed to follow the leader at tighter turns.

Transient behavior tests included u-turn and double lane change maneuvers. In u-turn test, Modified Pure Pursuit slightly out-performed Pure Pursuit by corresponding maximum lateral errors of 0,7 m and 0,8 m measured from the middle of the front axle. In DLC tests Pure Pursuit slightly out-performed Modified Pure Pursuit by corresponding maximum lateral errors of 0,4 m and 0,5 m (5 m/s) and 0,3 m and 0,4 m (10 m/s) measured from the middle of the front axle. In all transient behavior tests, Circular Pursuit followed poorly the leader bus and became oscillatory. Spline Pursuit performed the worst by following

poorly, becoming oscillatory and showing inability to get into the same lane with the leader after the maneuver.

Lateral errors produced by the Pure Pursuit and Modified Pure Pursuit do not meet the requirements originally placed in the study, which was under 0,1 m. Even though the requirement was tight, the lateral errors produced by the methods are not acceptable. Buses are large vehicles and are required to perform precise maneuvers when compared to their size. Especially u-turn must be usually performed very precisely. Lateral errors present in DLC tests were closer to being acceptable because such a maneuver does not require so precise movements. Therefore, Pure Pursuit and Modified Pure Pursuit could be used, if tuned, in controlling movements of a bus in lane changing operations but not for tight turns. The Spline Pursuit and Circular Pursuit methods seemed promising in theory, but they did not work in simulations as designed.

If a more precise lateral control method is found, Pure Pursuit or Modified Pure Pursuit could be used as a back-up control method in a case of failure of the main control method. These methods are computationally light so, if an application provides little computational power and does not require precise movements, these methods could be used.

The results of this study cannot be directly compared to other results in the literature because most of the existing research is conducted using an ordinary size car in simulations. A car has usually two times smaller dimensions than a bus, which obviously affects results. Wirtanen studied the control of a bus platoon and achieved promising results with a path following lateral control method named Polynomial algorithm. However, his simulation model might have been more idealistic than the one used in this study.

I should have included the comparison of an existing lateral control method into the study to be able to make a comparison. None of the studied lateral control methods have been implemented in the way they were in this study. Even though Pure Pursuit method has been studied may times in the literature, it has been implemented using path following approach, not direct following. These two approaches using Pure Pursuit cannot be compared, because they are fundamentally different. The idea here was to study if Pure Pursuit method would work with direct vehicle following approach.

Now, more insight has been gathered into the demands of tight turns on longitudinal controller. Also, two promising lateral control methods have been proposed that need further investigation.

## 5.2 Further research

Minimum target distance was arbitrarily and experimentally defined in this study to meet the demands of tight turns. Defining just a constant value for it did not meet the geometric requirements of extreme maneuvers. One possible way to define longitudinal control would be to control look ahead distance instead of distance. Look ahead distance means here the distance from the reference point of the follower to the corresponding reference point of the leader. It could be for instance the distance from the center of the follower's rear axle to the center of the leader's rear axle as defined in Pure Pursuit method. This change would decrease the complexity of the longitudinal controller and possibly affect the performance of the lateral controller. This is due to some of the lateral control laws proposed used look ahead distance as an input for the control law.

To be able to compare proposed control laws with other lateral control methods existing in the literature, it is mandatory to make a comparative study. Proposed Pure Pursuit and Modified Pure Pursuit methods could be compared to path following based methods. Straight conclusions about the performance between the methods cannot be made because different studies use different simulation models and parameters that affect the study results. Also, most of the research about lateral control of a vehicle use an ordinary size car as a simulation test vehicle, which makes it impossible to compare the results of this study to others.

Simulations were performed on a self-made platform that does not describe the reality thoroughly. It would be beneficial to conduct further simulations on a more sophisticated simulation software for instance CarSim to validate the results of this study.

# References


Ali, A., Garcia, G., & Martinet, P. (2013, July). Minimizing the Inter-vehicle Distances of the Time Headway Policy for Platoon Control on Highways. In ICINCO (2) (pp. 417-424).

Ali, A., Garcia, G., & Martinet, P. (2013, October). Minimizing the inter-vehicle distances of the time headway policy for urban platoon control with decoupled longitudinal and lateral control. In Intelligent Transportation Systems-(ITSC), 2013 16th International IEEE Conference on (pp. 1805-1810). IEEE. DOI: 10.1109/ITSC.2013.6728490. Electronic ISBN: 978-1-4799-2914-6 Print ISSN: 2153-0009 Electronic ISSN: 2153-0017.

Al-Mayyahi, A., Wang, W., & Birch, P. (2015, January). Path tracking of autonomous ground vehicle based on fractional order PID controller optimized by PSO. In Applied Machine Intelligence and Informatics (SAMI), 2015 IEEE 13th International Symposium on (pp. 109-114). IEEE. DOI: 10.1109/SAMI.2015.7061857. Electronic ISBN: 978-1-4799-8221-9.

Attia, R., Orjuela, R., & Basset, M. (2014). Combined longitudinal and lateral control for automated vehicle guidance. Vehicle System Dynamics, 52(2), 261-279. DOI: 10.1080/00423114.2013.874563.

Belkhouche, F., & Belkhouche, B. (2005, August). Modeling and controlling a robotic convoy using guidance laws strategies. IEEE Transactions on Systems, Man, and Cybernetics, Part B (Cybernetics), 35(4), 813-825. DOI: 10.1109/TSMCB.2005.846646. Print ISSN: 1083-4419 Online ISSN: 1941-0492.

Belkhouche, F., & Belkhouche, B. (2005, November). A method for robot navigation toward a moving goal with unknown maneuvers. Robotica, 23(06), 709-720. DOI:10.1017/S0263574704001523.

Bergenhem, C., Huang, Q., Benmimoun, A., & Robinson, T. (2010, October). Challenges of platooning on public motorways. In 17th world congress on intelligent transport systems (pp. 1-12).

Chan, E. (2014). SARTRE automated platooning vehicles. Towards Innovative Freight and Logistics, 137-150. DOI: 10.1002/9781119307785.ch10.

Chan, E., Gilhead, P., Jelinek, P., Krejci, P., & Robinson, T. (2012). Cooperative control of SARTRE automated platoon vehicles. In 19th ITS World Congress.

Continental. (2016). SRR 20X /-2 /-2C /-21 Short Range Radar. URL: http://www.conti-online.com/www/download/industrial_sensors_de_en/themes/download/srr20x_datasheet_en.pdf. Accessed: 10.5.2017.

Dávila, A., & Nombela, M. (2010, September). Sartre: Safe road trains for the environment. In Conference on Personal Rapid Transit PRT@ LHR (Vol. 3, pp. 2-3). URL: http://www.princeton.edu/~alaink/Orf467F10/PRT@LHR10_Conf/Arturo_Davila_prez_SafeTrains.pdf. Accessed: 16.5.2017.

Elbanhawi, M., Simic, M., & Jazar, R. N. (2015). Continuous path smoothing for car-like robots using B-spline curves. Journal of Intelligent & Robotic Systems, 80(1), 23-56. DOI: 10.1007/s10846-014-0172-0. ISSN: 0921-0296 (Print) 1573-0409 (Online).

Eskandarian, A. (Ed.). (2012). Handbook of intelligent vehicles. London: Springer. DOI 10.1007/978-0-85729-085-4. ISBN: 978-0-85729-084-7 e-ISBN: 978-0-85729-085-4.

Feng, S., Wang, W., & Zhang, H. (2013). Three-dimensional pursuer convoy by using guidance laws. Journal of Control Theory and Applications, 11(3), 442-453. DOI: 10.1007/s11768-013-2012-3.

Göhring, D., Wang, M., Schnürmacher, M., & Ganjineh, T. (2011, December). Radar/lidar sensor fusion for car-following on highways. In Automation, Robotics and Applications (ICARA), 2011 5th International Conference on (pp. 407-412). IEEE. DOI: 10.1109/ICARA.2011.6144918. Electronic ISBN: 978-1-4577-0330-0 Print ISBN: 978-1-4577-0329-4.

Götting. (2014). Laser Scanner HG 43600-A. URL: http://www.goetting-agv.com/dateien/downloads/HG_43600-A_E_data-sheet_R06_TD.pdf. Accessed: 12.5.2017.

Hellstrom, T., & Ringdahl, O. (2006). Follow the Past: a path-tracking algorithm for autonomous vehicles. International journal of vehicle autonomous systems, 4(2-4), 216-224. DOI: 10.1504/IJVAS.2006.012208. Print ISSN: 1471-0226 Online ISSN: 1741-5306.

Hoffmann, G. M., Tomlin, C. J., Montemerlo, M., & Thrun, S. (2007, July). Autonomous automobile trajectory tracking for off-road driving: Controller design, experimental validation and racing. In American Control Conference, 2007. ACC'07 (pp. 2296-2301). IEEE. DOI: 10.1109/ACC.2007.4282788. Print ISBN: 1-4244-0988-8 Print ISSN: 0743-1619 Electronic ISSN: 2378-5861.

HSL. (2014). Helsingin seudun liikenne. Ympäristöraportti 2014. URL: https://www.hsl.fi/sites/default/files/uploads/hsl_ymparistoraportti_2014.pdf. Accessed: 12.5.2017.

Jansen, W. L. (2016). Lateral Path-Following Control of Automated Vehicle Platoons. URL: http://resolver.tudelft.nl/uuid:8f04196b-e62b-4bfa-93c8-ccd21785f2c5.

Karl, J. Å., & Hägglund, T. (1995). PID controllers: theory, design and tuning. ISBN: 978-1-55617-516-9.

Khodayari, A., Ghaffari, A., Ameli, S., & Flahatgar, J. (2010, September). A historical review on lateral and longitudinal control of autonomous vehicle motions. In Mechanical and Electrical Technology (ICMET), 2010 2nd International Conference on (pp. 421-429). IEEE. DOI: 10.1109/ICMET.2010.5598396. Electronic ISBN: 978-1-4244-8102-6 Print ISBN: 978-1-4244-8100-2.

Kim, D. H., Han, C. S., & Lee, J. Y. (2013). Sensor-based motion planning for path tracking and obstacle avoidance of robotic vehicles with nonholonomic constraints. Proceedings of the Institution of Mechanical Engineers, Part C: Journal of Mechanical Engineering Science, 227(1), 178-191. DOI: 10.1177/0954406212446900. ISSN: 0954-4062 Online ISSN: 2041-2983.

Lam, S., & Katupitiya, J. (2013, June). Modeling and control of a platoon of autonomous buses. In Intelligent Vehicles Symposium (IV), 2013 IEEE (pp. 958-963). IEEE. DOI: 10.1109/IVS.2013.6629590. Electronic ISBN: 978-1-4673-2755-8 Print ISSN: 1931-0587.

Linkker. (2017). Technology. Linkker 12+. URL: http://www.linkkerbus.com/technology/. Accessed: 15.5.2017.

Litman, T. (2014). Autonomous vehicle implementation predictions. Victoria Transport Policy Institute, 28.

Mariottini, G. L., Morbidi, F., Prattichizzo, D., Vander Valk, N., Michael, N., Pappas, G., ... & Daniilidis, K. (2008). Vision-based Localization and Control of Leader-Follower Formations. In 2007 IEEE International Conference on Robotics and Automation (pp. 2403-2408). URL: http://www.cis.upenn.edu/~kostas/mypub.dir/mariottini08ro.pdf.

Matko, D., Klancar, G., Blazic, S., Simonin, O., Gechter, F., Contet, J. M., & Gruer, P. (2008, May). The Application of Reference-path Control to Vehicle Platoons. In ICINCO-RA (1) (pp. 145-150). URL: http://perso.citi.insa-lyon.fr/osimonin/OSimonin/travaux/ICINCO_Matko.pdf.

Milanés, V., Pérez, J., Onieva, E., González, C., & De Pedro, T. (2009, May). Electric power controller for steering wheel management in electric cars. In Compatibility and Power Electronics, 2009. CPE'09. (pp. 444-449). IEEE. DOI: 10.1109/CPE.2009.5156075. Print ISBN: 978-1-4244-2855-7 Print ISSN: 2166-9538 Electronic ISSN: 2166-9546.

Naranjo, J. E., González, C., García, R., De Pedro, T., & Haber, R. E. (2005). Power-steering control architecture for automatic driving. IEEE Transactions on Intelligent Transportation Systems, 6(4), 406-415. DOI: 10.1109/TITS.2005.858622. Print ISSN: 1524-9050 Online ISSN: 1558-0016.

Ng, T. C., Guzman, J. I., & Adams, M. D. (2005, August). Autonomous vehicle-following systems: A virtual trailer link model. In Intelligent Robots and Systems, 2005.(IROS 2005). 2005 IEEE/RSJ International Conference on (pp. 3057-3062). IEEE. DOI: 10.1109/IROS.2005.1545427. Print ISBN: 0-7803-8912-3.

Oshima, D. 2016. Development of an evaluation tool for the impact assessment of Automated Driving Systems on CO2 emissions. Pacific Consultants. 23 p. URL: http://en.sip-adus.jp/evt/workshop2016/file/evt_ws2016_s6_DaisukeOshima.pdf. Accessed: 12.5.2017.

Park, M., Lee, S., & Han, W. (2015). Development of steering control system for autonomous vehicle using geometry-based path tracking algorithm. ETRI Journal, 37(3), 617-625. DOI: 10.4218/etrij.15.0114.0123.

Pauwelussen, J. (2014). Essentials of vehicle dynamics. Butterworth-Heinemann. ISBN: 978-0-08-100036-6.

Petrov, P. (2009). Nonlinear adaptive control of a two-vehicle convoy. Open Cybernetics & Systemics Journal, 3, 70-78. URL: https://benthamopen.com/contents/pdf/TOCSJ/TOCSJ-3-70.pdf.

Pham, M., & Wang, D. (2004, June). A unified nonlinear controller for a platoon of car-like vehicles. In American Control Conference, 2004. Proceedings of the 2004 (Vol. 3, pp. 2350-2355). IEEE. Print ISBN: 0-7803-8335-4. Print ISSN: 0743-1619.

Rajamani, R., Tan, H. S., Law, B. K., & Zhang, W. B. (2000). Demonstration of integrated longitudinal and lateral control for the operation of automated vehicles in platoons. IEEE Transactions on Control Systems Technology, 8(4), 695-708. DOI: 10.1109/87.852914. Print ISSN: 1063-6536 Online ISSN: 1558-0865.

Schnelle, S., Wang, J., Su, H., & Jagacinski, R. (2017). A Driver Steering Model With Personalized Desired Path Generation. IEEE Transactions on Systems, Man, and Cybernetics: Systems, 47(1), 111-120. DOI: 10.1109/TSMC.2016.2529582. Print ISSN: 2168-2216 Online ISSN: 2168-2232.

Shieh, W. Y., Hsu, C. C. J., Chen, H. C., Wang, T. H., & Chen, C. C. (2015). Construction of infrared signal-direction discriminator for intervehicle communication. IEEE Transactions on Vehicular Technology, 64(6), 2436-2447. DOI: 10.1109/TVT.2014.2342262. Print ISSN: 0018-9545 Online ISSN: 1939-9359.

Snider, J. M. (2009). Automatic steering methods for autonomous automobile path tracking. Robotics Institute, Pittsburgh, PA, Tech. Rep. CMU-RITR-09-08.

Soltesz, K. (2008). Trajectory Tracking Control of an Autonomous Ground Vehicle. MSc Thesis. URL: http://lup.lub.lu.se/student-papers/record/8847589. ISSN: 0280-5316.

Subramanian, V., Burks, T. F., & Arroyo, A. A. (2006). Development of machine vision and laser radar based autonomous vehicle guidance systems for citrus grove navigation. Computers and electronics in agriculture, 53(2), 130-143. DOI: 10.1016/j.compag.2006.06.001.

Suomen Paikallisliikenneliitto. (2010). MITOITUSAJONEUVOT JA AJOURAMALLIT. URL: http://www.pllry.fi/liitteet/infrakortti_9.pdf. Accessed: 16.5.2017.

Tan, H. S., & Huang, J. (2014). Design of a high-performance automatic steering controller for bus revenue service based on how drivers steer. IEEE Transactions on Robotics, 30(5), 1137-1147. DOI: 10.1109/TRO.2014.2331092. Print ISSN: 1552-3098 Online ISSN: 1941-0468.

Tiehallinto. (2003). Linja-autopysäkit. URL: http://alk.tiehallinto.fi/thohje/pdf/2100015-02lautopys.pdf. Accessed: 15.5.2017. Print ISBN 951-726-900-5 Online ISBN 951-726-990-0.

Travis, W., & Bevly, D. M. (2008, May). Trajectory duplication using relative position information for automated ground vehicle convoys. In Position, Location and Navigation Symposium, 2008 IEEE/ION (pp. 1022-1032). IEEE. DOI: 10.1109/PLANS.2008.4570076. Print ISBN: 978-1-4244-1536-6 Print ISSN: 2153-358X Electronic ISSN: 2153-3598.

Villagra, J., Milanés, V., Pérez, J., & Godoy, J. (2012). Smooth path and speed planning for an automated public transport vehicle. Robotics and Autonomous Systems, 60(2), 252-265. DOI: 10.1016/j.robot.2011.11.001.

Wirtanen, K. (2017). Towing beam movement based algorithm to imitate leader vehicle trajectory. MSc Thesis. Aalto University. Espoo.

Wit, J. S. (2000). Vector pursuit path tracking for autonomous ground vehicles. Doctoral thesis. FLORIDA UNIV GAINESVILLE CENTER FOR INTELLIGENT MACHINES AND ROBOTICS.

Wu, W. (2012). DC motor parameter identification using speed step responses. Modelling and Simulation in Engineering, 2012, 30. DOI: 10.1155/2012/189757.

Yih, P. (2004). Steer-by-wire: implications for vehicle handling and safety (Doctoral dissertation, Stanford university).

Yin, G., Li, J., Jin, X., Bian, C., & Chen, N. (2015). Integration of motion planning and model-predictive-control-based control system for autonomous electric vehicles. Transport, 30(3), 353-360. DOI: 10.3846/16484142.2015.1089322. Print ISSN: 1648-4142 Online ISSN: 1648-3480.

Zakaria, M. A., Zamzuri, H., Mamat, R., & Mazlan, S. A. (2013). A path tracking algorithm using future prediction control with spike detection for an autonomous vehicle robot. International Journal of Advanced Robotic Systems, 10(8), 309. DOI: 10.5772/56658.

Zakaria, M. A., Zamzuri, H., Mazlan, S. A., & Zainal, S. M. H. F. (2012). Vehicle Path Tracking Using Future Prediction Steering Control. Procedia Engineering, 41, 473-479. DOI: 10.1016/j.proeng.2012.07.200.

Zhang, L., Ahamed, T., Zhang, Y., Gao, P., & Takigawa, T. (2016). Vision-Based Leader Vehicle Trajectory Tracking for Multiple Agricultural Vehicles. Sensors, 16(4), 578. DOI: 10.3390/s16040578.